

NOTE TO USERS

This reproduction is the best copy available.

UMI[®]

Switching Control using Generalized Sampled-Data Hold Functions

Shauheen Zahirazami

A Thesis
in
The Department
of
Electrical and Computer Engineering

Presented in Partial Fulfillment of the Requirements
for the Degree of Master of Applied Science at
Concordia University
Montréal, Québec, Canada

August 2005

© Shauheen Zahirazami, 2005



Library and
Archives Canada

Bibliothèque et
Archives Canada

Published Heritage
Branch

Direction du
Patrimoine de l'édition

395 Wellington Street
Ottawa ON K1A 0N4
Canada

395, rue Wellington
Ottawa ON K1A 0N4
Canada

Your file *Votre référence*

ISBN: 0-494-10258-6

Our file *Notre référence*

ISBN: 0-494-10258-6

NOTICE:

The author has granted a non-exclusive license allowing Library and Archives Canada to reproduce, publish, archive, preserve, conserve, communicate to the public by telecommunication or on the Internet, loan, distribute and sell theses worldwide, for commercial or non-commercial purposes, in microform, paper, electronic and/or any other formats.

The author retains copyright ownership and moral rights in this thesis. Neither the thesis nor substantial extracts from it may be printed or otherwise reproduced without the author's permission.

AVIS:

L'auteur a accordé une licence non exclusive permettant à la Bibliothèque et Archives Canada de reproduire, publier, archiver, sauvegarder, conserver, transmettre au public par télécommunication ou par l'Internet, prêter, distribuer et vendre des thèses partout dans le monde, à des fins commerciales ou autres, sur support microforme, papier, électronique et/ou autres formats.

L'auteur conserve la propriété du droit d'auteur et des droits moraux qui protègent cette thèse. Ni la thèse ni des extraits substantiels de celle-ci ne doivent être imprimés ou autrement reproduits sans son autorisation.

In compliance with the Canadian Privacy Act some supporting forms may have been removed from this thesis.

Conformément à la loi canadienne sur la protection de la vie privée, quelques formulaires secondaires ont été enlevés de cette thèse.

While these forms may be included in the document page count, their removal does not represent any loss of content from the thesis.

Bien que ces formulaires aient inclus dans la pagination, il n'y aura aucun contenu manquant.


Canada

ABSTRACT

Switching Control using Generalized Sampled-Data Hold Functions

Shauheen Zahirazami

In this thesis, switching control of linear time-invariant systems using generalized sampled-data hold functions (GSHF) is investigated. It is assumed that the plant model belongs to a finite set of known plants. The output of the system is periodically sampled and a control signal is being generated by using a suitable hold function from a set of GSHFs which solve the robust servomechanism problem for the family of plant models and a set of simultaneous stabilizing GSHFs for certain subsets of plant models. It is shown that by using the above sets of hold functions and choosing a proper switching sequence, one can minimize the number of switchings to destabilizing GSHFs. This can significantly improve the transient response of the system, which is one of the common weak points in most switching control schemes. Simulation results show the effectiveness of the proposed method in improving the transient response. It is also desirable to achieve a digital control law that reduces the complexity of online computations.

یک چنڊ بکودکی باستا دشیم
یک چنڊ زاستاومی خوشا دشیم
پایان سخن شنو که مارا چه رسید
از خاک درآیدیم بر باد دشیم

With them the seed of wisdom did I sow,
And with my own hand labour'd it to grow
And this was all the harvest that I reap'd
"I came from sand, and like wind I go"
Omar Khayyam, 1048 - 1123 CE

I dedicate this work to the imprisoned Iranian journalist Akbar Ganji, because of his fight for freedom of speech.

ACKNOWLEDGEMENTS

Thanks are due first to my supervisor, Dr. Amir G. Aghdam, for his great insights and guidance. I also appreciate the help and support I received from my colleagues at Dr. Amir G Aghdam's research group, especially my good friend Mr. Idin Karuei for his useful comments and brilliant ideas for the multi-layer scheme. I would also like to thank Dr. Siamak Yassemi, and Dr. Hamidreza Pezeshk for their help and encouragement.

TABLE OF CONTENTS

LIST OF FIGURES	viii
LIST OF ABBREVIATIONS AND SYMBOLS	xi
1 Introduction	1
1.1 Background	1
1.2 Notation and Abbreviations	2
1.3 Switching vs. Adaptive Control	3
1.3.1 Conventional Adaptive Control	4
1.3.2 Switching Control	5
Single-Layer Switching	7
Multi-Layer Switching	7
1.4 Generalized Sampled-Data Hold Function	11
1.5 Contributions of current work	13
1.6 Chapters Overview	14
2 Digital Control Using Generalized Sampled-Data Hold Functions	16
2.1 Design of Generalized sampled-Data Hold Functions	21
2.1.1 Inter-sample Ripple Effect	25
2.2 Switching Control of a Family of Plants	29
3 Single-Layer Switching Control using Generalized Sampled-Data Hold Functions	33
3.1 Problem Formulation	34

3.2	Main Results	39
3.3	Simulation Results	46
4	Multi-Layer Switching Control using Generalized Sampled-Data Hold Functions	51
4.1	Problem Formulation	53
4.2	Main Results	60
4.2.1	Switching Algorithm	60
4.2.2	Layers' Structure	64
4.2.3	Switching Mechanism	66
4.2.4	Transition Matrix	76
4.3	Simulation Results	77
5	Conclusions and Future work	92
5.1	Conclusions	92
5.2	Future Work	94
	Bibliography	99
A	Computing Integrals Involving Matrix Exponentials	110
A.1	An Efficient Matrix Exponential Integration Method	110
B	Simulation Codes	114
B.1	MATLAB Codes	114
B.1.1	Single-Layer	114
B.1.2	Multi-Layer	119

LIST OF FIGURES

1.1 Single-layer switching control structure, The plant model changes from \mathbf{P}_1 to \mathbf{P}_6	8
1.2 Multi-layer switching structure. The plant model changes from \mathbf{P}_1 to \mathbf{P}_6	9
1.3 Switching path in the multi-layer structure, when plant model changes from \mathbf{P}_1 to \mathbf{P}_5	10
1.4 The structure of a digital controller as a time-varying system.	12
1.5 The structure of a digital controller using a GSHF.	12
2.1 The structure of a digital controller.	17
2.2 Sampled-data system structure.	18
2.3 The output of the ZOH to a unit pulse.	19
2.4 An example of a sampled-data hold signals with a ZOH and a second order GSHF.	24
2.5 Three methods for evaluating inter-sample effect. (a) partial fraction expansion; (b) modified z -transform; (c) multi rate sampling.	27
3.1 Closed-loop model with GSHF.	35
3.2 The two-cart SISO system connected with spring and damper.	47
3.3 Switching instants, when the plant model changes from \mathbf{P}_4 to \mathbf{P}_2	49
3.4 Output signal of the closed-loop simulation results, when the plant model changes from \mathbf{P}_4 to \mathbf{P}_2	50
4.1 Switching control system with GSHFs.	55

4.2	Four layers of GSHFs for six plant models.	59
4.3	The flow chart of <i>Algorithm 1</i>	62
4.4	Switching in four layers. Solid arrows represent stable switchings and dashed arrow denotes an unstable switching.	63
4.5	A possible structure of layer 9 for eleven plant models, where the numbers inside the curly braces represent the indices of the plants that the GSHF cannot stabilize.	65
4.6	A possible multi-layer switching structure for eleven plants, where the numbers inside the curly braces represent the indices of the plants that the GSHF cannot stabilize.	67
4.7	Scenario No. 1 for switching, when the plant model changes from \mathbf{P}_1 to \mathbf{P}_4 . The dashed arrow shows an unstable switching, while the solid arrows show switching to a stabilizing GSHF.	79
4.8	Proposed model: Output of the closed-loop system with GSHFs (at discrete points of time) using the multi-layer scheme, when the plant model changes from \mathbf{P}_1 to \mathbf{P}_4	81
4.9	Continuous-time output of the closed-loop system in Example 1 with GSHFs using the proposed multi-layer scheme, when the plant model changes from \mathbf{P}_1 to \mathbf{P}_4 (Scenario one) using first set of GSHFs.	82
4.10	Continuous-time output of the closed-loop system in Example 1 with GSHFs using the proposed multi-layer scheme, when the plant model changes from \mathbf{P}_1 to \mathbf{P}_4 (Scenario one).	83

4.11	Continuous-time control signal of the closed-loop system in Example 1 with GSHFs using the proposed multi-layer scheme, when the plant model changes from \mathbf{P}_1 to \mathbf{P}_4 (Scenario one).	84
4.12	Switching instants of the multi-layer scheme in Example 1, when the plant model changes from \mathbf{P}_1 to \mathbf{P}_4	85
4.13	Scenario No. 2 for switching, when the plant model changes from \mathbf{P}_1 to \mathbf{P}_4 . The dashed arrow shows an unstable switching, while the solid arrow shows switching to a stabilizing GSHF.	86
4.14	Discrete output of the closed-loop system with GSHFs at discrete points of time using the single-layer scheme, when the plant model changes from \mathbf{P}_1 to \mathbf{P}_4	87
4.15	Continuous-time output of the closed-loop system for Example 1, using the single-layer scheme of [1], and first set of GSHFs when the plant model changes from \mathbf{P}_1 to \mathbf{P}_4	88
4.16	Continuous-time output of the closed-loop system for Example 1, using the single-layer scheme of [1], when the plant model changes from \mathbf{P}_1 to \mathbf{P}_4	89
4.17	Switching instants of the single-layer scheme for Example 1, when the plant model changes from \mathbf{P}_1 to \mathbf{P}_4	90
4.18	Output of the closed-loop system for Example 1 with optimal continuous-time LTI controllers using the single-layer scheme of [2], when the plant model changes from \mathbf{P}_1 to \mathbf{P}_4	91

LIST OF ABBREVIATIONS AND SYMBOLS

LTI	linear time-invariant
LTV	linear time-varying
ZOH	zero-order hold
GSHF	generalized sampled-data hold function
MIMO	multi-input multi-output
BIBO	bounded-input bounded-output
SISO	single-input single-output
FD	finite dimensional
CT	continuous time
DT	discrete time
DES	discrete event systems
A/D	analog to digital
D/A	digital to analog
DFM	decentralized fixed mode
PC	piece-wise continuous
RTOS	real time operating system
LQR	linear quadratic regulator
LQG	linear quadratic gaussian
PDF	probability distribution function

Chapter 1

Introduction

1.1 Background

The control of uncertain systems using discrete-time controllers is considered in this thesis by using both single-layer and multi-layer “switching control” technique.

This chapter is organized as follows. In section 1.2, some preliminary information about the notation and abbreviations used is given in Section 1.2, and then an overview of adaptive control and switching control as well as the advantages and disadvantages of each one is reviewed, and a new multi-layer switching structure is proposed in Section 1.3. In Section 1.4 digital control of systems using generalized sampling is discussed. The results will be used to design controllers in a multi-layer control structure. Section 1.5 briefly presents the contributions of the present work. Finally, this chapter will be concluded by an outline of this thesis in Section 1.6.

1.2 Notation and Abbreviations

Some of the terms and notation that appear throughout this thesis are defined as follows.

\mathbb{R} , \mathbb{R}^+ and \mathbb{N} represent the set of real, positive real, and natural numbers, respectively. Furthermore \mathbb{R}^n and $\mathbb{R}^{m \times n}$ denote the n -dimensional vector space and $m \times n$ matrix space, respectively.

In the state space representation of a system, capital letters A , B , C , E , and F are used to denote the system matrices of the continuous-time system, while the capital letters with hats \hat{A} , \hat{B} , \hat{C} , \hat{E} , and \hat{F} are used to denote the corresponding matrices for the discrete-time equivalent model.

$\|\cdot\|$ denotes the norm of a vector or the induced norm of a matrix. In Chapter 3 and Chapter 4, it is used to represent the 2-norm.

PC denotes the set of real vector-valued functions defined on $t \geq 0$ whose elements are piecewise continuous, and PC_∞ denotes the subset of PC functions which are bounded.

Given a set of plant models, the index of a model or the corresponding GSHF and parameters are denoted by subscripts. For example, K_i represents a parameter K corresponding to the plant $\#i$. To refer to a parameter related to the discrete-time equivalent of a plant using a particular GSHF, the index of the plant and the GSHF will be separated by a comma in the subscript. For example $K_{i,j}$ refers to the parameter K corresponding to plant i and GSHF $\#j$.

For continuous-time signals, the independent variable is enclosed in parentheses, whereas for discrete-time signals, brackets are used to enclose the corresponding independent variable. Furthermore throughout the thesis the sampling rate for discrete-time signals is assumed to be fixed.

In all examples, the international system of units (SI) has been assumed, unless noted otherwise. Also, all numerical values are assumed to be represented by at least 4 significant digits. Therefore, 3.49 will in fact be the same as 3.490 in the thesis.

All variables and parameters are denoted by italic fonts, while all sets and function names are represented by Roman fonts.

1.3 Switching vs. Adaptive Control

The study of control systems has experienced a huge advancement, which has resulted in very powerful tools and also has introduced new complicated problems. When one attempts to design and implement large-scale system problems such as power systems, socioeconomic systems, chemical process control, advanced flight control, etc. the classical methods such as simple PID control design would no more be effective for designing suitable control systems. Specifically introducing uncertainties in the plant model need to be addressed in a proper manner.

Servomechanism problem, known also as the output regulation problem, plays a crucial role in control theory. It concerns with the design of a feedback control law for the known system to achieve asymptotical tracking of the reference inputs and rejecting disturbances while maintaining the closed-loop stability. In many applications though the dynamics of the system which is to be controlled may change as time passes, and hence special techniques are required in the process of control. Adaptive control techniques were a major response to the problem of changes in the dynamics of the plant.

1.3.1 Conventional Adaptive Control

In adaptive control of system, it is desired to design a controller such that the behavior of the overall system remains close to that of a desirable model (reference model), in presence of uncertainties and variations in the plant parameters. Generally some assumptions have to be made in order to guarantee the asymptotical stability of the system. One of the shortcomings of classical adaptive control methods is that they are not suitable for highly uncertain systems, in general. For instance, in a power distribution network, slight changes of the power usage pattern in a particular area on the network might be possibly controlled using conventional adaptive techniques. However the sudden failure of a power plant could change the network dynamics completely and hence, classical adaptive techniques may fail to control the system.

In conventional adaptive control design, it is typically assumed that the actual plant is described by a LTI model whose parameters are unknown, but that some *a priori* information about the plant is available. Such information typically includes a knowledge of the upper bound on plant's order, the relative degree, the sign of the high-frequency gain, and minimum phase property.

There has been considerable amount of interest in adaptive control literature to relax some of the required assumptions in conventional adaptive control. For example, some improvements have been made to remove the required information on the sign of the high-frequency gain [3, 4, 5, 6], and to weaken the other assumptions [7, 8, 9, 10]. However, certain assumptions regarding the right half plane zeros are required [11]. Further attempts are made to design an adaptive controller in the presence of modelling uncertainties with robustness and performance analysis [12], [13] and also to extend this to time

varying systems [14].

1.3.2 Switching Control

Switching techniques have been the center of focus of many researchers in the past decade, specially when classical adaptive control methods fail to stabilize the systems due to, for instance, sudden changes in the dynamics of the model or insufficient *a priori* knowledge; e.g. see [4] [15, 16, 17, 18, 19, 20, 21, 22, 23, 24, 25, 26, 27, 28, 29, 30, 31, 32, 33, 34]. These methods can be very effective when wide-band tracking/disturbance rejection of a physical plant, which can be described by a family of plants models, is required.

The earliest research to weaken the classical *a priori* information required in adaptive methods can be traced back to Morse and Martensson's works [35], [36] in which a number of questions about the classical assumptions in conventional adaptive control were raised. In the adaptive switching control approach using a family of plants, it is typically assumed that the plant model changes between a finite set of plant models. As a result, it is required to have a finite set of controllers (obtained by using any design technique such as LQR method or tuning methods) so that at least one of the controllers can stabilize each model in the family of plant models. [17], [24], [30], [37], [2], [38], [39]. Then, using a so called "switching scheme", each controller is applied to the plant sequentially, and once the system switches to a stabilizing controller, it stops switching (this is accomplished in a finite time). This implies that as long as the plant remains unchanged, the system will also stay locked on the stabilizing controller.

Fu and Barmish [37] considered a compact set of LTI models to represent the plant

and imposed an *a priori* upper bound on the order of plants in this set. They showed that Lyapunov stability can be achieved in this case, by applying a finite set of controllers. Miller and Davison [2] reduced this *a priori* information, to the knowledge of the order of a LTI stabilizing compensator. They then simplified the compactness assumption required on the set of possible plant models to just a finite set of plant models. As a result, one can design a high-performance LTI controller, e.g. an optimal controller, for each plant model in the known set.

Branicky in [40] investigated many aspects of continuous-time switching control systems, and considered a realistic aircraft control problem using the extension of Bendixsons Theorem and the linear robustness criteria.

Chang and Davison proposed a switching mechanism [41], [39] and [42] using Strong bounding functions and showed that the system may switch to each controller more than once, before it locks on to a stabilizing controller. The only requirement for this method is that a set of controllers exists so that at least one of the controllers can stabilize the current plant. In other words, no information about the plant model is required to exist.

Aghdam and Davison have also investigated the problem of decentralized switching control in [43] and [44]. They also studied the inter-sample ripple effect in sampled-data systems using periodic feedback control in [45].

Liberzon studied several important issues of switching in systems and control and investigated hybrid systems in depth [46].

Single-Layer Switching

In switching control of a family of plant models $\{\mathbf{P}_i : i \in \bar{p} := \{1, 2, \dots, p\}\}$ using high performance LTI controllers introduced by Miller and Davison [2], [47] and [45], it is assumed that each plant-controller pair $(\mathbf{P}_i, \mathbf{K}_j)$ is stable iff $i = j, i, j \in \bar{p}$, and that a bound on the magnitude of the unmeasurable disturbance signal is available. It was shown that by using a proper switching mechanism which monitors the norm of error in the output, the system eventually locks onto a stabilizing controller after a number of switchings and would not switch to each controller more than once. One of the major shortcomings of most switching mechanisms is the large magnitude of the transient response. Several methods have been proposed to improve the transient response [48], [49]. One of the main reasons for undesirable transient response in switching control systems is that in the transition from the initial controller to the final one, the system may switch to several destabilizing controllers. For example suppose that initially plant \mathbf{P}_1 was the correct plant model, but due to some variations in the dynamics of the plant, the plant model changes to \mathbf{P}_6 as shown in Figure 1.1. The switching mechanism will search for the correct controller and will lock onto controller #6 after 4 unstable switchings.

Multi-Layer Switching

As mentioned before, one of the shortcomings of switching control methods is the bad transient response which is mainly contributed by switching to destabilizing controllers before the decision making unit finds the correct one. Each switching to a destabilizing controller will usually cause a big overshoot, which will be accumulated before the correct controller is found.

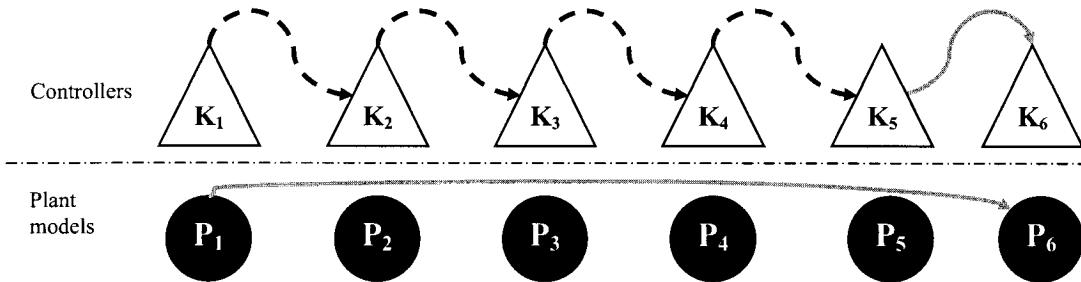


Figure 1.1: Single-layer switching control structure, The plant model changes from P_1 to P_6 .

A method is proposed here to improve the transient response of the switching control system by reducing the number of switchings to destabilizing controllers via introducing different layers of controllers with different properties [50]. In the multi-layer scheme, $p - 2$ layers of controllers are designed, where p denotes the number of models in the family of plants. Layer $k \in \{2, \dots, p - 2\}$ consists of a set of controllers which have the property that each one stabilizes k models in the family and destabilizes the remaining $p - k$ plants. Layer 1 consists of a set of p controllers, where each one solves the robust servomechanism problem for one of the models in the family. To obtain controllers for layers $2, \dots, p - 2$ one should use simultaneous stabilizer design techniques, which can be a difficult task in general. Furthermore the amount of on-line computations required to find the auxiliary signals which are to be compared with the norm of the error in the decision making unit according to the Miller and Davison's technique [2] will grow rapidly by introducing new layers of controllers.

Using a proper switching path between the controllers of different layers can lead the switching mechanism to identify the actual plant model more smoothly. Consider the

example given by Figure 1.1, and suppose that a set of simultaneous stabilizers exist for a multi-layer switching structure of Figure 1.2. Once the plant model changes from \mathbf{P}_1 to \mathbf{P}_6 , the system will switch from \mathbf{K}_1 to a higher level controller which does not stabilize \mathbf{P}_1 and one other plant model such as \mathbf{P}_6 . This controller is denoted by \mathbf{K}_{2345} (a controller that stabilizes plant models i_1, i_2, \dots, i_s and destabilizes plant models $i_{s+1}, i_{s+2}, \dots, i_p$ is denoted by $\mathbf{K}_{i_1 i_2 \dots i_s}$). Since this controller does not stabilize the actual plant model, the switching mechanism will identify \mathbf{P}_6 as the only possible actual plant model and will switch to \mathbf{K}_6 as illustrated in Figure 1.2.

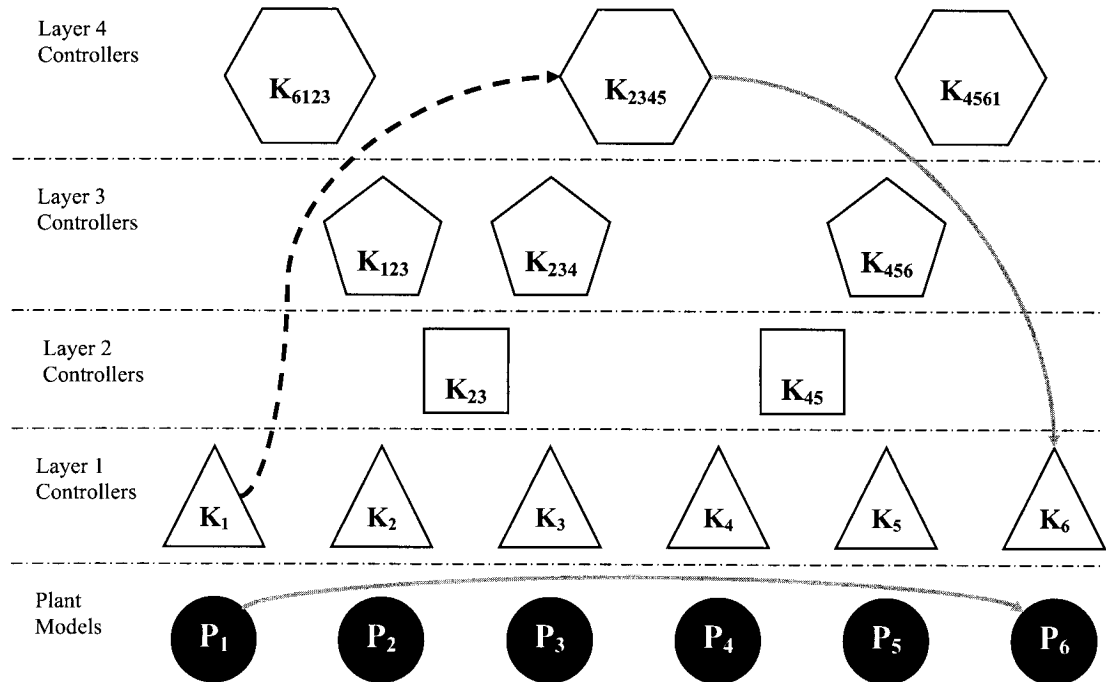


Figure 1.2: Multi-layer switching structure. The plant model changes from \mathbf{P}_1 to \mathbf{P}_6 .

Assume now that the plant model changes from \mathbf{P}_1 to \mathbf{P}_5 as illustrated in Figure 1.3. After one stable switching to \mathbf{K}_{2345} the actual plant model will known to be either \mathbf{P}_1 , \mathbf{P}_2 ,

P_3 , P_4 or P_5 . It would be enough to switch to a controller in the lower layer which does not stabilize one of these plant models. Assume, for example, that the system switches to K_{234} . This would be an unstable switching and thus, switching mechanism would identify P_5 as the actual plant model. Hence the system would eventually switch to K_5 .

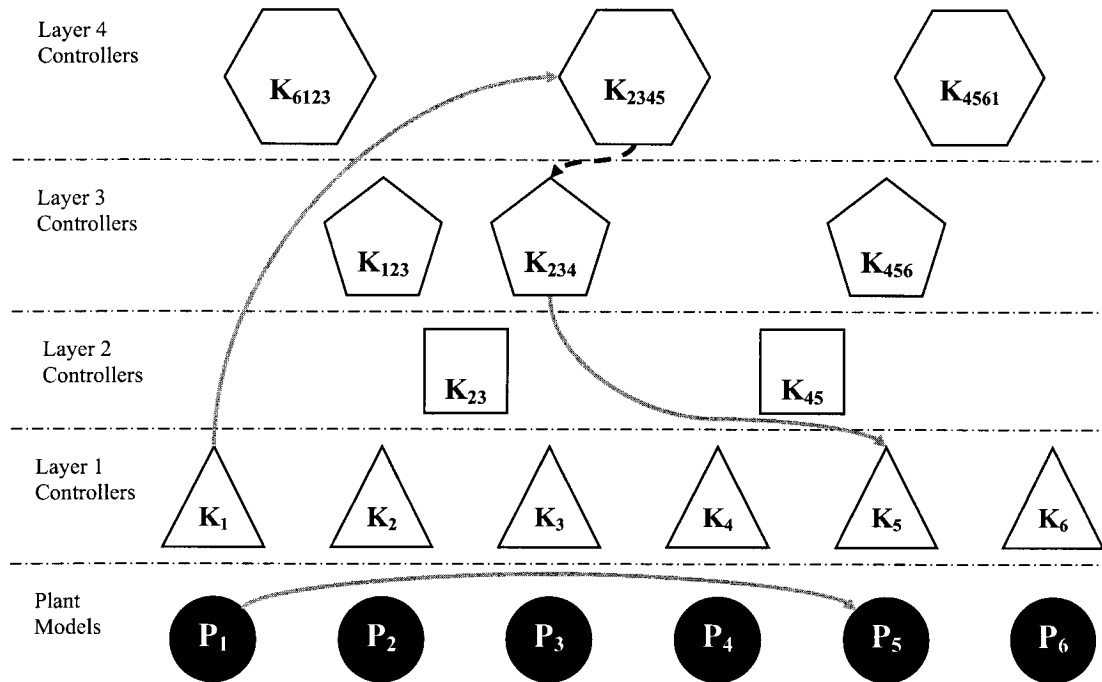


Figure 1.3: Switching path in the multi-layer structure, when plant model changes from P_1 to P_5 .

As elaborated in the above example, the switching sequence of the multi-layer algorithm requires that the system switches from the higher layer GSHFs to the lower layer GSHFs even if the system is stabilized in a higher layer. Unlike unstable switchings, stable switchings cannot be identified through the upper-bound signals. In order to detect

stability, a sufficiently long time-interval will be required such that if the norm of the error does not meet the upper-bound signal during this time interval, it is concluded that the system is stable. This time-interval can be obtained either experimentally or by considering worst-case scenario associated with the initial state, reference input and disturbance signal. This time duration will be referred to as safety time and will be denoted by t_d .

In [39], a class of multivariable switching control algorithms was introduced which does not require a knowledge of the actual family of plant models. The only requirement of this procedure, is that a set of controllers, corresponding to the set of plant models, which contains a stabilizing controller for each plant model is given. The norm of the error will be compared to an increasing bounding function in order to find the correct controller. The system, however, may switch to each controller several times before it locks onto the correct controller.

1.4 Generalized Sampled-Data Hold Function

The combination of a sampler, a DT LTI controller and a hold operator can be considered as a linear time-varying continuous time controller for the CT system, as shown in Figure 1.4. Suppose that the following SISO CT FD LTI system is given

$$x[k+1] = A_d x[k] + B_d u[k] \quad (1.1a)$$

$$y[k] = C_d x[k] + D_d u[k] \quad (1.1b)$$

A GSHF can be formulated as follows

$$\begin{aligned} u(t) &= \mathbf{f}(t) \cdot \tilde{u}[k] \\ \mathbf{f}(t+T) &= \mathbf{f}(t), \quad t > 0 \end{aligned} \quad (1.2)$$

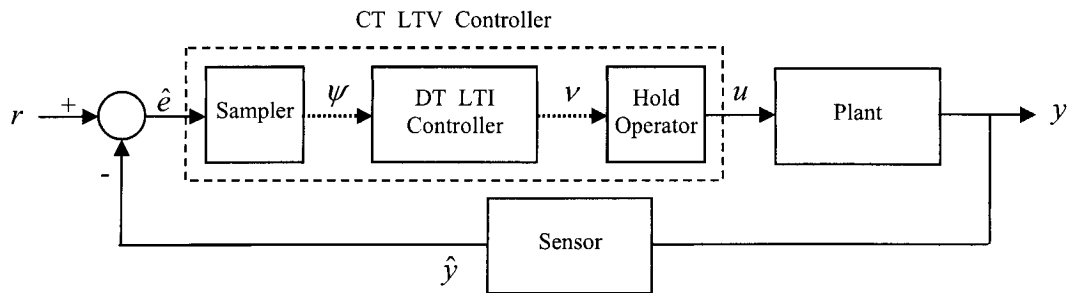


Figure 1.4: The structure of a digital controller as a time-varying system.

The samples of the control input $\tilde{u}[k]$ are multiplied by the function $\mathbf{f}(t)$ to construct the control signal which will then be applied to the system as illustrated in Figure 1.5. It can be shown that if the CT system is stabilizable and a non-pathological sampling frequency is used, then the closed-loop CT system is stable if the corresponding discrete-time model is stable.

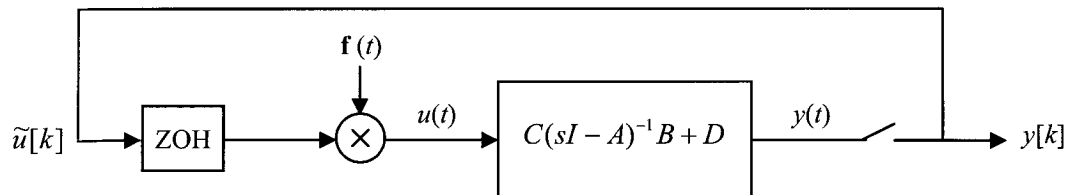


Figure 1.5: The structure of a digital controller using a GSDF.

The idea of using generalized sampled-data hold functions (GSDF) instead of a simple zero-order hold (or first-order hold) in control systems, was first introduced by Chammas and Leondes [51]. Kabamba presented several advantages of using GSDFs in control systems, and showed that by using GSDFs, one can obtain many of the advantages

of state feedback controllers, without the requirement of state estimation. A method was presented in [52] to design GSHFs, based on the dynamics of the system. The input signal is constructed as a function of the output samples in each sampling interval. Design of simultaneous stabilizing GSHFs was also investigated in [53].

In this thesis, GSHFs are employed in both single-layer and multi-layer switching structure instead of LTI controllers. The switching scheme used here is the discrete time version of the approach presented in [50]. It is assumed that layer $k \in \{2, \dots, p-2\}$ consists of a set of GSHFs which have the property that each one stabilizes k plant models in the family of plants and destabilizes the remaining $p-k$ models. The first layer consists of a set of p high-performance GSHFs, where each one stabilizes a plant \mathbf{P}_i in the family of plant models.

One of the objectives of this work is to propose a switching controller which is computationally efficient in obtaining bounding functions or auxiliary signals compared to the existing methods [2], [50]. The required control computations are also much less than the continuous-time counterparts. Moreover, the proposed switching control method utilizes the benefits of output control using GSHFs which can, in general, outperform traditional LTI controllers.

1.5 Contributions of current work

In the present work, switching mechanism as proposed by Miller and Davison [2] has been implemented using generalized sampled-data hold functions. The proposed method has several advantages compared to the switching control using LTI controllers. First of all, the design and implementation of the GSHFs can be much easier than those of LTI

controllers. Digital controllers are specially of interest in decentralized systems, where the structure of the decentralized setup can be changed using a suitable GSHF to weaken the effect of interconnections in the system [44]. They can also be used to control decentralized systems with certain type of unstable decentralized fixed modes (DFM) [54], [55]. Moreover, the amount of online computations required is reduced significantly, since in switching between CT controllers continuous signals are to be compared with the output of the system, while in case of GSHFs the auxiliary signals are to be compared with the output at discrete points of time. This can be very important when the number of auxiliary signals is increased due to introducing new controllers in the switching mechanism. Simulation results also show a significant reduction in the maximum overshoot in the output.

Switching control using GSHFs has also been extended to a multi-layer architecture which introduces new layers of simultaneous stabilizer GSHFs. The advantage is that the proposed algorithm guarantees not more than only one unstable switching during the switching process, which can reduce the maximum overshoot significantly.

1.6 Chapters Overview

The remainder of this thesis is organized as follows. In Chapter 2, the application of digital controllers in control systems is discussed. It will be shown that the effectiveness of digital control strategies can be improved significantly by using a more general form of sampled-data hold functions instead of a simple zero-order hold. Some efficient computational tools are introduced in section A.1 which will be used in order to simplify some of the required calculations encountered throughout the thesis. Also some practical and

theoretical issues concerning the inter-sample ripple effect are discussed.

In Chapter 3, a single-layer switching controller using generalized sampled-data hold functions (GSHF) is introduced. The proposed switching scheme is a discrete-time version of the method introduced by Miller and Davison in [2]. It is assumed that the plant model belongs to a known finite set of plant models which is referred to as a family of plant models. It is also assumed that the unmeasurable disturbance signal is bounded. The switching mechanism will start switching as soon as the norm of the error signal hits an upper bound. It is guaranteed that under certain conditions the switching mechanism will eventually find the correct GSHF and lock onto it. However the switching mechanism of Chapter 3 may switch to several destabilizing GSHFs before it finds the correct GSHF. This can potentially generate a bad transient response.

In Chapter 4 generalized sampled-data hold functions are used in a multi-layer switching architecture. In this approach, additional GSHFs are added to the set of GSHFs used in the switching control of Chapter 3. When the system detects instability it will first try to switch to a GSHF which can stabilize a number of other plants. An algorithm is given which guarantees that by using suitable GSHFs, the correct GSHF can be found after at most one unstable switching. This can significantly reduce the magnitude of the transient response. Simulation results show effectiveness of multi-layer structure in improving the performance of the system.

Finally, the thesis closes with Chapter 5, the concluding remarks and suggested future work.

Chapter 2

Digital Control Using Generalized Sampled-Data Hold Functions

Sampled-data systems are hybrid systems which operate in continuous-time (CT) but involve discrete-time (DT) signals too which are samples of some CT signals. In these systems usually the continuous controllers are replaced by digital (micro)controllers with the necessary input/output hardware to implement them. The control system is often implemented on a microprocessor using a realtime programming language such as *Ada 95* or *Modula 2* with a realtime kernel or runtime system, or using a sequential programming language such as C or C++ together with a realtime operating system (RTOS). The realtime kernel or OS uses multiprogramming to multiplex the execution of the tasks on the CPU. Simplicity of implementation of digital control laws is one of the advantages of sampled-data systems in control. Figure 2.1 shows a typical sampled-data system setup, which involves A/D and D/A units, and a digital controller.

Two basic elements in a digital systems are sampler and hold circuit. In practice,

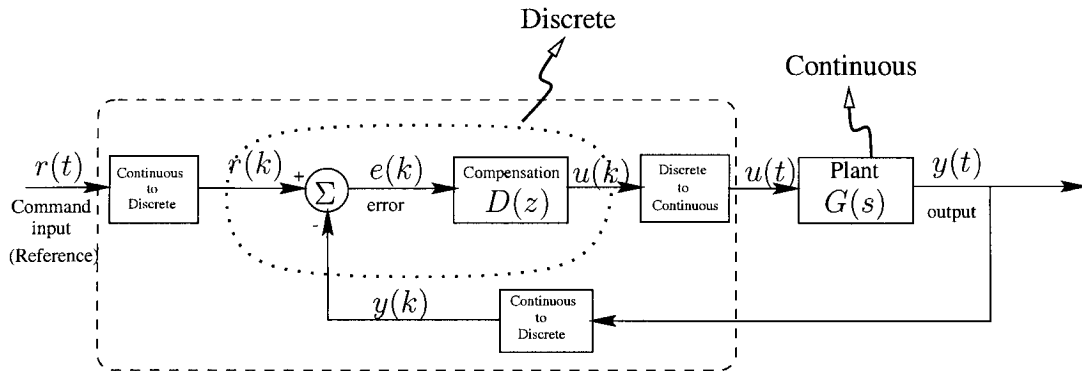


Figure 2.1: The structure of a digital controller.

an analog-to-digital converter (A/D) consists of an ideal sampler followed by a quantizer and a digital-to-analog converter (D/A) is the hold operator, generating a constant signal equal to the latest sample up to the next sampling instant. In general, A/D and D/A can be multi-input, multi-output (MIMO) operators. A discretized system with sampler and hold is shown in Figure 2.2.

Let the sampling period be denoted by T . In the sampler discrete samples of the CT signal are taken, where in the hold device, each sample of the signal is multiplied by the hold function. It is to be noted that the combination of sampler, DT time-invariant controller and hold operator is equivalent to a time-varying controller. Since shifting the input signal by any non integer multiple of T will not shift the output of the system.

The easiest conversion method is to hold voltage constant across a sampling period, that is, the value of the continuous signal $u(t)$ will be held constant at $u[k]$ within the interval $[kT, (k+1)T)$. This method is called zero-order hold (ZOH), where a polynomial of degree zero is used to connect the sample points, and a piece-wise constant continuous-time signal is generated. It would also be possible to multiply the sample by any given

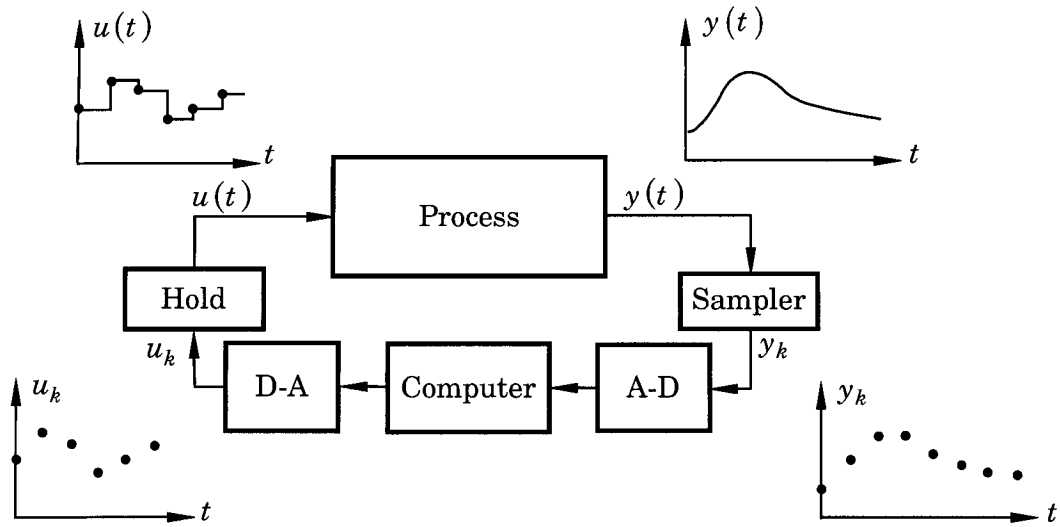


Figure 2.2: Sampled-data system structure.

function defined on the interval $[0, T)$.

In general, the output of the DT model obtained from the combination of an ideal sampler, a CT system and a ZOH is exactly equal to the samples of the original CT system.

It is possible to find the transfer function of the discrete equivalent model obtained by using a ZOH. The response of the ZOH to a unit impulse is a rectangular function as shown in Figure 2.3. The Laplace transform of the rectangular function is $\frac{1-e^{-Ts}}{s}$. Hence the output of the system in the Laplace domain will be:

$$\begin{aligned}
 Y(s) &= (1 - e^{-Ts}) \frac{G(s)}{s} \\
 &= \frac{G(s)}{s} - e^{-Ts} \frac{G(s)}{s}
 \end{aligned}
 \tag{2.1}$$

Let

$$x(t) = L^{-1} \left[\frac{G(s)}{s} \right]
 \tag{2.2}$$

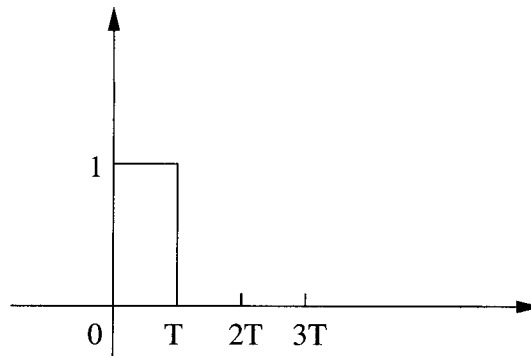


Figure 2.3: The output of the ZOH to a unit pulse.

Then applying the inverse laplace transform to both sides of (2.1) will yield the following expression for the output $y(t)$ in the time domain:

$$y(t) = x(t) - x(t - T) \quad (2.3)$$

which in discrete-time domain will be:

$$y[k] = x[k] - x[k - 1] \quad (2.4)$$

Taking the z -transform of both sides of the above equation will result in:

$$G(z) = (1 - z^{-1})Z\left[\frac{G(s)}{s}\right] \quad (2.5)$$

The DT equivalent model obtained here is called step-invariant transformed DT equivalent. The reason is that if a DT unit step signal is applied to the system, the output $y[k]$ will be the step response of the DT system. Since $y[k]$ is equal to the samples of $y(t)$, it can be said that the step response of the DT equivalent model is equal to the samples of the step response of the CT system.

To obtain the state equation of the DT equivalent model under step invariance transformation, consider a CT LTI system as follows,

$$\begin{cases} \dot{x}(t) = Ax(t) + Bu(t) \\ y(t) = Cx(t) + Du(t) \end{cases} \quad (2.6)$$

where $x(t) \in \mathbb{R}^n$ is the state vector, $u(t) \in \mathbb{R}^m$ is the input vector, and $y(t) \in \mathbb{R}^r$ is the output vector, and A , B , C and D are constant matrices of proper dimension. For simplicity and without loss of generality assume that $m = r$.

The transfer function matrix for this system is denoted by $G(s) = \begin{bmatrix} A & B \\ C & D \end{bmatrix}$ and is equal to $G(s) = C(sI - A)^{-1}B + D$

The state space equations for the DT equivalent model resulted from the step invariant transformation, are represented by:

$$\begin{aligned} x[k+1] &= A_d x[k] + B_d u[k] \\ y[k] &= C_d x[k] + D_d u[k] \end{aligned} \quad (2.7)$$

First the state of the CT system at time $t = t_2$ is written in terms of the state at time $t_1 < t_2$,

$$x(t_2) = e^{(t_2-t_1)A}x(t_1) + \int_{t_1}^{t_2} e^{(t_2-\tau)A}Bu(\tau)d\tau \quad (2.8)$$

Let $t_1 = kT$ and $t_2 = (k+1)T$ then

$$x((k+1)T) = e^{TA}x(kT) + \int_{kT}^{(k+1)T} e^{[(k+1)T-\tau]A}Bu(\tau)d\tau \quad (2.9)$$

Since $u(t)$ is the output of the ZOH, it is constant over $kT \leq \tau < (k+1)T$. In fact $u(\tau) = u(kT) = u[k]$ for $kT \leq \tau < (k+1)T$. Hence,

$$x[k+1] = e^{TA}x[k] + \left[\int_{kT}^{(k+1)T} e^{[(k+1)T-\tau]A} B d\tau \right] u[k] \quad (2.10)$$

Using the change of variable $s := (k+1)T - \tau$ one can write,

$$\int_{kT}^{(k+1)T} e^{[(k+1)T-\tau]A} d\tau = \int_T^0 e^{sA} (-ds) = \int_0^T e^{sA} ds = \int_0^T e^{\tau A} d\tau \quad (2.11)$$

Therefore,

$$\begin{aligned} x[k+1] &= e^{TA}x[k] + \left[\int_0^T e^{\tau A} B d\tau \right] u[k] \\ y[k] &= Cx[k] + Du[k] \end{aligned} \quad (2.12)$$

It can be shown that the step invariant transformation maps the state space matrices as follows [56]:

$$(A, B, C, D) \longmapsto (A_d, B_d, C, D) \quad (2.13)$$

where:

$$A_d = e^{TA}, \quad B_d = \int_0^T e^{\tau A} B d\tau \quad (2.14)$$

It is evident from the above equations that type of discretization only affects the matrices A and B .

2.1 Design of Generalized sampled-Data Hold Functions

The idea of using generalized sampled-data hold functions (GSHF) instead of a simple zero-order hold (or first-order hold) in control systems, which was first introduced by Chammas and Leondes [51] was extensively investigated by many researchers [1], [52], [44], [57], [58], [59].

Digital control of systems using GSHF has several advantages. First, it has the efficiency of state feedback without the requirement of state estimation. Second, it does not introduce additional state variables; hence, it does not require many on-line computations. As a result it may be suitable for the on-line control of high order systems. Third, its practical implementation only requires computer memory to store the time history of the hold function gain over one period. Computer memory is now highly reliable, compact, and affordable. These characteristics make practical implementation of GSHF promising. An example of input and output signals for a sampled-data system with a ZOH and also with a second order GSHF is given in Figure 2.4.

Consider the CT FD LTI SISO system in equation (2.6). The impulse response of the system is given by:

$$h(t) = Ce^{(At)}B \quad (2.15)$$

Using the GSHF $\mathbf{f}(t) \in \mathbb{R}^m$, one can write:

$$\begin{aligned} u(t) &= \mathbf{f}(t) \cdot \tilde{u}[k], & kT \leq t < (K+1)T \\ \mathbf{f}(t+T) &= \mathbf{f}(t), & t > 0 \end{aligned} \quad (2.16)$$

The DT equivalent model can then be obtained as follows:

$$\begin{aligned} x(kT+T) &= e^{AT}x(kT) + \int_0^T e^{A(T-\tau)}\mathbf{B}\mathbf{f}(\tau)\tilde{u}[k]d\tau \\ \Rightarrow x[k+1] &= e^{AT}x[k] + \left(\int_0^T e^{A(T-\tau)}\mathbf{B}\mathbf{f}(\tau)d\tau\right)\tilde{u}[k] \end{aligned} \quad (2.17)$$

with the following transfer function,

$$\begin{aligned} H_0(z) &= C[zI - e^{AT}]^{-1} \cdot \int_0^T e^{A(T-t)}\mathbf{B}\mathbf{f}(\tau)d\tau \\ &= \sum_{k=1}^{\infty} z^{-k} \int_0^T h(kT - \tau)\mathbf{f}(\tau)d\tau \end{aligned} \quad (2.18)$$

This shows that in the DT equivalent model:

$$\begin{aligned} A_d &= e^{AT} \\ B_d &= \int_0^T e^{A(T-\tau)} B \mathbf{f}(\tau) d\tau \end{aligned} \quad (2.19)$$

and the matrices C_d and D_d will remain the same as the CT counterparts. In order to achieve closed-loop control, one can set,

$$\tilde{u}[k] = y[k] \quad (2.20)$$

Hence the modes of the DT closed-loop system will be the eigenvalues of the matrix $A_d + B_d C$. The resulting CT equivalent system is stable if all of the modes of this matrix are inside the unit circle. From the definition of controllability, it is known that a CT LTI system is controllable if there exists an unconstrained control signal u that can transfer the state of the system from the origin $x_0 = 0$ to any arbitrary point in the state space in a finite time. From the definition of controllability and comparing it to (2.19), it can be concluded that using a proper GSHF $\mathbf{f}(t)$, the vector B_{d_i} in the DT equivalent model can be set arbitrarily if the pair (A, B_i) is controllable, where B_{d_i} and B_i for $i = 1, 2, \dots, m$ represent the i 'th column of the matrices B_d and B , respectively. More generally, using a proper GSHF, B_{d_i} can be made equal to any vector in the controllability subspace of (A, B_i) .

One can use GSHFs of polynomial form, piece-wise constant form or any other form to achieve the desired B_d . One possible choice for the GSHF (which is not unique) to get a desired B_d in the DT equivalent model is given by:

$$\mathbf{f}(t) = B^H e^{(A^H(T-t))} W^{-1} B_d \quad (2.21)$$

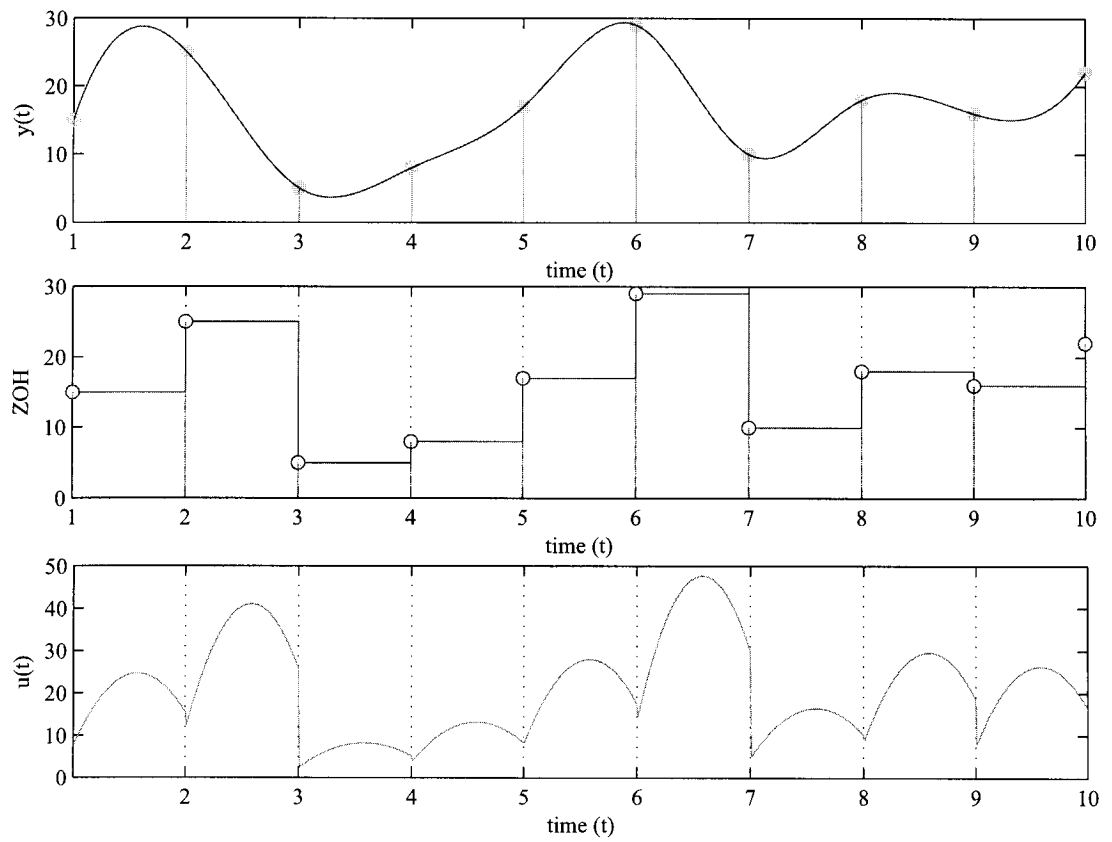


Figure 2.4: An example of a sampled-data hold signals with a ZOH and a second order GSHF.

where W is the controllability gramian on the interval $[0, T]$ which can be obtained from the following equation:

$$W = \int_0^T e^{A(T-\tau)} B B^H e^{A^H(T-\tau)} d\tau \quad (2.22)$$

The following proposition can be used to find a GSHF for a given system.

Proposition 1 *If the triple (A, B, C) is minimal, then for almost all $T > 0$, the optimal noise rejection problem is solvable and a solution is given by:*

[52]

$$F(t) = B^H e^{A^H(T-t)} W^{-1}(A, B, T) \bar{F} \quad (2.23)$$

where

$$\bar{F} \triangleq -e^{AT} K C^H [C K C^H + 1]^{-1} \quad (2.24)$$

and $K \in \mathbb{R}^{n \times n}$ is the unique positive solution of the discrete Riccati equation

$$e^{AT} K e^{A^H T} - e^{AT} K C^H [C K C^H + 1]^{-1} C K e^{A^H T} - K = 0 \quad (2.25)$$

2.1.1 Inter-sample Ripple Effect

Applying a given input signal to a sampled-data system, the output of the system can be computed using the z -transform. In practice, however, it is desirable to know the behavior of the original CT system between the sampling instants. It is to be noted that the sampled-data system with a good discrete-time response may have a very poor inter-sample behavior. In other words, in the control design for a sampled-data system, one

should take the inter-sample ripple effect into consideration as the samples of the output signal may not be a good indication of the overall system behavior. Three techniques are used to compute the inter-sample ripple. The first method suggested by J. Sklansky in [60] is based on the partial fraction expansion of $\frac{G(s)}{s}$. The second one suggested by E. Jury [61], is based on introducing a time shift in the sampler at the output of the system. If this shift is less than the sampling period, the new samples are taken between the system samples. The modified transform from input samples to shifted samples is called the modified z -transform of $\frac{G(s)}{s}$. The third technique is based on sampling the output at a faster rate than the feedback loop is updated. These techniques are illustrated in the block diagrams of Figure 2.5.

One can use a simple technique to reduce the inter-sample ripple effect when a GSHF is to be used. After designing the GSHFs using any desired method, find its polynomial approximation by using interpolation methods. Suppose that the GSHF is approximated by $ax^2 + bx + c$, and that this polynomial is a stabilizing hold function for the system. Hence, to minimize the inter-sample ripple effect, a constrained optimization problem has to be solved. Using the $\langle a, b, c \rangle$ as an initial point, one can define a performance index such as maximum error magnitude (infinity norm of the error) or energy of the error (2-norm of the error). A proper optimization algorithm such as Nelder-Mead's direct search simplex method can be used to improve the inter-sample ripple effect.

Regarding the optimal control problem, consider the CT FD LTI system in equation (2.6), and assume that the DT equivalent model is given by equation (2.7). A continuous time cost function which takes the inter-sample ripple effect into account is given below:

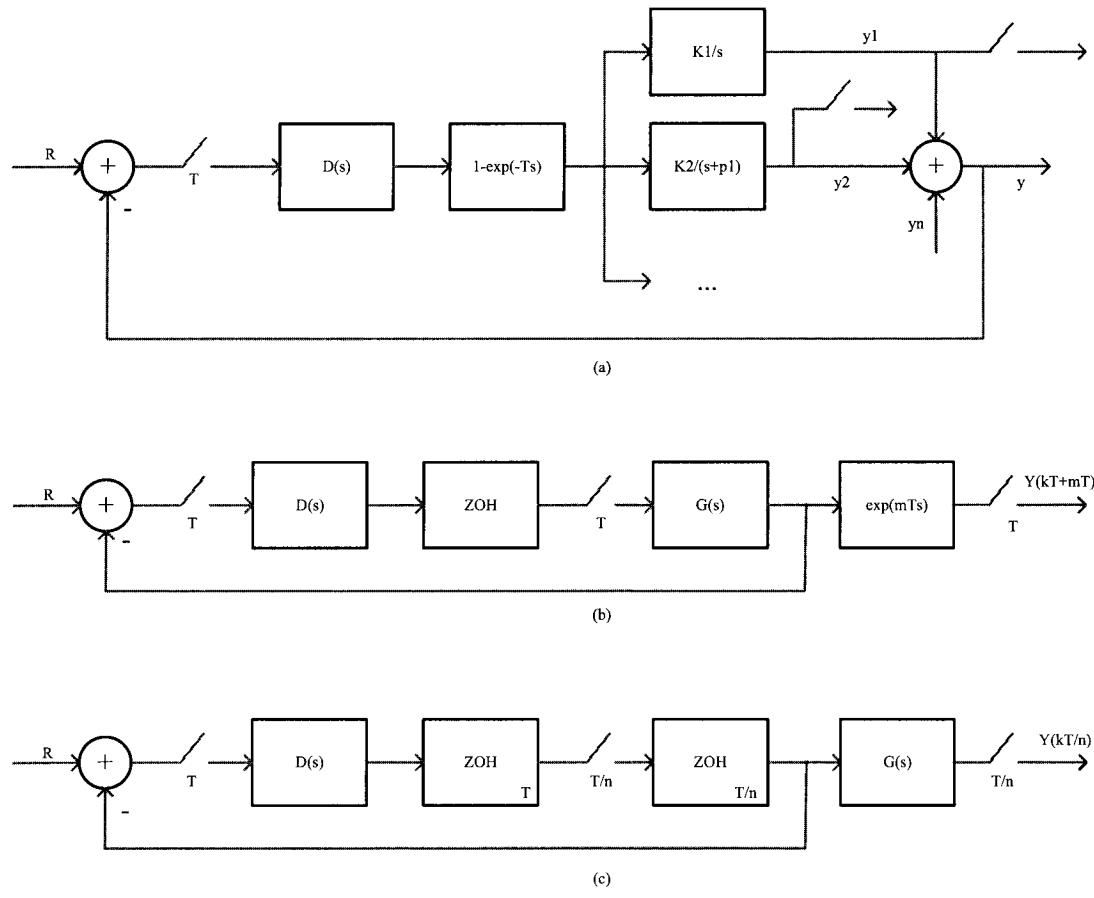


Figure 2.5: Three methods for evaluating inter-sample effect. (a) partial fraction expansion; (b) modified z-transform; (c) multi rate sampling.

$$J_c = \frac{1}{2} \int_0^{NT} [x^H(t)Q_{c_1}x(t) + u^H(t)Q_{c_2}u(t)]dt \quad (2.26)$$

where Q_{c_1} and Q_{c_2} are positive definite symmetric weighting matrices which are, in fact, design parameters. This cost function can be rewritten as follows:

$$J_c = \sum_{k=0}^{N-1} \frac{1}{2} \int_{kT}^{(k+1)T} [x^H(t)Q_{c_1}x(t) + u^H(t)Q_{c_2}u(t)] dt \quad (2.27)$$

On the other hand

$$x(kT + t) = \Phi(t)x(kT) + \Gamma(t)u(kT) \quad (2.28)$$

where

$$\Phi(t) = e^{At}, \quad \Gamma(t) = \int_0^t e^{A\tau} d\tau B \quad (2.29)$$

Substituting (2.28) in (2.27) results in

$$J_c = \sum_{k=0}^{N-1} \frac{1}{2} \begin{pmatrix} x^H[k] & u^H[k] \end{pmatrix} \begin{pmatrix} Q_{11} & Q_{12} \\ Q_{21} & Q_{22} \end{pmatrix} \begin{pmatrix} x[k] \\ u[k] \end{pmatrix} \quad (2.30)$$

where

$$\begin{pmatrix} Q_{11} & Q_{12} \\ Q_{21} & Q_{22} \end{pmatrix} = \int_0^T \begin{pmatrix} \Phi^H(t) & 0 \\ \Gamma^H(t) & I \end{pmatrix} \begin{pmatrix} Q_{c_1} & 0 \\ 0 & Q_{c_2} \end{pmatrix} \begin{pmatrix} \Phi(t) & \Gamma(t) \\ 0 & I \end{pmatrix} dt \quad (2.31)$$

This means that the CT cost function (2.26) is equivalent to a DT cost function given by (2.30). However the latter one has cross terms that weight the product of the state and

control input. It is possible to formulate the LQR solution so that it can account for the cross terms.

A very efficient method of computing integrals involving exponentials of matrices which can be used to compute the matrix in (2.31) [62] is given in Appendix A.

Using the results of Theorem 4 in the Appendix A the matrices in (2.31) can be obtained as follows:

$$\exp \begin{bmatrix} -A^H & 0 & Q_{c_1} & 0 \\ -B^H & 0 & 0 & Q_{c_2} \\ 0 & 0 & A & B \\ 0 & 0 & 0 & 0 \end{bmatrix} T \triangleq \begin{bmatrix} M_{11} & M_{12} \\ 0 & M_{22} \end{bmatrix} \quad (2.32)$$

$$\begin{bmatrix} Q_{11} & Q_{12} \\ Q_{21} & Q_{22} \end{bmatrix} = M_{22}^H M_{12} \quad (2.33)$$

2.2 Switching Control of a Family of Plants

If a plant is prone to unpredictable environmental influences or component failures, then it may be necessary to consider logic based mechanisms for detecting such events and providing counteractions. If the desired system trajectory is composed of several pieces of significantly different types (e.g. aircraft maneuvers), then one might need to employ different controllers at different stages. The need for logic based decision also arises when the state space of the process contains obstacles. Perhaps more interestingly, there exists systems that are smooth and defined on spaces with no obstacles (e.g. \mathbb{R}^n) yet do not admit continuous feedback laws for tasks as basic as asymptotical stabilization. In

other words, an obstruction to continuous stabilization may come from the mathematics of the system itself. A well known class of such systems is given by nonholonomic control systems [46]. Also optimal control of systems with sensor and/or actuator limitations involves switching control. More importantly, systems with large modelling uncertainty require switching techniques to be applied in order to achieve stability.

In [2] Miller and Davison assume that the actual plant belongs to a finite set of known LTI plants (family of plants). Hence, they consider the following strictly proper, controllable and observable LTI system \mathbf{P}_i , $i \in \bar{p} := \{1, 2, \dots, p\}$

$$\begin{aligned} \dot{x} &= A_i x + B_i u + E_i \omega \\ y &= C_i x + F_i \omega \\ e &= y_{ref} - y \end{aligned} \tag{2.34}$$

Then suitable high performance LTI controllers are designed for each of the possible plants, as described below:

$$\begin{aligned} \dot{z} &= G_i z + H_i y + J_i y_{ref} \\ u &= K_i z + L_i y + M_i y_{ref} \end{aligned} \tag{2.35}$$

It is assumed that each \mathbf{K}_i is designed such that it stabilizes the closed-loop system corresponding to \mathbf{P}_i , i.e. the closed-loop system matrix has all of its eigenvalues in the open left half of the complex plane, and it performs satisfactory disturbance rejection and/or tracking for \mathbf{P}_i , depending on the control objective. Using a switching mechanism or logic to switch between these controllers at appropriate points of time, the overall system ultimately locks onto the correct controller and becomes stable.

For this purpose, first it is assumed that a bound on the disturbance is known in advance. Then a bound is obtained for the initial condition as follows,

$$\|x(0)\|^2 \leq \alpha_{i_1} \int_0^T \|y(\tau)\|^2 d\tau + \alpha_{i_2} \sup \|\omega(t)\|^2 \quad (2.36)$$

where $\omega \in PC_\infty$ is disturbance. Assuming that W_i is the observability grammian of the i th plant, and

$$\begin{aligned} W_i &= \int_0^T e^{A_i^T \tau} C_i^T C_i e^{A_i \tau} d\tau \\ \alpha_{i_3} &\triangleq \min svds(W_i) \\ \alpha_{i_1} &\triangleq \frac{2}{\alpha_{i_3}} \\ \alpha_{i_2} &\triangleq \alpha_{i_2} \int_0^T \left[\int_0^t \|C_i e^{A_i(t-\tau)} E_i\| d\tau + \|F_i\| \right]^2 dt \end{aligned} \quad (2.37)$$

then for every $\tilde{u}, y_{ref}, \omega \in PC$ and every initial condition $\tilde{x}(0)$ a bound is obtained on the state of the augmented controllable and observable system, as follows:

$$\begin{aligned} \|\tilde{x}(t)\| &\leq \gamma_{i_1} \|\tilde{x}(0)\| e^{\lambda_i t} \\ &+ \int_0^t e^{\lambda_i(t-\tau)} [\gamma_{i_2} \|\tilde{u}(\tau) - \tilde{K}_i(\tilde{y}(\tau) - \tilde{D}_i y_{ref}(\tau))\| + \gamma_{i_3} \|\omega(\tau)\|] d\tau \end{aligned} \quad (2.38)$$

where

$$\tilde{K}_i = \begin{bmatrix} L_i & K_i & M_i \\ H_i & G_i & J_i \end{bmatrix} \quad (2.39)$$

and $\gamma_{i_1} > 0$ and $\lambda_i < 0$ can be found such that for $t \geq 0$ and \tilde{A}_i, \tilde{B}_i and \tilde{C}_i (the matrices of the augmented system), one can write, $\|e^{(\tilde{A}_i + \tilde{B}_i \tilde{K}_i \tilde{C}_i)t}\| \leq \gamma_{i_1} e^{\lambda_i t}$

Furthermore, define the following constants:

$$\begin{aligned} \gamma_{i_2} &\triangleq \gamma_{i_1} \|\tilde{B}_i\| \\ \gamma_{i_3} &\triangleq \gamma_{i_1} \|\tilde{E}_i + \tilde{B}_i \tilde{K}_i \tilde{F}_i\| \end{aligned} \quad (2.40)$$

Therefore one can use the knowledge of the upper bound on the disturbance along with the equation (2.36) to construct an upper bound on the initial condition, and then combine the result with equation (2.38) to construct a signal r_i which is an upper bound on the state of the augmented system if the plant is \mathbf{P}_i . At this point it is possible to compare $\tilde{y} - \tilde{D}_i y_{ref}$ with r_i to see if it is too large, implying that the real plant model is not \mathbf{P}_i . As soon as these two signals meet, then the switching control logic will switch gains, and use another controller. It is shown in [2] that the gain will eventually will remain at one of \mathbf{K}_i s and that the state of the overall system will remain bounded.

Chapter 3

Single-Layer Switching Control using Generalized Sampled-Data Hold Functions

Switching of a family of plant models $\{\mathbf{P}_i : i \in \bar{p} = \{1, 2, \dots, p\}\}$ using high performance LTI controllers was first introduced by Miller and Davison in [2], [47] and [45], where it is assumed that each plant-controller combination $(\mathbf{P}_i, \mathbf{K}_j)$ is stable iff $i = j$, $i, j \in \bar{p}$, and that a bound on the unmeasurable disturbance signal is given as *a priori* information. It was shown that the system would not switch to each controller more than once.

The advantages of the using generalized sampled-data hold functions (GSHF) instead of simple LTI controllers were discussed in Chapter 2.

In this chapter, GSHFs are employed in the switching mechanism instead of LTI controllers used in traditional switching control. The switching scheme used here is the discrete time version of the approach presented in [2]. It is assumed that a GSHF denoted

by \mathbf{f}_i , is designed for each plant model \mathbf{P}_i , in the family of plant models,

$$\Pi := \{\mathbf{P}_i : i \in \bar{p} = \{1, 2, \dots, p\}\} \quad (3.1)$$

and that the system switches between different GSHFs in proper time instants, until it finds the correct GSHF to control the system. It is also assumed that each plant-GSHF pair $(\mathbf{P}_i, \mathbf{f}_j)$ gives a stable equivalent discrete time model iff $i = j$ and that a bound on the disturbance signal is given.

One of the objectives of this work is to propose a switching controller which is computationally efficient in obtaining bounding functions or auxiliary signals compared to the existing methods [2],[50]. The required control computations are also much less than continuous-time switching control techniques. Moreover, the proposed switching control method utilizes the benefits of output control using GSHFs which can, in general, outperform traditional LTI controllers. On the other hand it is known that discrete-time controllers are very effective in decentralized systems. Thus, the proposed method can be applied in a decentralized manner to achieve better performance.

3.1 Problem Formulation

Consider a strictly proper, controllable and observable, LTI system $\mathbf{P}_i(t)$, in a given finite set of plant models Π defined in (3.1).

$$\forall t : \mathbf{P}_i(t) \in \Pi \quad (3.2)$$

The plant model is defined by the following state-space formulation:

$$\begin{cases} \dot{x}(t) = A_i x(t) + B_i u(t) + E_i \omega(t) \\ y(t) = C_i x(t) + F_i \omega(t) \end{cases} \quad (3.3a)$$

$$e = y_{ref} - y \quad (3.3b)$$

where $x(t) \in R^n, i \in \bar{p}$ is the state, $u(t) \in R^m$ is the control input, $y(t) \in R^r$ is the output, $\omega(t) \in R^v$ is the disturbance signal and $e(t) \in R^r$ is the error signal, which is the difference between the output and the reference signals. For simplicity and without loss of generality it will be assumed that $m = r$.

Figure 3.1 shows the closed-loop model of the system.

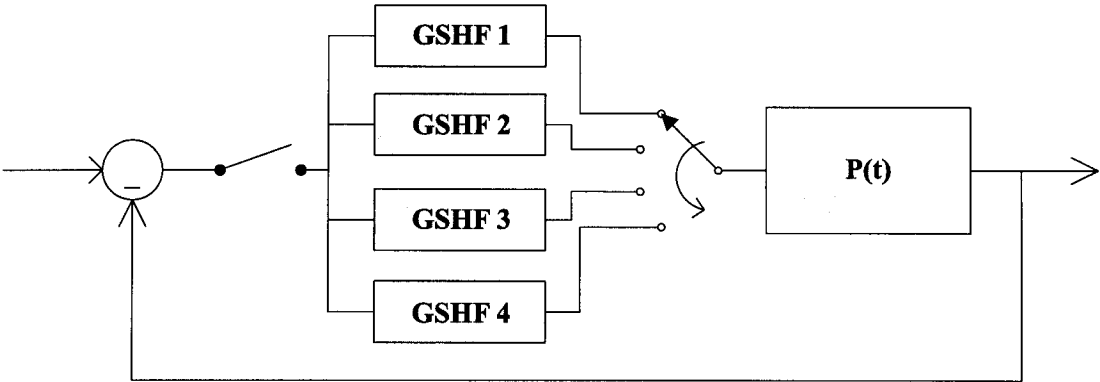


Figure 3.1: Closed-loop model with GSHF.

The control signal is constructed by multiplying the discrete samples of the input and the GSHF, i.e.

$$\begin{aligned}
u(t) &= \mathbf{f}_i(t) \cdot \tilde{u}[k] \\
\mathbf{f}_i(t+T) &= \mathbf{f}_i(t), \quad i = 1, \dots, p \quad t > 0
\end{aligned} \tag{3.4}$$

let the five-tuple $(A_i, B_i, C_i, E_i, F_i)$ represent the i^{th} plant model \mathbf{P}_i of the family Π and the five-tuple $(A_a, B_a, C_a, E_a, F_a)$ represent the actual system \mathbf{P}_a , the regulation of which is the control objective. Sampling the error signal will result in,

$$\tilde{u}[k] = e[k] = y_{ref}[k] - y[k] \tag{3.5}$$

The control signal will then be

$$\begin{aligned}
u(t) &= \mathbf{f}_i(t) \cdot [y_{ref}[k] - y[k]] \\
&= \mathbf{f}_i(t) \cdot [y_{ref}[k] - [\hat{C}_i x[k] + \hat{F}_i \omega[k]]] \\
&= \mathbf{f}_i(t) \cdot y_{ref}[k] - \mathbf{f}_i(t) \cdot \hat{C}_i x[k] - \mathbf{f}_i(t) \cdot \hat{F}_i \omega[k]
\end{aligned} \tag{3.6}$$

The corresponding sampled-data system for (3.3) is given by the following equation,

$$\begin{aligned}
x[(k+1)T] &= e^{A_i T} x[kT] + \int_{kT}^{(k+1)T} e^{A_i((k+1)T-t)} B_i u(t) dt \\
&\quad + \int_{kT}^{(k+1)T} e^{A_i((k+1)T-t)} E_i \omega(t) dt
\end{aligned} \tag{3.7}$$

Define

$$\begin{aligned}\hat{A}_i &:= e^{A_i T} \\ \hat{B}_i &:= \int_0^T e^{A_i(T-t)} B_i \mathbf{f}_i(t) dt \\ \hat{E}_i &:= \int_0^T e^{A_i(T-t)} E_i dt \\ \hat{C}_i &:= C_i \\ \hat{F}_i &:= F_i\end{aligned}$$

Assuming that the closed-loop system is stable and correct GSHF is being used, substituting $u(t)$ from (3.6) into (3.7) will result in,

$$\begin{aligned}x[k+1] &= e^{A_i T} x[k] + \int_{kT}^{(k+1)T} e^{A_i((k+1)T-t)} B_i \\ &\quad \cdot [\mathbf{f}_i(t) \cdot y_{ref}[k] - \mathbf{f}_i(t) \cdot \hat{C}_i x[k] - \mathbf{f}_i(t) \cdot \hat{F}_i \omega[k]] dt \\ &\quad + \int_{kT}^{(k+1)T} e^{A_i((k+1)T-t)} E_i \omega(t) dt\end{aligned}$$

Hence, the discrete-time equivalent model for the resultant closed-loop system will be given by,

$$\begin{aligned}x[k+1] &= \hat{A}_i x[k] + \hat{B}_i y_{ref}[k] - \hat{B}_i \hat{C}_i x[k] - \hat{B}_i \hat{F}_i \omega[k] + \hat{E}_i \omega[k] \\ &= (\hat{A}_i - \hat{B}_i \hat{C}_i) x[k] + \hat{B}_i (y_{ref}[k] - \hat{F}_i \omega[k]) + \hat{E}_i \omega[k]\end{aligned}\tag{3.8a}$$

$$y[k] = \hat{C}_i x[k] + \hat{F}_i \omega[k]\tag{3.8b}$$

Having $x[k+1] = \phi x[k] - \psi[k]$ we can write,

$$\begin{aligned}
x[k+1] &= \phi x[k] - \psi[k] \\
x[k+2] &= \phi^2 x[k] - \phi \psi[k] - \psi[k+1] \\
x[k+3] &= \phi^3 x[k] - \phi^2 \psi[k] - \phi \psi[k+1] - \psi[k+2] \\
x[j] &= \phi^{j-m} x[m] - \sum_{i=m}^{j-1} \phi^{j-i-1} \psi[i]; \quad j > m \\
x[k] &= \phi^k x[0] - \sum_{i=0}^{k-1} \phi^{k-i-1} \psi[i]
\end{aligned} \tag{3.9}$$

So the state of the closed-loop system at each sampling instant can be related to the initial state and input signals through the following equation,

$$\begin{aligned}
x[k] &= (\hat{A}_i - \hat{B}_i \hat{C}_i)^k x[0] \\
&+ \sum_{v=0}^{k-1} \left[(\hat{A}_i - \hat{B}_i \hat{C}_i)^{k-v-1} [\hat{B}_i (y_{ref}[v] - \hat{F}_i \omega[v]) + \hat{E}_i \omega[v]] \right]
\end{aligned} \tag{3.10}$$

Since it is assumed that the unmeasurable disturbance signal is bounded, one can write:

$$\bar{\omega} := \max_t \|\omega(t)\|$$

where $\bar{\omega}$ represents an upper bound on the norm of the disturbance $\omega(t)$ and will later be used to derive inequalities corresponding to the upper bound on the state of the system.

A switching control method will be developed in the next section using periodic feedback control and the switching scheme of [17].

3.2 Main Results

We need to prove the following inequality which will be used later in the proof of *Lemma 1*.

Preliminary: Assume that $y[k] = y_1[k] + y_2[k]$ hence we can write

$$\begin{aligned}\|y_2[k]\| + \|y[k]\| &\geq \|y_2[k] - y[k]\| = \|y_1[k]\| \\ \|y_1[k]\|^2 &\leq \|y[k]\|^2 + \|y_2[k]\|^2 + 2\|y[k]\| \cdot \|y_2[k]\|\end{aligned}$$

we also know that $(\|y_2[k]\| - \|y[k]\|)^2 \geq 0$, By adding this later inequality to the former we can obtain,

$$\|y_1[k]\|^2 \leq 2\|y[k]\|^2 + 2\|y_2[k]\|^2 \quad (3.11)$$

This will later be used in the proofs.

To make sure that the switching mechanism acts properly, we will have to find a bound on the initial condition of the system. Same as the algorithm in [2] our method will be performed in two phases: before applying the control signal and after that. The following lemma gives a bound on the norm of the initial state of the system with the assumption that the disturbance is bounded and the control input is set to zero.

Lemma 1: Consider the system (3.8) and assume that the control input $u(t)$ in (3.3) is equal to zero for $0 \leq t \leq mT$, for any arbitrary integer $m > 0$. There exists constants $\alpha_{1,i}$ and $\alpha_{2,i}$, such that for any initial condition $x[0]$ and disturbance ω , the following inequality on the norm of the initial state holds:

$$\|x[0]\|^2 \leq \alpha_{1,i} \sum_{k=0}^m \|y[k]\|^2 + \alpha_{2,i} \bar{\omega}^2 \quad (3.12)$$

Proof of Lemma 1: The samples of the output obtained from the discrete equivalent system the output is given by:

$$y[k] = \hat{C}_i x[k] + \hat{F}_i \omega[k] \quad (3.13)$$

Since the control input is set to zero for $0 \leq t \leq mT$, it can be concluded from (3.10) that

$$x[k] = \hat{A}_i^k x[0] + \sum_{v=0}^{k-1} [\hat{A}_i^{k-v-1} \hat{E}_i \omega[v]] \quad (3.14)$$

Substituting (3.14) in (3.13) will result in:

$$\begin{aligned} y[k] &= \hat{C}_i [\hat{A}_i^k x[0] + \sum_{v=0}^{k-1} \hat{A}_i^{k-v-1} \hat{E}_i \omega[v]] + \hat{F}_i \omega[k] \\ &= \hat{C}_i \hat{A}_i^k x[0] + \hat{C}_i \sum_{v=0}^{k-1} \hat{A}_i^{k-v-1} \hat{E}_i \omega[v] + \hat{F}_i \omega[k] \end{aligned} \quad (3.15)$$

Define

$$y_1[k] := \hat{C}_i \hat{A}_i^k x[0] \quad (3.16a)$$

$$y_2[k] := \hat{C}_i \sum_{i=0}^{k-1} \hat{A}_i^{k-i-1} \hat{E}_i \omega[i] + \hat{F}_i \omega[k] \quad (3.16b)$$

Taking norm of the terms in both sides of (3.16b) results in:

$$\begin{aligned} \|y_2[k]\| &\leq \|\omega[k]\| \cdot \left(\sum_{v=0}^{k-1} \|\hat{C}_i \hat{A}_i^{k-v-1} \hat{E}_i\| + \|\hat{F}_i\| \right) \\ &\leq \bar{\omega} \cdot \left(\sum_{v=0}^{k-1} \|\hat{C}_i \hat{A}_i^{k-v-1} \hat{E}_i\| + \|\hat{F}_i\| \right) \end{aligned} \quad (3.17)$$

Define now:

$$W_i := \sum_{k=0}^m (\hat{A}_i^k)^k \hat{C}_i' \hat{C}_i \hat{A}_i^k$$

then

$$\sum_{k=0}^m \|y_1[k]\|^2 = x[0]' W_i x[0]$$

Now let

$$\alpha_{3,i} := \text{smallest singular value of } W_i \quad (3.18)$$

It can be concluded from (3.16a) that:

$$\begin{aligned} \sum_{k=0}^m \|y_1[k]\|^2 - \alpha_{3,i} \|x[0]\|^2 &= x[0]' [W_i - \alpha_{3,i} I] x[0] \geq 0 \\ \sum_{k=0}^m \|y_1[k]\|^2 &\geq \alpha_{3,i} \|x[0]\|^2 \end{aligned} \quad (3.19)$$

On the other hand, it follows from the preliminary results in (3.11), that

$$\sum_{k=0}^m \|y_1[k]\|^2 \leq 2 \sum_{k=0}^m \|y[k]\|^2 + 2 \sum_{k=0}^m \|y_2[k]\|^2 \quad (3.20)$$

Substituting $y_1[k]$ from (3.19) in (3.20) and dividing both sides by $\alpha_{3,i}$ will result in:

$$\|x[0]\|^2 \leq \frac{2}{\alpha_{3,i}} \sum_{k=0}^m \|y[k]\|^2 + \frac{2}{\alpha_{3,i}} \sum_{k=0}^m \|y_2[k]\|^2 \quad (3.21)$$

Now define $\alpha_{1,i}$ and $\alpha_{2,i}$ as follows

$$\begin{aligned} \alpha_{1,i} &:= \frac{2}{\alpha_{3,i}} \\ \alpha_{2,i} &:= \frac{2}{\alpha_{3,i}} \sum_{k=0}^m \left[\sum_{v=0}^{k-1} \|\hat{C}_i \hat{A}_i^{k-v-1} \hat{E}_i\| + \|\hat{F}_i\| \right]^2 \end{aligned}$$

Then using (3.17), one can obtain the following inequality,

$$\|x[0]\|^2 \leq \alpha_{1,i} \sum_0^m \|y[k]\|^2 + \alpha_{2,i} \bar{\omega}^2$$

■

Lemma 1 states that if a bound $\bar{\omega}$ on the norm of disturbance ω exists, then one can find a bound on the norm of the initial condition as long as the control input is zero.

It is desired now to obtain an upper bound on the state of the system at each sampling instant, and at the presence of the control signal. This bound will be used in the decision maker unit to verify weather the current GSHF is correct or it needs to be changed. Since the closed-loop system is not necessarily stable hence the equation obtained in (3.10) cannot be used for $x[k]$, therefore we need to find $x[k]$ related to the initial state and the input signal, even if the correct GSHF is not being applied to the system, Having (3.7) and (3.4) we can write,

$$\begin{aligned} x[k+1] &= e^{A_i T} x[k] \\ &+ \int_{kT}^{(k+1)T} e^{A_i((k+1)T-t)} B_i \cdot [\mathbf{f}_j(t) \cdot \tilde{u}[k]] dt \\ &+ \int_{kT}^{(k+1)T} e^{A_i((k+1)T-t)} E_i \omega(t) dt \end{aligned}$$

To find the bound on the state even if the GSHF used in the system is not the correct one (This happens while the system switches to different GSHFs to find the correct one, Define $\hat{B}_{i,j}$ as the discrete-time equivalent matrix for B_i , when the GSHF \mathbf{f}_j corresponding to the plant \mathbf{P}_j is used in the closed-loop system. $\hat{B}_{i,j}$ can be obtained as follows:

$$\hat{B}_{i,j} := \int_0^T e^{A_i(T-t)} B_i \mathbf{f}_j(t) dt$$

Apparently, when $i = j$ we have $\hat{B}_{i,j} = \hat{B}_i$ hence,

$$\begin{aligned} x[k+1] &= \hat{A}_i x[k] + \hat{B}_{i,j} \tilde{u}[k] + \hat{E}_i \omega[k] \\ &= (\hat{A}_i - \hat{B}_i \hat{C}_i) x[k] + \hat{B}_i \hat{C}_i x[k] + \hat{B}_{i,j} \tilde{u}[k] + \hat{E}_i \omega[k] \\ &= (\hat{A}_i - \hat{B}_i \hat{C}_i) x[k] + \hat{B}_i [y[k] - \hat{F}_i \omega[k]] + \hat{B}_{i,j} \tilde{u}[k] + \hat{E}_i \omega[k] \end{aligned}$$

according to (3.9) we can now write:

$$\begin{aligned}
x[k] &= (\hat{A}_i - \hat{B}_i \hat{C}_i)^k x[0] \\
&+ \sum_{v=0}^{k-1} \left[(\hat{A}_i - \hat{B}_i \hat{C}_i)^{k-v-1} [\hat{B}_i y[v] + \hat{B}_{i,j} \tilde{u}[v] + (\hat{E}_i - \hat{B}_i \hat{F}_i) \omega[v]] \right]
\end{aligned} \tag{3.22}$$

The following lemma gives an upper bound on the state of the system in terms of the system parameters and norms of the disturbance ω and reference signal y_{ref} denoted by $\bar{\omega}$ and \bar{y}_{ref} respectively.

Lemma 2: There exists constants $\gamma_{1,i}$, $\gamma_{2,i}$ and λ_i such that for the control signal $u(t)$ and bounded disturbance ω and initial state $x[0]$ the following inequality holds:

$$\begin{aligned}
\|x[k]\| &\leq \lambda_i \gamma_{1,i}^k \|x[0]\| \\
&+ \sum_{v=0}^{k-1} \left[\lambda_i \gamma_{1,i}^{k-v-1} [\|\hat{B}_i y[v]\| + \|\hat{B}_{i,j} \tilde{u}[v]\| + \gamma_{2,i}] \right]
\end{aligned} \tag{3.23}$$

Proof of Lemma 2: It follows from (3.22) that:

$$\begin{aligned}
\|x[k]\| &\leq \|(\hat{A}_i - \hat{B}_i \hat{C}_i)^k\| \|x[0]\| + \sum_{v=0}^{k-1} \left[\|(\hat{A}_i - \hat{B}_i \hat{C}_i)^{k-v-1}\| \right. \\
&\left. \cdot [\|\hat{B}_i y[v]\| + \|\hat{B}_{i,j} \tilde{u}[v]\| + \bar{\omega} \|\hat{E}_i - \hat{B}_i \hat{F}_i\|] \right]
\end{aligned} \tag{3.24}$$

A proper λ_i can be found such that

$$\|(\hat{A}_i - \hat{B}_i \hat{C}_i)^k\| \leq \lambda_i \cdot \max |eig(\hat{A}_i - \hat{B}_i \hat{C}_i)|^k$$

by choosing $\gamma_{1,i} = \max |eig(\hat{A}_i - \hat{B}_i \hat{C}_i)|$ and $\gamma_{2,i} = \bar{\omega} \|\hat{E}_i - \hat{B}_i \hat{F}_i\|$ we can prove the lemma, and hence find a norm on the state of the system.

■

Having $\gamma_{3,i} = \bar{\omega} \|\hat{C}_i(\hat{E}_i - \hat{B}_i\hat{F}_i)\|$ a bound on the norm of the output can now be found by using (3.13) as follows:

$$\begin{aligned} \|y[k]\| \leq & \|\hat{C}_i\| \lambda_i \gamma_{1,i}^k \|x[0]\| + \sum_{v=0}^{k-1} \left[\lambda_i \gamma_{1,i}^{k-v-1} \right. \\ & \left. \cdot [\|\hat{C}_i\hat{B}_{i,y}[v] + \hat{C}_i\hat{B}_{i,j}\tilde{u}[v]\| + \gamma_{3,i}] \right] + \bar{\omega} \|\hat{F}_i\| \end{aligned} \quad (3.25)$$

Assuming that the disturbance is bounded, By substituting the bound on the initial condition given by *Lemma 1* into (3.25), one can find an auxiliary signal which gives a bound on the state of the system at any point of time. let r_i denote the auxiliary signal which is a bound on the norm of the output of the closed-loop system corresponding to the plant model \mathbf{P}_i . In other words r_i is a bound on the output of the plant \mathbf{P}_i , regardless of which GSHF is used to control the system. This auxiliary signal is given by:

$$\begin{aligned} r_i[k] = & \|\hat{C}_i\| \lambda_i \gamma_{1,i}^k \|x[0]\| \\ & + \sum_{v=0}^{k-1} \left[\lambda_i \gamma_{1,i}^{k-v-1} \cdot [\|\hat{C}_i(\hat{B}_{i,y}[v] + \hat{B}_{i,j}\tilde{u}[v])\| + \gamma_{3,i}] \right] + \bar{\omega} \|\hat{F}_i\| \\ r_i[k+1] = & \|\hat{C}_i\| \lambda_i \gamma_{1,i}^{k+1} \|x[0]\| \\ & + \sum_{v=0}^k \left[\lambda_i \gamma_{1,i}^{k-v} \cdot [\|\hat{C}_i(\hat{B}_{i,y}[v] + \hat{B}_{i,j}\tilde{u}[v])\| + \gamma_{3,i}] \right] + \bar{\omega} \|\hat{F}_i\| \end{aligned} \quad (3.26)$$

In order to come up with a difference equation to update the auxiliary signals at each step one can write,

$$\begin{aligned} r_i[k+1] = & \gamma_{1,i} r_i[k] + \lambda_i [\|\hat{C}_i(\hat{B}_{i,y}[k] + \hat{B}_{i,j}\tilde{u}[k])\| + \gamma_{3,i}] \\ & + (1 - \gamma_{1,i}) \bar{\omega} \|\hat{F}_i\| \end{aligned} \quad (3.27)$$

Note that,

$$r_i[0] = \|\hat{C}_i\| \cdot \lambda_i \|x[0]\| + \bar{\omega} \|\hat{F}_i\|$$

Using the results of the *Lemma 1* and substituting the upper bound on the initial state into the above equation, for $0 \leq t \leq mT$, and for any arbitrary integer $m > 0$ with no input, results in:

$$r_i[t] \leq \lambda_i \|\hat{C}_i\| \cdot [\alpha_{1,i} \sum_{k=0}^m \|y[k]\|^2 + \alpha_{2,i} \bar{\omega}^2]^{\frac{1}{2}} + \bar{\omega} \|\hat{F}_i\|$$

Choosing proper constants to satisfy the inequalities in *Lemma 1* and *Lemma 2*, one can break the control process into two phases, as follows,

Phase 1: Setting the control signal to zero for $0 \leq t \leq mT$ where m is any non-zero integer and T is the sampling period results in the following upper bound on the norm of the output of the system.

$$r_i[k] = \lambda_i \|\hat{C}_i\| \cdot [\alpha_{1,i} \sum_{v=0}^m \|y[v]\|^2 + \alpha_{2,i} \bar{\omega}^2]^{\frac{1}{2}} + \bar{\omega} \|\hat{F}_i\|$$

Phase 2: The equation (3.27) can now be used to update the new values of the auxiliary signals for $k > m$. It is to be noted that the norm of the output is compared with the corresponding upper bound only at the sampling instants (the discrete model will be used in the decision making unit of the switching control.)

It is now desired to find the switching instants using the auxiliary signals obtained above.

Switching Controller 1: Set $t_1 = mT$, and for every $i \in \{2, \dots, p+1\}$ for which $t_{i-1} \neq \infty$, define:

$$t_i := \min\{t \geq t_{i-1}, \exists \tilde{k} \in [mT, t] \mid \|y[\tilde{k}]\| \geq r_i[\tilde{k}]\}$$

Theorem 1 Suppose that the reference input and the disturbance signals are piecewise constant and bounded, i.e. $\|\omega(t)\| \leq \bar{\omega}$ and $y_{ref}(t) \leq \bar{y}_{ref}$ for $t \geq 0$. For every initial condition $x(0)$, when the *Switching Controller 1* is applied to the uncertain plant, where model belongs to the known family of plant models Π the closed-loop system has the following properties:

- a) the GSHF will ultimately remain unchanged at an element of $\{\mathbf{f}_j; j \in \bar{p}\}$ and;
- b) the state of the system will be bounded.

Proof: It was shown in (3.25) that $\|y[k]\| \leq r_i[k]$ for $k \geq mT$. Thus, it can be concluded from *Switching Controller 1*, that t_{i+1} must be ∞ . Hence part (a) holds. On the other hand, boundedness of the state of the system follows immediately from *Lemma 2*. ■

3.3 Simulation Results

Consider the two cart mass-spring-damper system of Figure 3.2 as shown in [63]. The control force is applied to the mass m_1 , and the output of the system is the position of the second cart (m_2). The state-space model is represented by the following matrices:

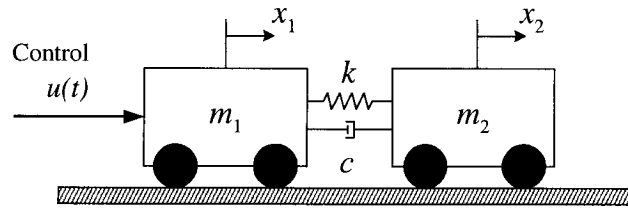


Figure 3.2: The two-cart SISO system connected with spring and damper.

$$A = \begin{bmatrix} 0 & 0 & 1 & 0 \\ 0 & 0 & 0 & 1 \\ \frac{-k}{m_1} & \frac{k}{m_1} & \frac{-c}{m_1} & \frac{c}{m_1} \\ \frac{k}{m_2} & \frac{-k}{m_2} & \frac{c}{m_2} & \frac{-c}{m_2} \end{bmatrix}$$

$$B^T = \begin{bmatrix} 0 & 0 & \frac{1}{m_1} & 0 \end{bmatrix}$$

$$C = \begin{bmatrix} 0 & 1 & 0 & 0 \end{bmatrix}$$

where k and c are the spring constant and the damping coefficient, respectively. It is assumed that the disturbance signal $\omega(t)$ is equal to zero, and that the reference input is

the unit step signal. Consider a family of four plant models given by:

$$\mathbf{P}_1 : m_1 = 6.2032, \quad m_2 = 5.0660,$$

$$k = 1.0011, \quad c = 0.0104$$

$$\mathbf{P}_2 : m_1 = 7.8113, \quad m_2 = 9.5371,$$

$$k = 1.1226, \quad c = 0.2168$$

$$\mathbf{P}_3 : m_1 = 5.9745, \quad m_2 = 8.9869,$$

$$k = 0.8837, \quad c = 0.1359$$

$$\mathbf{P}_4 : m_1 = 2.1017, \quad m_2 = 1.2885,$$

$$k = 0.5548, \quad c = 0.0561$$

A GSHF is designed for each plant model using the method proposed in [52].

Assume now that the actual plant model was initially \mathbf{P}_4 and at some point of time it suddenly changes to \mathbf{P}_2 . Using the proposed switching mechanism given by *Switching Controller 1* the system will first switch from \mathbf{f}_4 to \mathbf{f}_1 and then to \mathbf{f}_2 . The system locks onto \mathbf{f}_2 as it is the only GSHF that stabilizes \mathbf{P}_2 , which is the new plant model. The switching instants are shown in Figure 3.3. The output of the system is given in Figure 3.4. This figure shows good regulation for the given system parameters.

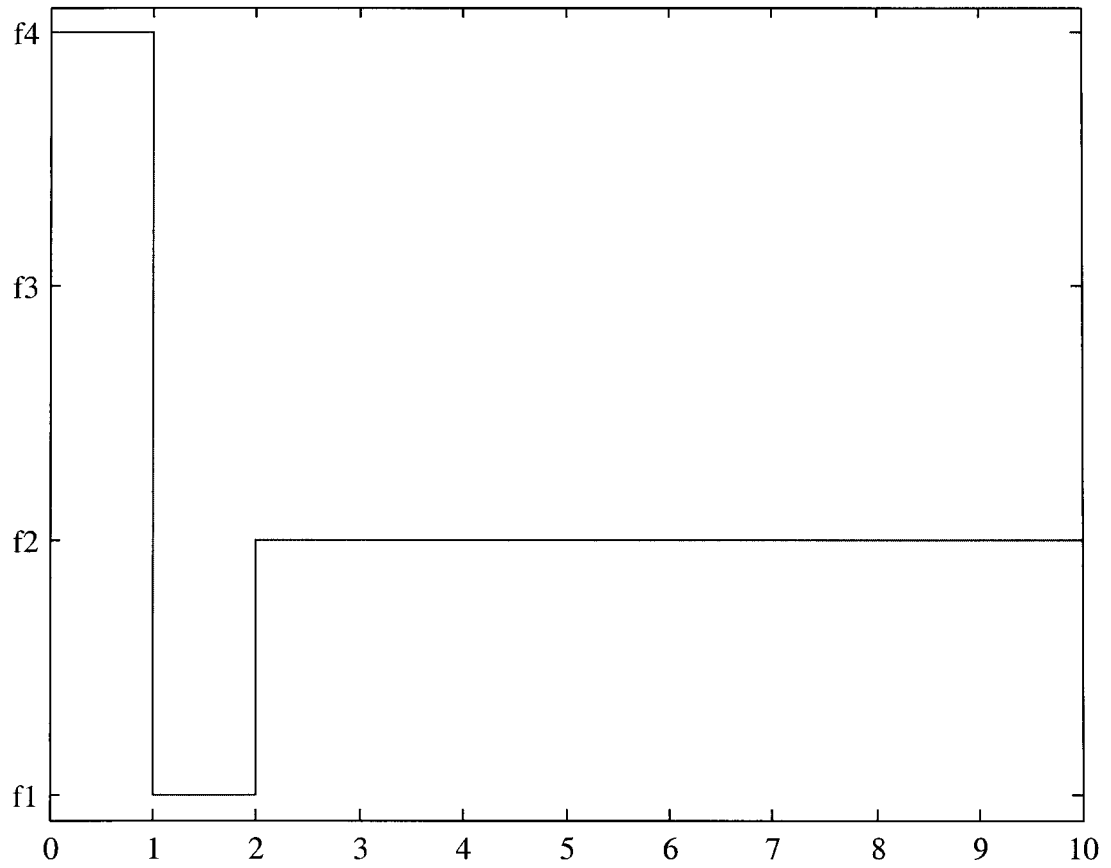


Figure 3.3: Switching instants, when the plant model changes from \mathbf{P}_4 to \mathbf{P}_2 .

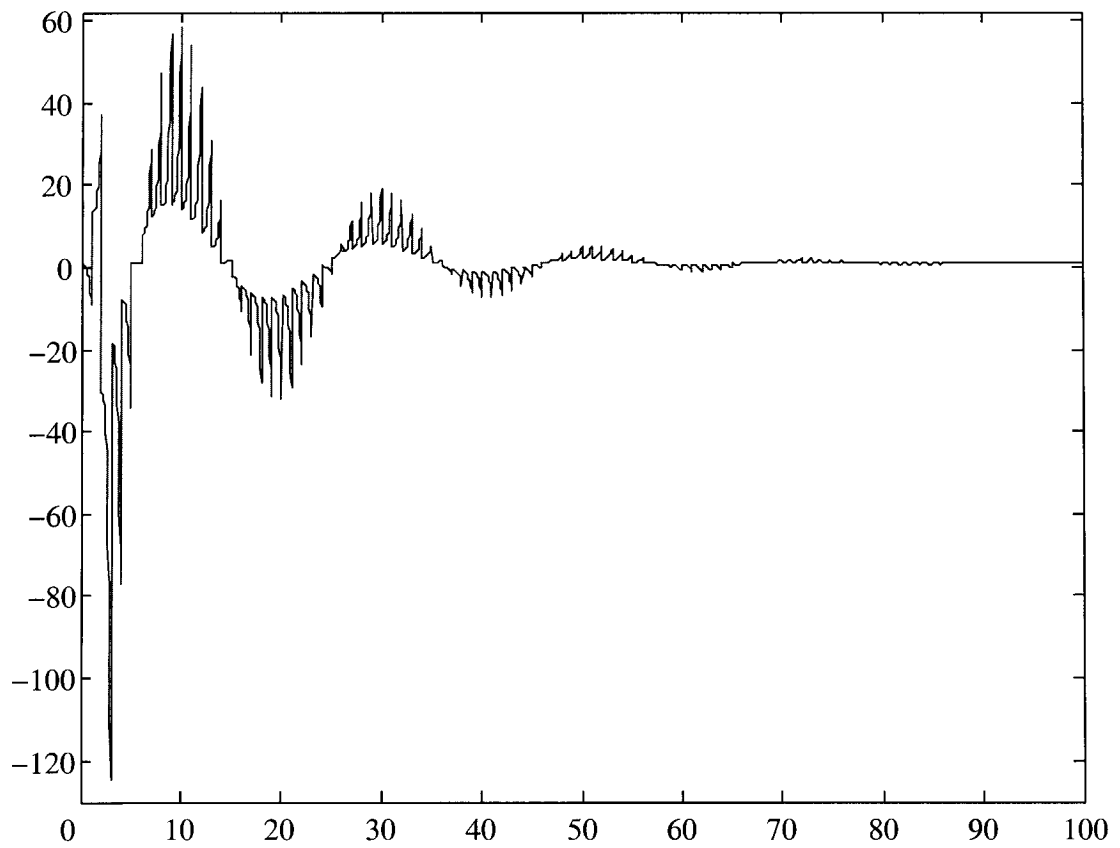


Figure 3.4: Output signal of the closed-loop simulation results, when the plant model changes from \mathbf{P}_4 to \mathbf{P}_2 .

Chapter 4

Multi-Layer Switching Control using Generalized Sampled-Data Hold Functions

It was shown in Chapter 3 that by using a proper switching logic in a single-layer switching mechanism using GSHFs which monitors the norm of error in the output, the system eventually locks onto a stabilizing GSHF after a number of switchings and would not switch to each GSHF more than once. Several methods have been proposed to reduce the magnitude of the transient response [48], [49]. One of the main reasons for undesirable transient response in switching control systems is that in the transition from the initial controller to the final one, the system may switch to several destabilizing controllers. Although using GSHFs has resulted in reduction of the maximum overshoot and the complexity of computations compared to the case with CT controllers, since the system may switch to many destabilizing GSHFs before it finds the correct GSHF, the output can still

have a bad transient response.

A method was proposed in [50] to improve the transient response of the switching control system by reducing the number of switchings to destabilizing controllers via introducing different layers of controllers with different properties. The method relies on $p - 2$ layers of controllers with different properties, where p denotes the number of models in the family of plants. Layer #1 consists of a set of p high-performance controllers, where each one solves the robust servomechanism problem for one of the models in the family. Layer # $\rho \in \{2, \dots, p - 2\}$ consists of a set of controllers which have the property that each one stabilizes ρ plant models in the family and destabilizes the remaining $p - \rho$ models. However, to obtain controllers for layers $2, \dots, p - 2$ one should use simultaneous stabilizer design techniques, which can be a difficult task in general. Furthermore, the amount of on-line computations required to find the upper-bound signals which are to be compared with the norm of the error in the decision making unit will grow rapidly by introducing new layers of controllers. One can overcome these difficulties to some extent by using discrete-time controllers with generalized hold functions instead of continuous-time LTI controllers.

In this chapter, GSHFs are employed in a multi-layer switching structure instead of LTI controllers. The switching scheme used here is the discrete time version of the approach presented in [50]. It is assumed that layer $k \in \{2, \dots, p - 2\}$ consists of a set of GSHFs which have the property that each one stabilizes k plants in the family while destabilizing the remaining $p - k$ plants. The first layer consists of a set of p GSHFs, where each one stabilizes a plant \mathbf{P}_i in the family of plant models,

$$\Pi := \{\mathbf{P}_i : i \in \bar{p} = \{1, 2, \dots, p\}\} \quad (4.1)$$

iff $i = j$. The system switches between different GSHFs in proper time instants, until it finds the correct GSHF to control the system.

Notation: Throughout this chapter, a sample of a continuous-time signal $z(t)$ at $t = KT$ will be denoted by $z[k]$. Also the norm of $x \in \mathbb{R}^n$ which is denoted by $\|x\|$ is the Holder 2-norm; with $A \in \mathbb{R}^{n \times m}$, $\|A\|$ denotes the corresponding induced norm of A . $2^{\bar{p}}$ is the powerset of \bar{p} (The set of all subsets of \bar{p}).

This chapter is organized as follows. The problem formulation is given in section 4.1. A multi-layer switching system is proposed in section 4.2 and in section 4.3 the method is compared to a single-layer counterpart.

4.1 Problem Formulation

Consider a strictly proper, controllable and observable LTI system $\mathbf{P}_i(t)$ in a given finite set of plant models Π defined in (4.1).

$$\forall t : \mathbf{P}_i(t) \in \Pi \quad (4.2)$$

The plant model $\mathbf{P}_i(t)$ has the following state-space representation:

$$\begin{cases} \dot{x}(t) = A_i x(t) + B_i u(t) + E_i \omega(t) \\ y(t) = C_i x(t) + F_i \omega(t) \end{cases} \quad (4.3a)$$

$$e = y_{ref} - y \quad (4.3b)$$

where $x(t) \in R^{n_i}, i \in \bar{p}$ is the state, $u(t) \in R^q$ is the control input, $y(t) \in R^r$ is the output, $\omega(t) \in R^v$ is the disturbance signal, $y_{ref}(t) \in R^r$ is the reference input and $e(t) \in R^r$ is the error signal. For simplicity and without loss of generality, it will be assumed that $q = r$. Also y_{ref} and ω are bounded piecewise continuous time functions.

Let Φ_1 represent the set of GSHFs in the first layer of our proposed multi-layer architecture, i.e. for each $i \in \bar{p}$, there exists a GSHF $\mathbf{f}_i \in \Phi_1, i \in \bar{p}$. Thus:

$$\Phi_1 = \{\mathbf{f}_i : i \in \bar{p}\}, \quad N(\Phi_1) = p \quad (4.4)$$

Which solves robust servomechanism problem for the plant model $\mathbf{P}_i, i \in \bar{p}$. On the other hand, the set of GSHFs of layer $\# \rho, \rho = 2, \dots, p$ is denoted by Φ_ρ as follows

$$\Phi_\rho = \{\mathbf{f}_{i_1 i_2 \dots i_\rho} | i_1, i_2, \dots, i_\rho \in \bar{p}\} \quad (4.5)$$

where $i_j, j = 1, \dots, \rho$ are distinct integers and the indices of each GSHF represent the plants that can be stabilized by that GSHF, e.g. $\mathbf{f}_{i_1 i_2 \dots i_\rho}$ “only” stabilizes plant models $\mathbf{P}_{i_1}, \mathbf{P}_{i_2}, \dots, \mathbf{P}_{i_\rho}$, and destabilizes the other plants in the set Π .

According to the above definition, in each layer $\# \rho \in \bar{p}$, there exist $N(\Phi_\rho) \times \rho$ combinations of stable closed-loop configurations. The total number of all stable configurations corresponding to all layers is given by

$$\phi = \sum_{\rho=1}^{p-2} N(\Phi_\rho) \times \rho$$

Figure 4.1 shows the closed-loop model of the system. The control signal is constructed by multiplying the discrete samples of the input and the GSHF, i.e.

$$\begin{aligned} u(t) &= \mathbf{f}_{i_1 i_2 \dots i_\rho}(t) \cdot \tilde{u}[k], \quad kT \leq t < (K+1)T, \quad k \in \mathbb{Z} \\ \mathbf{f}_{i_1 i_2 \dots i_\rho}(t+T) &= \mathbf{f}_{i_1 i_2 \dots i_\rho}(t), \quad \{i_1, i_2, \dots, i_\rho\} \subseteq \bar{p}, \quad t > 0 \end{aligned} \quad (4.6)$$

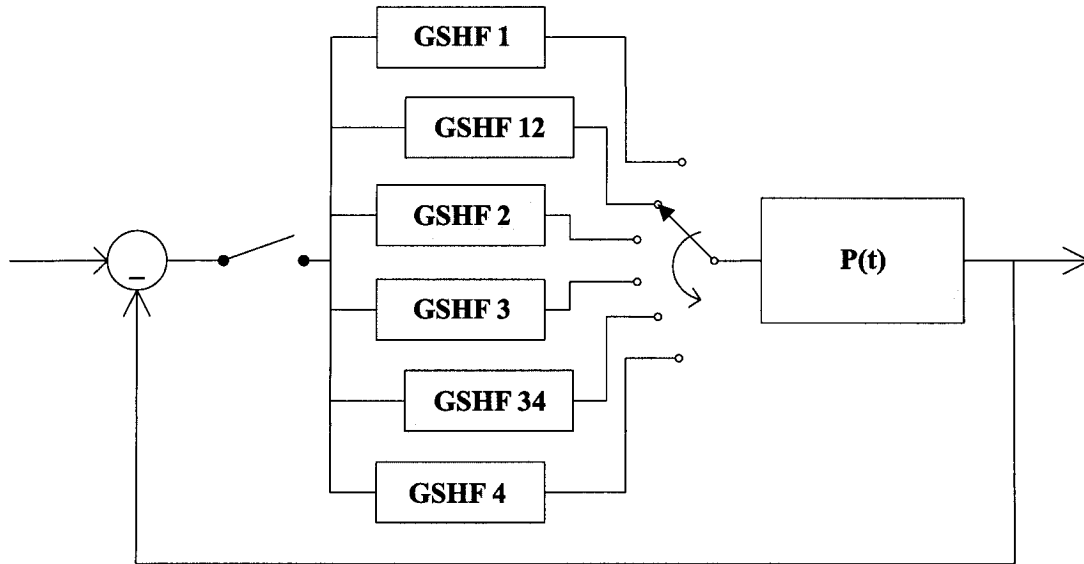


Figure 4.1: Switching control system with GSHFs.

which results in a stable closed-loop system corresponding to the controllable and observable plant $\mathbf{P}_i, i \in \{i_1, i_2, \dots, i_p\}$. Let the five-tuple $(A_i, B_i, C_i, E_i, F_i)$ represent the i^{th} plant model \mathbf{P}_i of the family Π and the five-tuple $(A_a, B_a, C_a, E_a, F_a)$ represent the actual system \mathbf{P}_a , the regulation of which is the control objective. Sampling the error signal will result in:

$$\tilde{u}[k] = e[k] = y_{ref}[k] - y[k] \quad (4.7)$$

Set $\tilde{u}[k]$ in (4.6) equal to $e[k]$ to obtain a feedback control system. The control signal will then be

$$\begin{aligned}
u(t) &= \mathbf{f}_{i_1 i_2 \dots i_\rho}(t) \cdot (y_{ref}[k] - y[k]) \\
&= \mathbf{f}_{i_1 i_2 \dots i_\rho}(t) \cdot (y_{ref}[k] - \hat{C}_i x[k] - \hat{F}_i \omega[k]) \\
&= \mathbf{f}_{i_1 i_2 \dots i_\rho}(t) \cdot y_{ref}[k] - \mathbf{f}_{i_1 i_2 \dots i_\rho}(t) \cdot \hat{C}_i x[k] - \mathbf{f}_{i_1 i_2 \dots i_\rho}(t) \cdot \hat{F}_i \omega[k]
\end{aligned} \tag{4.8}$$

$k \in \mathbb{Z}$

The state of the corresponding sampled-data system for (4.3) is given by the following equation:

$$\begin{aligned}
x[(k+1)T] &= e^{A_i T} x[kT] + \int_{kT}^{(k+1)T} e^{A_i((k+1)T-t)} B_i u(t) dt \\
&\quad + \int_{kT}^{(k+1)T} e^{A_i((k+1)T-t)} E_i \omega(t) dt
\end{aligned} \tag{4.9}$$

Now for any $i \in \{i_1, i_2, \dots, i_\rho\}$ and $\sigma = i_1 i_2 \dots i_\rho$, where $i_1, i_2, \dots, i_\rho \in \bar{p}$ are ρ distinct integers, define:

$$\begin{aligned}
\hat{A}_i &:= e^{A_i T} \\
\hat{B}_{i,\sigma} &:= \int_0^T e^{A_i(T-t)} B_i \mathbf{f}_{i_1 i_2 \dots i_\rho}(t) dt, \quad \sigma = i_1 i_2 \dots i_\rho \\
\hat{E}_i &:= \int_0^T e^{A_i(T-t)} E_i dt \\
\hat{C}_i &:= C_i \\
\hat{F}_i &:= F_i
\end{aligned}$$

Note that since i is assumed to belong to $\{i_1, i_2, \dots, i_\rho\}$, the above matrices represent a stable closed-loop system. Substituting $u(t)$ from (4.8) into (4.9) will result in:

$$\begin{aligned}
x[k+1] &= e^{A_i T} x[k] + \int_{kT}^{(k+1)T} e^{A_i((k+1)T-t)} B_i \\
&\cdot [\mathbf{f}_{i_1 i_2 \dots i_p}(t) \cdot y_{ref}[k] - \mathbf{f}_{i_1 i_2 \dots i_p}(t) \cdot \hat{C}_i x[k] - \mathbf{f}_{i_1 i_2 \dots i_p}(t) \cdot \hat{F}_i \omega[k]] dt \\
&+ \int_{kT}^{(k+1)T} e^{A_i((k+1)T-t)} E_i \omega(t) dt
\end{aligned}$$

Hence, the discrete-time equivalent model for the resultant closed-loop system will be given by:

$$\begin{aligned}
x[k+1] &= \hat{A}_i x[k] + \hat{B}_{i,\sigma} y_{ref}[k] - \hat{B}_{i,\sigma} \hat{C}_i x[k] - \hat{B}_{i,\sigma} \hat{F}_i \omega[k] + \hat{E}_i \omega[k] \\
&= (\hat{A}_i - \hat{B}_{i,\sigma} \hat{C}_i) x[k] + \hat{B}_{i,\sigma} (y_{ref}[k] - \hat{F}_i \omega[k]) + \hat{E}_i \omega[k] \tag{4.10a}
\end{aligned}$$

$$y[k] = \hat{C}_i x[k] + \hat{F}_i \omega[k] \tag{4.10b}$$

Define:

$$\begin{aligned}
\phi &:= (\hat{A}_i - \hat{B}_{i,\sigma} \hat{C}_i) \\
\psi[k] &:= \hat{B}_{i,\sigma} (y_{ref}[k] - \hat{F}_i \omega[k]) + \hat{E}_i \omega[k]
\end{aligned} \tag{4.11}$$

Thus, (4.10) can be rewritten as:

$$x[k] = \phi^k x[0] - \sum_{v=0}^{k-1} \phi^{k-v-1} \psi[v] \tag{4.12}$$

So, the state of the closed-loop system at each sampling instant is related to the initial state and the input signals through the following equation:

$$\begin{aligned}
x[k] &= (\hat{A}_i - \hat{B}_{i,\sigma} \hat{C}_i)^k x[0] \\
&+ \sum_{v=0}^{k-1} \left[(\hat{A}_i - \hat{B}_{i,\sigma} \hat{C}_i)^{k-v-1} (\hat{B}_{i,\sigma} (y_{ref}[v] - \hat{F}_i \omega[v]) + \hat{E}_i \omega[v]) \right]
\end{aligned} \tag{4.13}$$

Assume that the following bound on the norm of the disturbance signal is given:

$$\bar{\omega} := \max_t \|\omega(t)\|$$

Since multiple layers of GSHFs are used in this approach, The following definitions are inevitable;

Definition 1 *Throughout this chapter, a switching to a destabilizing GSHF will be called an unstable switching,*

Definition 2 *A GSHF whose indices include all but one of the indices of another GSHF is called a parent of that GSHF.*

For instance, $\mathbf{f}_{i_1 i_2 \dots i_{p-1}}$ is a parent of $\mathbf{f}_{i_1 i_2 \dots i_p}$. On the other hand, any GSHF in a layer other than layer # 1 is called a *child* to its parent in the lower layer.

Definition 3 *A child-parent switching route is a switching path from a GSHF in one of the higher layers to a GSHF in the first layer, consisting of only child-to-parent switchings.*

It is desired now to find a switching path which consists of *at most one* unstable switching between the GSHFs of different layers.

Figure 4.2 shows a family of 6 plant models and the architecture of different layers, where the plant models are represented by black circles and GSHFs of layer 1, 2, 3 and 4 are represented by triangles, squares, pentagons and hexagons, respectively.

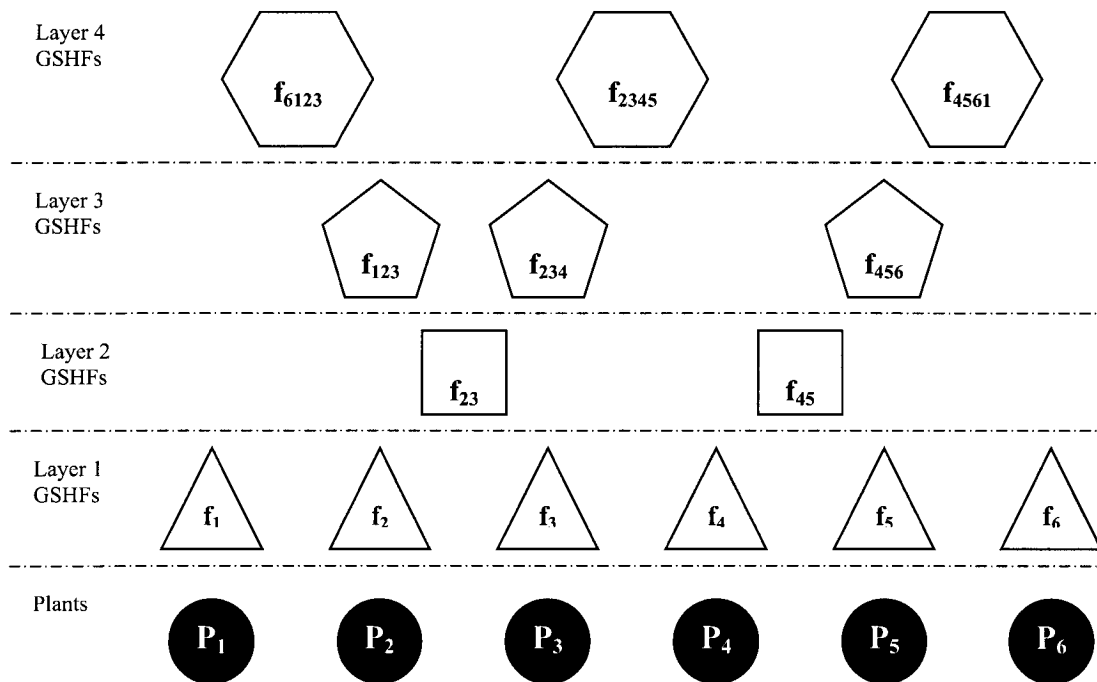


Figure 4.2: Four layers of GSHFs for six plant models.

4.2 Main Results

One of the shortcomings of most switching control methods is the bad transient response, which is mainly contributed by switching to many destabilizing controllers before the system locks onto the correct one. Each switching to a destabilizing controller will usually cause a big overshoot, which will be accumulated before the correct controller is found. Addition of new layers of controllers can potentially reduce the number of *unstable switchings* as shown in the following Algorithm.

4.2.1 Switching Algorithm

Assumption 1: Suppose that there exists a GSHF in layer $p - 2$ which destabilizes two of plant models and stabilizes all other models and each of the plant models is destabilized by at least one GSHF in layer $p - 2$. Assume also that there exists at least one child-parent route from any of the GSHFs in layer $p - 2$ to a GSHF in the first layer.

Initially let the correct plant model be \mathbf{P}_{i_1} which is stabilized by GSHF \mathbf{f}_{i_1} in the first layer. Once a change in the model occurs, the new plant model is known to be one of the remaining $p - 1$ models $\bar{p} - \{i_1\} = \{i_2, i_3, \dots, i_p\}$, which results in instability of the closed-loop system.

Algorithm 1:

Step 1: Set $l = 1$ and $\bar{\mathbf{I}} = \{i_1, i_2, \dots, i_p\}$

Step 2: Switch to a GSHF in layer $p - (l + 1)$ which destabilizes \mathbf{P}_{i_1} . Denote the other plant model which is also destabilized by this GSHF with \mathbf{P}_{i_κ} . Let this GSHF be represented by $\mathbf{f}_{\bar{\mathbf{I}} - \{i_\kappa, i_1\}}$. Set $\bar{\mathbf{I}} = \bar{\mathbf{I}} - \{i_1\}$ and $q = i_\kappa$.

Step 3: If the closed-loop system is known to be unstable, the actual plant model is identified to be \mathbf{P}_q . Switch to \mathbf{f}_q and stop. Otherwise, set $l = l + 1$ and $\bar{\mathbf{I}} = \bar{\mathbf{I}} - \{q\}$.

Step 4: At this point, it is known that the actual plant model belongs to the set $\{\mathbf{P}_i | i \in \bar{\mathbf{I}}\}$. If $l = p - 2$ then stop; otherwise switch to one of the *parent* GSHFs of \mathbf{f}_l in layer $p - (l + 1)$. Let this GSHF be denoted by $\mathbf{f}_{\bar{\mathbf{I}} - i_{\kappa_l}}$. Set $q = i_{\kappa_l}$. Go to Step 3.

It can be easily verified that using the switching sequence described in *Algorithm 1*, it is guaranteed that the system will eventually switch to the correct GSHF with at most one unstable switching. The flow chart of *Algorithm 1* is given in figure 4.3.

Example 1 *As an example, consider a family of 6 plants as shown in Figure 4.4. Initially, the actual plant model is \mathbf{P}_6 which is stabilized by GSHF \mathbf{f}_6 . Assume that at some point of time the plant model changes to \mathbf{P}_4 which is the new (unknown) plant model, and as a result the system becomes unstable. Following the Algorithm 1, the system switches to \mathbf{f}_{2345} which stabilizes $\mathbf{P}_2, \mathbf{P}_3, \mathbf{P}_4, \mathbf{P}_5$ and destabilizes \mathbf{P}_6 and \mathbf{P}_1 (Step 1 and Step 2). The system becomes stable and switches to \mathbf{f}_{234} which is the parent of the previous GSHF \mathbf{f}_{2345} (Step 3 and Step 4). The system remains stable and hence should switch to a parent of the current GSHF \mathbf{f}_{234} . Assume that the system switches to \mathbf{f}_{23} as shown in the figure, (Step 3 and Step 4). This is the only time that the system becomes unstable. At this point, the actual plant model is identified to be \mathbf{P}_4 and the system switches to \mathbf{f}_4 (Step 3).*

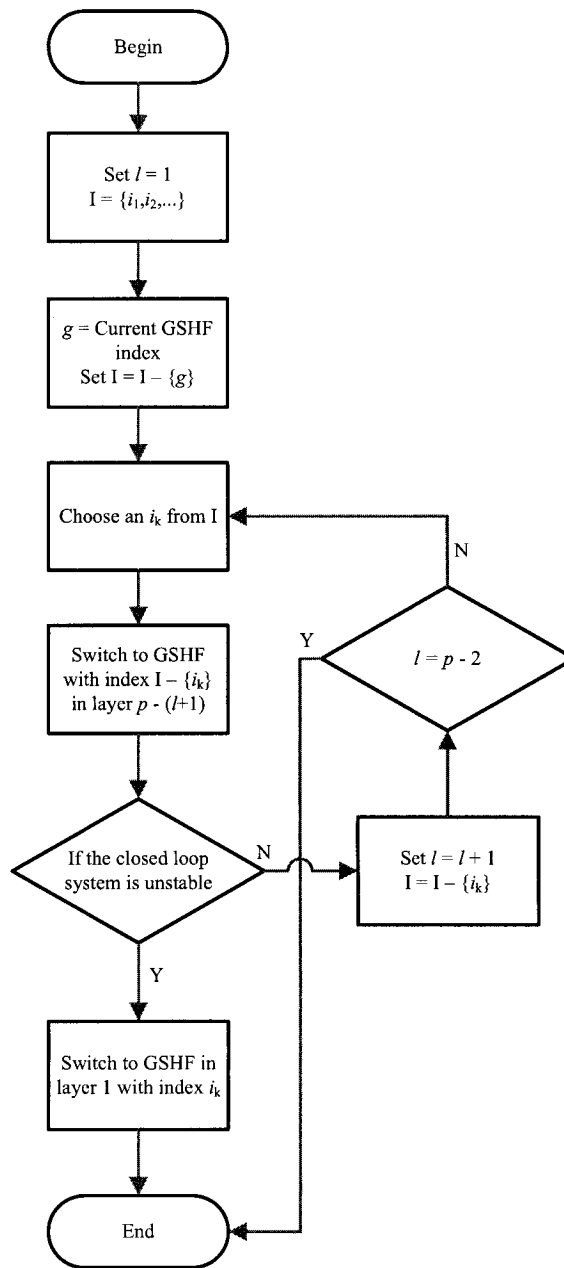


Figure 4.3: The flow chart of *Algorithm 1*.

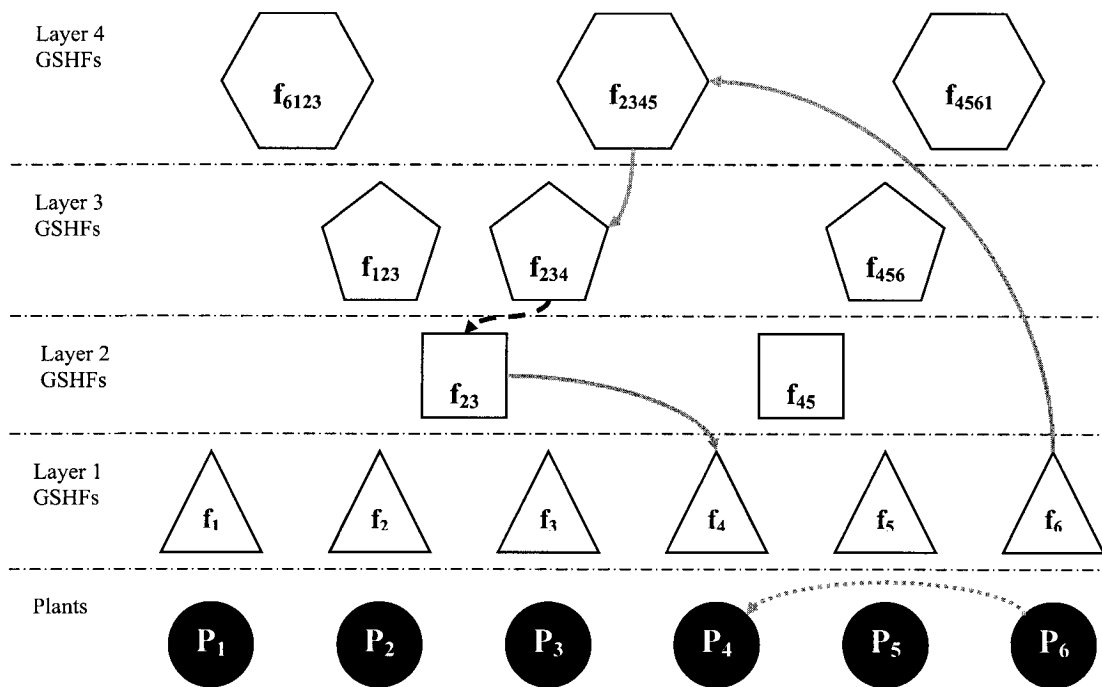


Figure 4.4: Switching in four layers. Solid arrows represent stable switchings and dashed arrow denotes an unstable switching.

4.2.2 Layers' Structure

It is to be noted that the number of GSHFs for layer $\# \rho$ that can stabilize ρ plant models and destabilize the remaining $p - \rho$ models is equal to the number of unordered combinations of p choose ρ which is $\frac{p!}{\rho!(p-\rho)!}$. Thus, the total number of all GSHFs in the multi-layer structure is equal to $\sum_{\rho=1}^{p-2} \frac{p!}{\rho!(p-\rho)!}$. More specifically, the number of all possible GSHFs for layer $p - 2$ is equal to p choose $p - 2$ or $\frac{p!}{(p-2)!2!} = \frac{p(p-1)}{2}$, since each GSHF in layer $p - 2$ should stabilize $p - 2$ plants. However it can be verified that only p GSHFs for layer $\# 1$ is needed. Furthermore, when switching mechanism switches from GSHF i in the first layer to layer $p - 2$, it has to choose a GSHF which does not stabilize plant i and one other plant such as j . This is the same, when it switches from GSHF j in the first layer. Therefore each pair of plants can have only one simultaneous stabilizer in the layer $p - 2$. Hence, $\text{fix}(\frac{p+1}{2})$ GSHFs for other layers would suffice, where $\text{fix}(\cdot)$ represents the nearest integer towards zero. One will need to design at most $(p - 3) \times \text{fix}(\frac{p+1}{2})$ simultaneous stabilizer GSHFs such that the conditions of *Assumption 1* are satisfied.

For example, suppose that 11 plant models are given. In this case 9 layers of GSHFs are needed in which the number of all possible GSHFs in layer 9 would be equal to 55. Yet only $\text{fix}(\frac{11}{2})$ or 6 GSHFs are sufficient to satisfy the conditions of *Assumption 1* (See Figure 4.5).

Since the multi-layer approach introduces new GSHFs in the system, it would be of great interest to find the minimum number of GSHFs required so that the proposed algorithm can be used. As discussed earlier it is very easy to verify that $p - 2$ layers are required in this scheme, where layer 1 consists of p GSHFs and layer $p - 2$ must

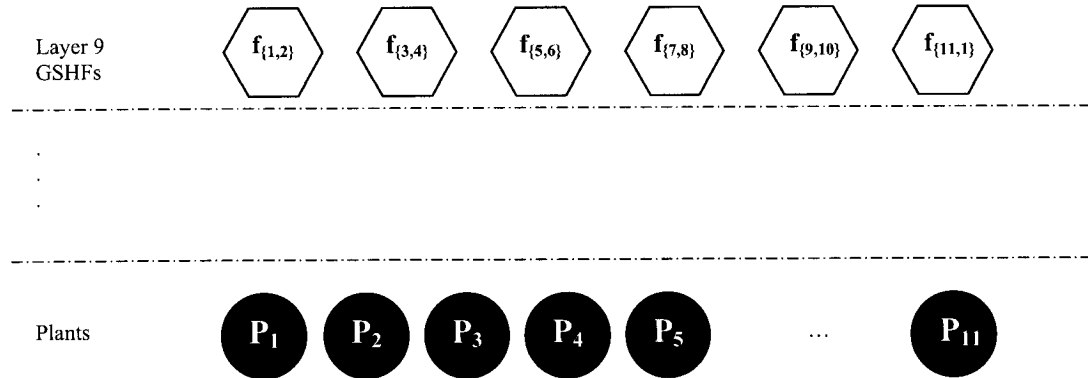


Figure 4.5: A possible structure of layer 9 for eleven plant models, where the numbers inside the curly braces represent the indices of the plants that the GSHF cannot stabilize.

have at least $\lceil \frac{p+1}{2} \rceil$ GSHFs, with $\lceil x \rceil$ denoting the largest integer smaller than or equal to x (i.e. $\lceil \frac{p+1}{2} \rceil$ is equal to $\frac{p}{2}$ for an even p and is equal to $\frac{p+1}{2}$ for an odd p). It is also to be noted that a GSHF in a higher layer can stabilize more plant models compared to one at a lower layer. While a GSHF at layer $p - 2$ can stabilize $p - 2$ plants, at layer $p - 3$ its corresponding parent GSHF will stabilize $p - 3$ plants. Furthermore, it can be easily verified that if two GSHFs in a layer differ in only one index, which means that they have a common parent, the number of the required GSHFs in the immediate lower layer will be smaller.

Since it is desired to minimize the number of GSHFs, it is preferable to use GSHFs with indices which lead to common parents. As a result it can be verified that in the multi-layer configuration of Figure 4.6, since $f_{1,2}$ and $f_{3,4}$ are in layer #9, GSHFs $f_{1,2,3}$ and $f_{2,3,4}$ have been considered as a part of GSHFs in layer #8. Notice that two of the indices of GSHFs in layer $p - 2$ are different and as a result layer $p - 3$ cannot have fewer GSHFs than layer $p - 2$ which is $\lceil \frac{p+1}{2} \rceil$. For constructing layer $p - 4$ only one parent GSHF can

be used for each pair of GSHFs in layer $p - 3$, and hence, the number of GSHFs required would be $\lceil \frac{p+1}{2} \rceil + 1$. For instance, for a family of eleven plant models, only three GSHFs are required in layer 7 (see Figure 4.6). At layer $p - 4$, GSHFs will have indices that are different in four places. Hence, in order to find common parents, four layers of the same number of GSHFs should be introduced. It is easy to verify that the number of reduction of GSHFs at a layer is equal to $\lceil \log_2 p \rceil + 1$. Therefore the multi-layer structure has blocks of p GSHFs each, and the overall number of GSHFs required is less than or equal to $p(\lceil \log_2 p \rceil + 1)$.

One can define a discrete event system (DES) model for the present problem, to determine the minimum number of required GSHFs for different specifications such as different number of permitted unstable switchings or different cost functions for each route in the multi-layer structure.

4.2.3 Switching Mechanism

To make sure that the switching mechanism acts properly, a bound on the initial condition of the system needs to be found first. This method will be performed in two phases: before applying the control signal and after that. The following Lemma will be used in the development of the main result.

Lemma 1: For any $y[k], y_1[k], y_2[k] \in \mathbb{R}^r$ where $y[k] = y_1[k] + y_2[k]$ the following inequality holds:

$$\|y_1[k]\|^2 \leq 2\|y[k]\|^2 + 2\|y_2[k]\|^2 \quad (4.14)$$

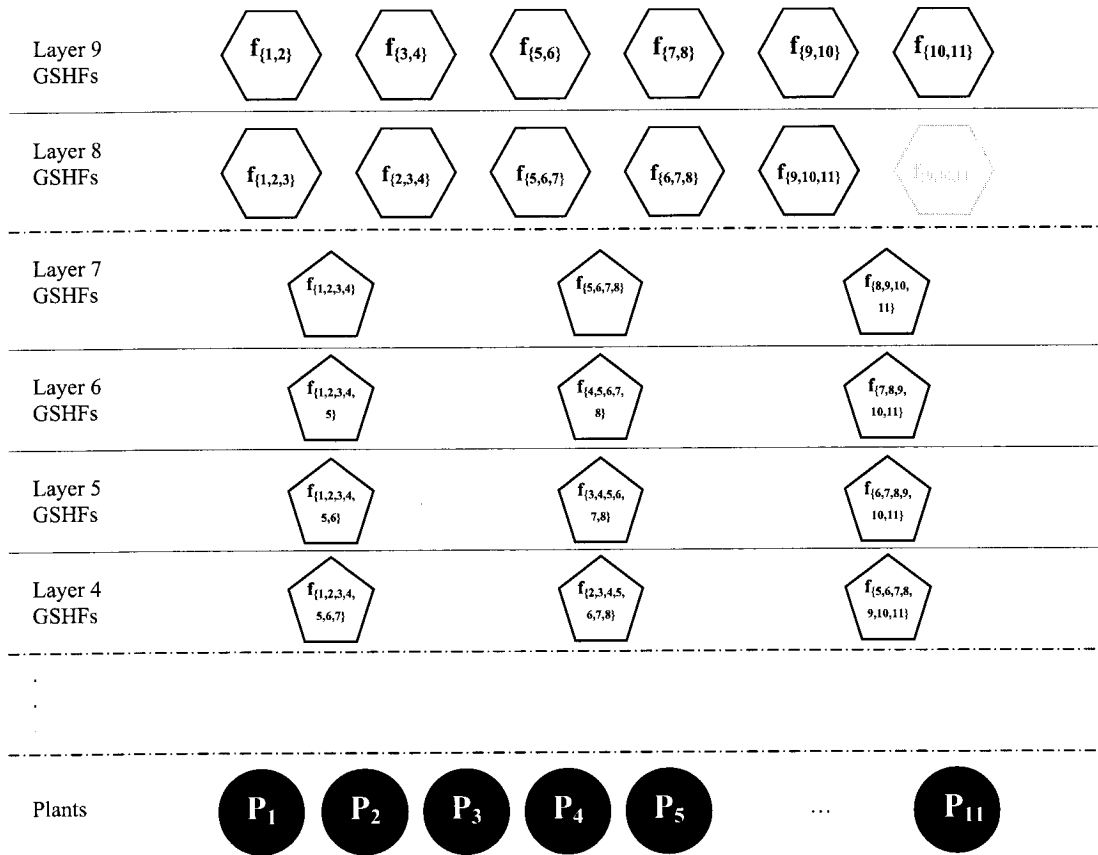


Figure 4.6: A possible multi-layer switching structure for eleven plants, where the numbers inside the curly braces represent the indices of the plants that the GSHF cannot stabilize.

Proof of Lemma 1: One can write:

$$\begin{aligned} \|y_2[k]\| + \|y[k]\| &\geq \|y_2[k] - y[k]\| = \|y_1[k]\| \\ \|y_1[k]\|^2 &\leq \|y[k]\|^2 + \|y_2[k]\|^2 + 2\|y[k]\| \cdot \|y_2[k]\| \end{aligned} \quad (4.15)$$

it is also known that:

$$(\|y_2[k]\| - \|y[k]\|)^2 \geq 0 \quad (4.16)$$

combining the inequalities (4.15) and (4.16) results in:

$$\|y_1[k]\|^2 \leq 2\|y[k]\|^2 + 2\|y_2[k]\|^2$$

■

The following Lemma is the discrete-time version of *Lemma 2* in [2], and gives a bound on the norm of the initial state of the system with the assumption that the disturbance is bounded and the control input is set to zero.

Lemma 2: Consider the discretized system (4.10) and assume that the control input $u(t)$ in (4.3) is equal to zero for $0 \leq t \leq mT$, for any arbitrary integer $m > 0$. For any initial state $x[0]$ and disturbance ω , whose norm is bounded by $\bar{\omega}$, there exist constants $\alpha_{1,i}$ and $\alpha_{2,i}$ so that the following inequality on the norm of the initial state holds

$$\|x[0]\|^2 \leq \alpha_{1,i} \sum_{k=0}^m \|y[k]\|^2 + \alpha_{2,i} \bar{\omega}^2 \quad (4.17)$$

Proof of Lemma 2: The samples of the output obtained from the discrete-time equivalent model is given by:

$$y[k] = \hat{C}_i x[k] + \hat{F}_i \omega[k] \quad (4.18)$$

Since the control input is set to zero for $0 \leq t \leq mT$, it can be concluded from (4.13) that

$$x[k] = \hat{A}_i^k x[0] + \sum_{v=0}^{k-1} [\hat{A}_i^{k-v-1} \hat{E}_i \omega[v]] \quad (4.19)$$

Substituting (4.19) in (4.18) will result in:

$$\begin{aligned} y[k] &= \hat{C}_i [\hat{A}_i^k x[0] + \sum_{v=0}^{k-1} \hat{A}_i^{k-v-1} \hat{E}_i \omega[v]] + \hat{F}_i \omega[k] \\ &= \hat{C}_i \hat{A}_i^k x[0] + \hat{C}_i \sum_{v=0}^{k-1} \hat{A}_i^{k-v-1} \hat{E}_i \omega[v] + \hat{F}_i \omega[k] \end{aligned} \quad (4.20)$$

Define

$$y_1[k] := \hat{C}_i \hat{A}_i^k x[0] \quad (4.21a)$$

$$y_2[k] := \hat{C}_i \sum_{v=0}^{k-1} \hat{A}_i^{k-v-1} \hat{E}_i \omega[v] + \hat{F}_i \omega[k] \quad (4.21b)$$

Taking norm of the terms in both sides of (4.21b) results in:

$$\begin{aligned} \|y_2[k]\| &\leq \|\omega[k]\| \left(\sum_{v=0}^{k-1} \|\hat{C}_i \hat{A}_i^{k-v-1} \hat{E}_i\| + \|\hat{F}_i\| \right) \\ &\leq \bar{\omega} \left(\sum_{v=0}^{k-1} \|\hat{C}_i \hat{A}_i^{k-v-1} \hat{E}_i\| + \|\hat{F}_i\| \right) \end{aligned} \quad (4.22)$$

Define now:

$$W_i := \sum_{k=0}^m (\hat{A}_i')^k \hat{C}_i' \hat{C}_i \hat{A}_i^k$$

Then:

$$\sum_{k=0}^m \|y_1[k]\|^2 = x[0]' W_i x[0]$$

Define also:

$$\alpha_{3,i} := \text{smallest singular value of } W_i \quad (4.23)$$

It can be concluded from (4.21a) that:

$$\begin{aligned} \sum_{k=0}^m \|y_1[k]\|^2 - \alpha_{3,i} \|x[0]\|^2 &= x[0]' [W_i - \alpha_{3,i} I] x[0] \geq 0 \\ \sum_{k=0}^m \|y_1[k]\|^2 &\geq \alpha_{3,i} \|x[0]\|^2 \end{aligned} \quad (4.24)$$

On the other hand, it follows from *Lemma 1* that:

$$\sum_{k=0}^m \|y_1[k]\|^2 \leq 2 \sum_{k=0}^m \|y[k]\|^2 + 2 \sum_{k=0}^m \|y_2[k]\|^2 \quad (4.25)$$

Substituting $y_1[k]$ from (4.24) in (4.25) and dividing both sides by $\alpha_{3,i}$ will result in:

$$\|x[0]\|^2 \leq \frac{2}{\alpha_{3,i}} \sum_{k=0}^m \|y[k]\|^2 + \frac{2}{\alpha_{3,i}} \sum_{k=0}^m \|y_2[k]\|^2 \quad (4.26)$$

Now, define $\alpha_{1,i}$ and $\alpha_{2,i}$ as follows:

$$\alpha_{1,i} := \frac{2}{\alpha_{3,i}}$$

$$\alpha_{2,i} := \frac{2}{\alpha_{3,i}} \sum_{k=0}^m \left[\sum_{v=0}^{k-1} \|\hat{C}_i \hat{A}_i^{k-v-1} \hat{E}_i\| + \|\hat{F}_i\| \right]^2$$

Then using (4.22), one can obtain the following inequality:

$$\|x[0]\|^2 \leq \alpha_{1,i} \sum_{k=0}^m \|y[k]\|^2 + \alpha_{2,i} \bar{\omega}^2$$

■

It is now necessary to obtain an upper bound on the state of the system at each sampling instant, and at the presence of the control signal. This bound will be used in the decision-making unit to verify whether the current GSHF is correct or it needs to be changed. Since it is required to find $x[k]$ related to the initial state and the input signal, even if the correct GSHF is not being applied to the system, let $j \in 2^{\bar{p}} - \emptyset$. From (4.9) and (4.6) one can write,

$$\begin{aligned}
x[k+1] &= e^{A_i T} x[k] \\
&+ \int_{kT}^{(k+1)T} e^{A_i((k+1)T-t)} B_i \cdot [\mathbf{f}_j(t) \cdot \tilde{u}[k]] dt \\
&+ \int_{kT}^{(k+1)T} e^{A_i((k+1)T-t)} E_i \omega(t) dt
\end{aligned}$$

Define $\hat{B}_{i,j}$ as the discrete-time equivalent matrix for B_i , when the GSHP \mathbf{f}_j corresponding to the plant \mathbf{P}_j is used in the closed-loop system. $\hat{B}_{i,j}$ can be obtained as follows:

$$\hat{B}_{i,j} := \int_0^T e^{A_i(T-t)} B_i \mathbf{f}_j(t) dt$$

Define:

$$\bar{\sigma} = \text{the subset of GSHPs that stabilize } \mathbf{P}_i$$

Apparently, for $j = \sigma \in \bar{\sigma}$, we have $\hat{B}_{i,j} = \hat{B}_{i,\sigma}$ and hence:

$$\begin{aligned}
x[k+1] &= \hat{A}_i x[k] + \hat{B}_{i,j} \tilde{u}[k] + \hat{E}_i \omega[k] \\
&= (\hat{A}_i - \hat{B}_{i,\sigma} \hat{C}_i) x[k] + \hat{B}_{i,\sigma} \hat{C}_i x[k] + \hat{B}_{i,j} \tilde{u}[k] + \hat{E}_i \omega[k] \\
&= (\hat{A}_i - \hat{B}_{i,\sigma} \hat{C}_i) x[k] + \hat{B}_{i,\sigma} [y[k] - \hat{F}_i \omega[k]] + \hat{B}_{i,j} \tilde{u}[k] + \hat{E}_i \omega[k]
\end{aligned}$$

It can be concluded from (4.12) that:

$$\begin{aligned}
x[k] &= (\hat{A}_i - \hat{B}_{i,\sigma} \hat{C}_i)^k x[0] + \sum_{v=0}^{k-1} \left[(\hat{A}_i - \hat{B}_{i,\sigma} \hat{C}_i)^{k-v-1} \right. \\
&\quad \left. \cdot [\hat{B}_{i,\sigma} y[v] + \hat{B}_{i,j} \tilde{u}[v] + (\hat{E}_i - \hat{B}_{i,\sigma} \hat{F}_i) \omega[v]] \right]
\end{aligned} \tag{4.27}$$

The following lemma provides an upper bound on the state of the system in terms of the system parameters and maximum norms of the disturbance ω and reference signal y_{ref} denoted by $\bar{\omega}$ and \bar{y}_{ref} respectively.

Lemma 3: There exists constants $\gamma_{1,i}$, $\gamma_{2,i}$ and λ_i such that for any bounded piecewise continuous signal $u(t)$ and reference signal y_{ref} and disturbance ω , and any initial

state $x[0]$, the following inequality holds:

$$\begin{aligned} \|x[k]\| &\leq \lambda_i \gamma_{1,i}^k \|x[0]\| \\ &+ \sum_{v=0}^{k-1} \left[\lambda_i \gamma_{1,i}^{k-v-1} [\|\hat{B}_{i,\sigma} y[v] + \hat{B}_{i,j} \tilde{u}[v]\| + \gamma_{2,i}] \right] \end{aligned} \quad (4.28)$$

Proof of Lemma 3: Choose λ_i such that

$$\|(\hat{A}_i - \hat{B}_{i,\sigma} \hat{C}_i)^k\| \leq \lambda_i \cdot \max |eig(\hat{A}_i - \hat{B}_{i,\sigma} \hat{C}_i)|^k$$

The proof immediately follows by choosing $\gamma_{1,i} = \max |eig(\hat{A}_i - \hat{B}_{i,\sigma} \hat{C}_i)|$ and $\gamma_{2,i} = \bar{\omega} \|\hat{E}_i - \hat{B}_{i,\sigma} \hat{F}_i\|$, and using (4.27). ■

The output of the system is:

$$\begin{aligned} y[k] &= \hat{C}_i \cdot \left[(\hat{A}_i - \hat{B}_{i,\sigma} \hat{C}_i)^k x[0] + \sum_{v=0}^{k-1} \left[(\hat{A}_i - \hat{B}_{i,\sigma} \hat{C}_i)^{k-v-1} \right. \right. \\ &\quad \left. \left. \cdot [\hat{B}_{i,\sigma} y[v] + \hat{B}_{i,j} \tilde{u}[v] + (\hat{E}_i - \hat{B}_{i,\sigma} \hat{F}_i) \omega[v]] \right] \right] + \bar{\omega} \hat{F}_i \end{aligned} \quad (4.29)$$

Hence, using the same approach as in *Lemma 3* and having $\gamma_{3,i} = \bar{\omega} \|\hat{C}_i (\hat{E}_i - \hat{B}_{i,\sigma} \hat{F}_i)\|$ one can write:

$$\begin{aligned} \|y[k]\| &\leq \|\hat{C}_i\| \cdot \lambda_i \gamma_{1,i}^k \|x[0]\| \\ &+ \sum_{v=0}^{k-1} \left[\lambda_i \gamma_{1,i}^{k-v-1} [\|\hat{C}_i \hat{B}_{i,\sigma} y[v] + \hat{C}_i \hat{B}_{i,j} \tilde{u}[v]\| + \gamma_{3,i}] \right] \\ &+ \bar{\omega} \|\hat{F}_i\| \end{aligned} \quad (4.30)$$

Assuming that the disturbance is bounded, by substituting the bound on the initial condition into (4.30), one can find an auxiliary signal which gives a bound on the state of the system at any point of time. Let $r_{i,\sigma}$ denote the auxiliary signal which is a bound on the

norm of the output of the closed-loop system corresponding to the plant model \mathbf{P}_i with GSHF \mathbf{f}_σ . In other words $r_{i,\sigma}$ is a bound on the output of the discrete-equivalent, model for the plant \mathbf{P}_i with GSHF \mathbf{f}_σ . This auxiliary signal is given by:

$$\begin{aligned}
r_{i,\sigma}[k] &= \|\hat{C}_i\| \cdot \lambda_i \gamma_{i,i}^k \|x[0]\| \\
&+ \sum_{v=0}^{k-1} \left[\lambda_i \gamma_{i,i}^{k-v-1} \cdot [\|\hat{C}_i(\hat{B}_{i,\sigma}y[v] + \hat{B}_{i,j}\tilde{u}[v])\| + \gamma_{3,i}] \right] + \bar{\omega} \|\hat{F}_i\| \\
r_{i,\sigma}[k+1] &= \|\hat{C}_i\| \cdot \lambda_i \gamma_{i,i}^{k+1} \|x[0]\| \\
&+ \sum_{v=0}^k \left[\lambda_i \gamma_{i,i}^{k-v} \cdot [\|\hat{C}_i(\hat{B}_{i,\sigma}y[v] + \hat{B}_{i,j}\tilde{u}[v])\| + \gamma_{3,i}] \right] + \bar{\omega} \|\hat{F}_i\|
\end{aligned} \tag{4.31}$$

In order to come up with a difference equation to update the auxiliary signals at each step one, can write:

$$\begin{aligned}
r_{i,\sigma}[k+1] &= \gamma_{i,i} \cdot r_{i,\sigma}[k] + \lambda_i [\|\hat{C}_i(\hat{B}_{i,\sigma}y[k] + \hat{B}_{i,j}\tilde{u}[k])\| + \gamma_{3,i}] \\
&+ (1 - \gamma_{i,i}) \bar{\omega} \|\hat{F}_i\|
\end{aligned} \tag{4.32}$$

Note that:

$$r_{i,\sigma}[0] = \|\hat{C}_i\| \cdot \lambda_i \|x[0]\| + \bar{\omega} \|\hat{F}_i\|$$

Consequently, for $0 \leq t \leq mT$, and for any arbitrary integer $m > 0$ with no control signal,

$$r_{i,\sigma}[t] \leq \lambda_i \|\hat{C}_i\| \cdot [\alpha_{1,i} \sum_{k=0}^m \|y[k]\|^2 + \alpha_{2,i} \bar{\omega}^2]^{\frac{1}{2}} + \bar{\omega} \|\hat{F}_i\|$$

Hence one can break the control process into two phases, as follows:

Phase 1: Setting the control signal to zero for $0 \leq t \leq mT$ where m is any non-zero integer and T is the sampling period, results in the following upper bound on the norm of

the output of the system.

$$r_{i,\sigma}[k] = \lambda_i \|\hat{C}_i\| \cdot [\alpha_{1,i} \sum_{v=0}^m \|y[v]\|^2 + \alpha_{2,i} \bar{\omega}^2]^{\frac{1}{2}} + \bar{\omega} \|\hat{F}_i\|$$

Phase 2: The equation (4.32) can now be used to update the new values of the auxiliary signals for $k > m$. It is to be noted that the norm of the output is compared with the corresponding upper bound only at the sampling instants (the discrete model will be used in the decision making unit of the switching control).

It is desired now to find the switching instants using the auxiliary signals obtained above.

Switching Controller 1: Define $t_1 = mT$, and for every $i \in \{2, \dots, p+1\}$ for which $t_{i-1} \neq \infty$, define:

$$t_i := \min\{t \geq t_{i-1}, \exists \tilde{k} \in [mT, t]; \|y[\tilde{k}]\| \geq r_{i,\sigma}[\tilde{k}]\}$$

The following theorem states that the switching mechanism will finally lock onto the correct GSHF, and the state of the system will remain bounded.

Theorem 2 Suppose that the reference input and the disturbance signals are piece-wise continuous and bounded with $\|\omega(t)\| \leq \bar{\omega}$ and $\|y_{ref}(t)\| \leq \bar{y}_{ref}$ for $t \geq 0$. For every initial condition $x(0)$, when the *switching controller 1* is applied to the uncertain plant whose model belongs to the known family of plant models Π , the closed-loop system has the following properties:

a) the GSHF will ultimately be equal to an element of $\{\mathbf{f}_j; j \in \bar{p}\}$ and will remain unchanged afterwards; and

b) the state of the system will be bounded.

Proof: It has already been shown that $\|y[k]\| \leq r_{i,\sigma}[k]$ for $k \geq mT$. Therefore, if t_{i+1} is defined, then according to the *switching controller 1* t_{i+1} must be ∞ . Hence part (a) holds, and a bound on the state of the system is obtained in *Lemma 3* is obtained, which is bounded itself. ■

The switching sequence of the multi-layer algorithm requires that the system switches from the higher layer GSHFs to the lower layer GSHFs even if the system is stabilized in a higher layer. Unlike unstable switchings, stable switchings cannot be identified through the upper-bound signals. In order to detect stability, a sufficiently long time-interval will be used such that if the norm of the error does not meet the upper-bound signal during this time interval, the system is stable. This time-interval can be obtained either experimentally or by considering worst-case scenario associated with the initial state, reference input and disturbance signal. This time duration will be referred to as safety time and will be denoted by t_d .

Remark 1: One can conclude from (4.32) that there are more than one boundary signal related to higher layer GSHF (associated with different plant models that it can stabilize). Thus, the system is known to be unstable when the output hits the bound with larger value at any time.

Theorem 3 Consider the system (4.10). Using the multi-layer GSHF structure and the switching sequence of Algorithm 1, with the switching instants $t_s = \min(t_{i-1} + t_d, t_i)$ where t_i represents the time instants given in Theorem 1 ($t_0 := 0$) and t_d is the safety time,

the system will eventually switch to the correct GSHF with no more than one unstable switching.

Proof of Theorem 3: The proof follows immediately from the results of *Theorem 1* and by noting that the auxiliary signals can be obtained as given by (4.32) for any stabilizing or destabilizing GSHF in different layers. ■

4.2.4 Transition Matrix

The process of switching from one GSHF to another can be regarded as an stochastic process with a transition matrix $\Theta_p = [\theta_{i,j}(t)]$, $i, j = 1 \dots p$, where $\theta_{i,j}(t)$ is the probability that \mathbf{P}_i would change to \mathbf{P}_j at time t , and obviously for all i formula (4.33) holds.

$$\sum_{j=1}^p \theta_{i,j} = 1 \quad (4.33)$$

Generally, when there is no information available on the probable sequence in which the plants dynamics might change, one can assume that the distribution function is uniform and hence if the initial plant model which has becomes unstable is denoted by \mathbf{P}_i then,

$$\theta_{i,j}(t_1) = \begin{cases} 0, & i=j; \\ \frac{1}{p-1}, & \text{otherwise.} \end{cases} \quad (4.34)$$

where t_1 is the time when *Algorithm 1* first detects an instability. On the other hand if statistical data would be available, it would be possible that *Algorithm 1* chooses a GSHF

which would stabilize the plant model with better chances, depending on the switching strategy. The matrix Θ_p can be updated at each switching instant to reflect the changes made in the dynamics of the system, and since *Algorithm 1* is guaranteed to visit each GSHF only once, hence as the Algorithm proceeds the steps, better decision can be made.

4.3 Simulation Results

Example 1: Consider the following unstable non-minimum phase plant model used in [64] and [65]:

$$\mathbf{P} = \lambda \frac{s-1}{(s-2)(s+1)}, \quad 0.95 < \lambda(t) < 1.9$$

A family of four plant models $\mathbf{P}_i = \{\mathbf{P}_1, \mathbf{P}_2, \mathbf{P}_3, \mathbf{P}_4\}$ is then considered as follows

$$\mathbf{P}_1 = \frac{s-1}{(s-2)(s+1)}, \quad \mathbf{P}_2 = 1.2\mathbf{P}_1, \quad \mathbf{P}_3 = 1.2\mathbf{P}_2, \quad \mathbf{P}_4 = 1.2\mathbf{P}_3.$$

One can obtain the high-performance GSHFs of the first layer using the method presented in [52]:

$$\begin{aligned} \mathbf{f}_1 &= 1015.7e^{(t-1)} + 110.3e^{(2-2t)} - 994.5, \\ \mathbf{f}_2 &= 0.83\mathbf{f}_1, \quad \mathbf{f}_3 = 0.69\mathbf{f}_1, \quad \mathbf{f}_4 = 0.58\mathbf{f}_1. \end{aligned}$$

The second layer consists of three GSHFs as follows:

$$\mathbf{f}_{12} = 0.91\mathbf{f}_1, \quad \mathbf{f}_{23} = 0.76\mathbf{f}_1, \quad \mathbf{f}_{34} = 0.63\mathbf{f}_1.$$

Which will be the first set of possible GSHFs. It can be easily verified that GSHF \mathbf{f}_{12} stabilizes the plant models $\mathbf{P}_1, \mathbf{P}_2$ and destabilizes $\mathbf{P}_3, \mathbf{P}_4$. Similarly, $(\mathbf{f}_{23}, \mathbf{P}_2)$, $(\mathbf{f}_{23}, \mathbf{P}_3)$, $(\mathbf{f}_{34}, \mathbf{P}_3)$ and $(\mathbf{f}_{34}, \mathbf{P}_4)$ will result in stable closed-loop systems while $(\mathbf{f}_{23}, \mathbf{P}_1)$, $(\mathbf{f}_{23}, \mathbf{P}_4)$,

$(\mathbf{f}_{34}, \mathbf{P}_1)$ and $(\mathbf{f}_{34}, \mathbf{P}_2)$ are unstable pairs. However the design of these GSHFs are based on maximum noise rejection, and the objective here is to reduce the maximum overshoot at the output. Notice that although a digital control law is being used but the inter-sample ripples can significantly increase the continuous-time output in between the samples. Direct search methods such as Nelder-Mead simplex method or other methods such as steepest descent can be used in design of GSHFs, so that the following continuous-time performance index is minimized:

$$J = E\left\{\int_0^{\infty} (x^T Qx + u^T Ru) dt\right\}$$

where $E\{\cdot\}$ represents the expected value over the following set of uniformly distributed initial conditions:

$$x_0^1 = \begin{bmatrix} 1 \\ 0 \\ 0 \\ \vdots \\ 0 \end{bmatrix}, \quad x_0^2 = \begin{bmatrix} 0 \\ 1 \\ 0 \\ \vdots \\ 0 \end{bmatrix}, \quad \dots \quad x_0^n = \begin{bmatrix} 0 \\ 0 \\ 0 \\ \vdots \\ 1 \end{bmatrix}$$

With appropriate R and Q . Nevertheless, one can also achieve the goal with an easier approach. Using interpolation techniques a quadratic polynomial approximation of each GSHF is obtained. The coefficients of the interpolating polynomials are used as initial point for a constrained optimization problem. One has to make sure that while searching for new coefficients the conditions of stabilizing only a suitable set of plants is always satisfied. Although finding an optimal set of coefficients depends on the convexity of space in which the search is performed, and even in case of existence of an optimal point the procedure to find it can be very complicated and almost impossible, but better coefficients

in terms of reducing the output between the samples can be found with little effort. This leads to the following set of optimal GSHFs, which will be used in the simulations:

$$f_1 = 957.34t^2 - 987.63t + 174.58,$$

$$f_2 = 800.67t^2 - 825.82t + 145.92,$$

$$f_3 = 670.75t^2 - 692.28t + 122.47,$$

$$f_4 = 561.08t^2 - 578.50t + 102.13.$$

Assume that initially the actual plant model is P_1 and at some point of time it changes to P_4 . Figure 4.7

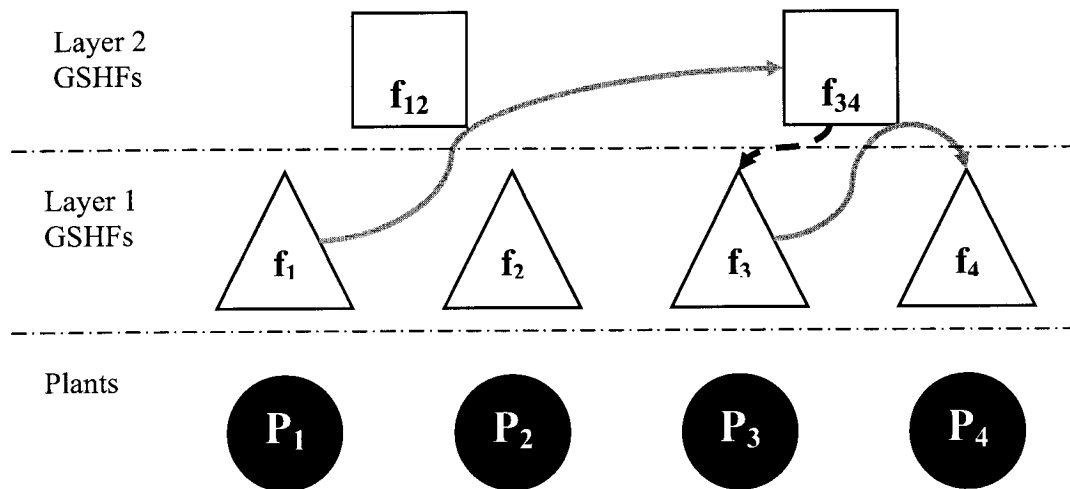


Figure 4.7: Scenario No. 1 for switching, when the plant model changes from P_1 to P_4 . The dashed arrow shows an unstable switching, while the solid arrows show switching to a stabilizing GSHF.

In the single-layer approach, the system will switch from f_1 to f_2 , then to f_3 , and

finally to \mathbf{f}_4 . The first two switching instants are unstable. In the multi-layer approach, the system will switch from \mathbf{f}_1 to \mathbf{f}_{34} , and then to \mathbf{f}_3 which is the only unstable switching. The plant is finally known to be \mathbf{P}_4 , and the last GSHF would be \mathbf{f}_4 . Figures 4.10 and 4.12 show the closed-loop simulation results using the proposed multi-layer algorithm and the corresponding switching instants, respectively. Note that figure 4.8 shows the digital output without the inter sample effect. Figures 4.15, 4.16 and 4.17 show the single-layer switching results.

Notice that Figure 4.9 shows the CT output of the system, when the first set of GSHFs are used, while Figure 4.10 shows the output of the system using the optimal GSHFs. Also Figure 4.11 shows the CT control signal.

For comparison the response of single-layer switching control system using the GSHFs of the first layer for this example is given in Figure 4.16. It can be seen from these figures that the magnitude of the transient response corresponding to the proposed multi-layer structure is 60% smaller than its single-layer counterpart. It is to be noted that the switching sequence as presented in this multi-layer example is the worst case scenario as it includes one unstable switching. As mentioned earlier, the total number of unstable switchings in the proposed multi-layer structure is zero or one. If no unstable switching occurs the transient magnitude will be smaller. For example, after the system becomes stable using \mathbf{f}_{34} , one may switch to either \mathbf{f}_3 or \mathbf{f}_4 . Switching to \mathbf{f}_4 instead of \mathbf{f}_3 will lead to a smaller transient magnitude as there will be no unstable switching instant. Scenario 2: Consider a multi-layer structure with the second layer composed of \mathbf{f}_{14} and \mathbf{f}_{23} . After the change of plant model from \mathbf{P}_1 to \mathbf{P}_4 , the system will switch to \mathbf{f}_{23} which does not stabilize the system and hence the correct GSHF is found immediately as shown in Figure 4.13. The simulation results for the single-layer switching using the continuous-time

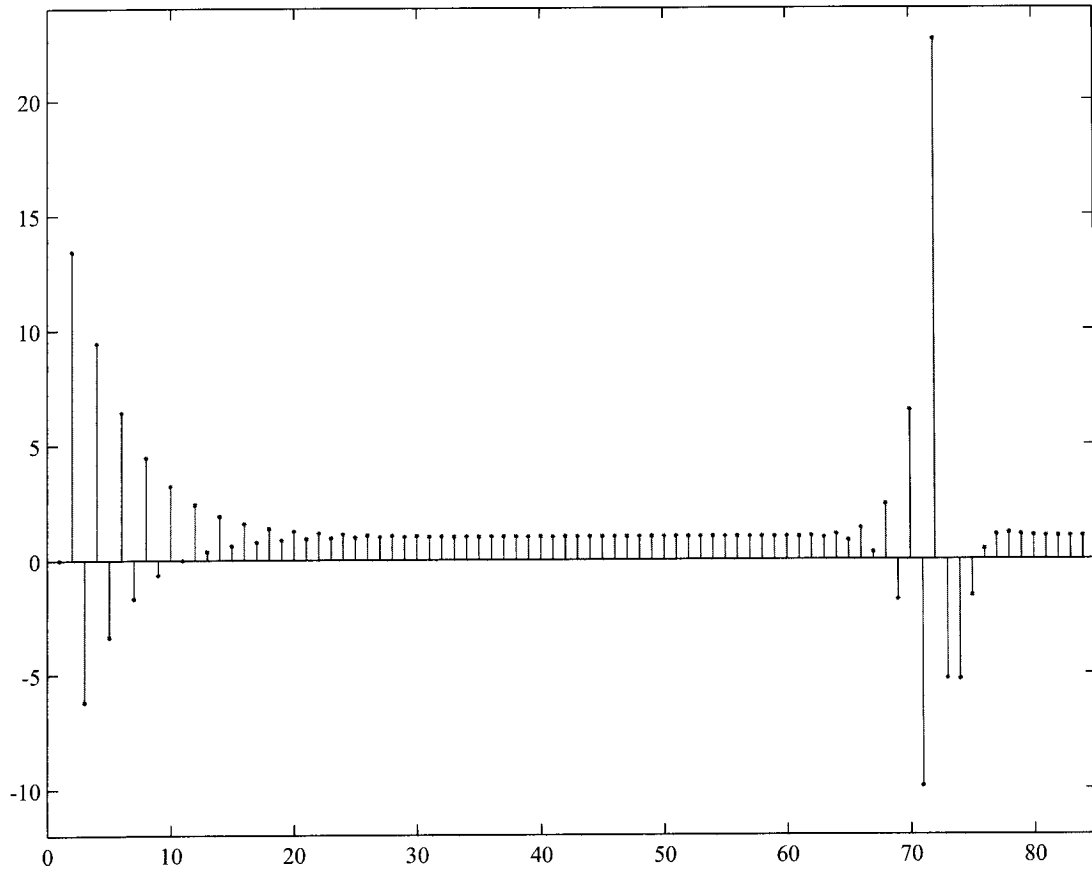


Figure 4.8: Proposed model: Output of the closed-loop system with GSHFs (at discrete points of time) using the multi-layer scheme, when the plant model changes from \mathbf{P}_1 to \mathbf{P}_4 .

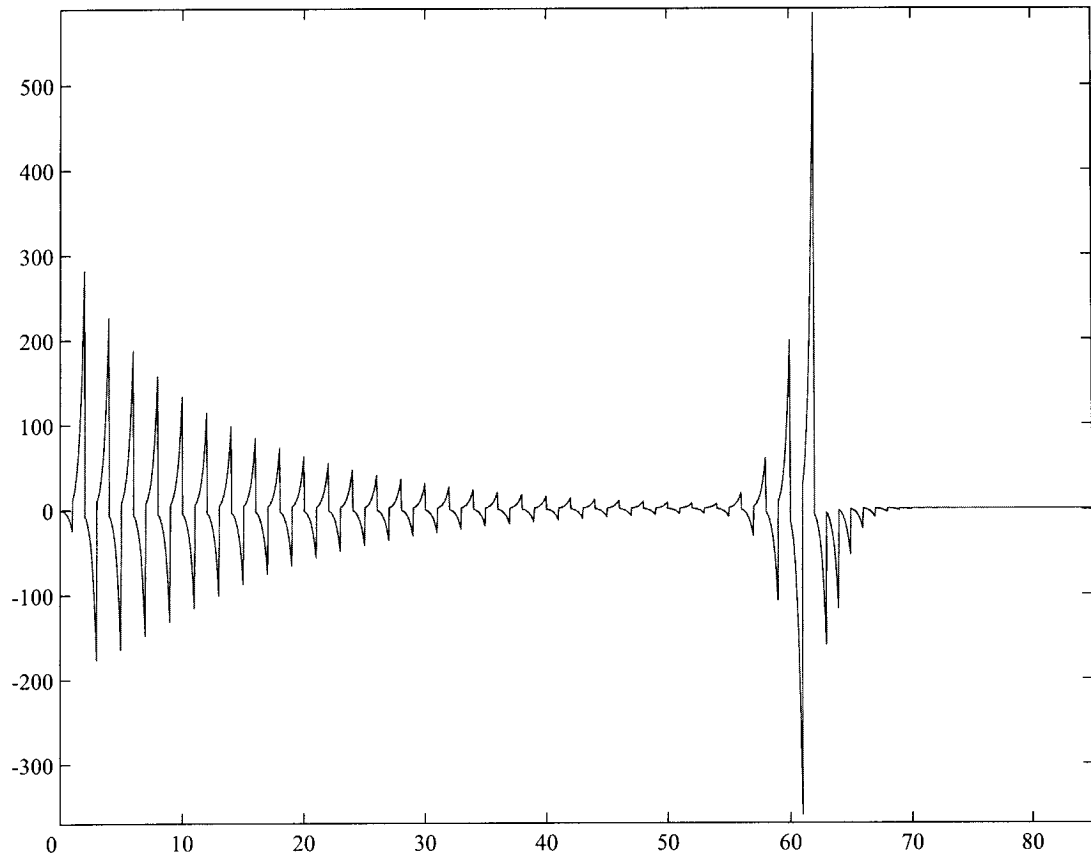


Figure 4.9: Continuous-time output of the closed-loop system in Example 1 with GSHFs using the proposed multi-layer scheme, when the plant model changes from \mathbf{P}_1 to \mathbf{P}_4 (Scenario one) using first set of GSHFs.

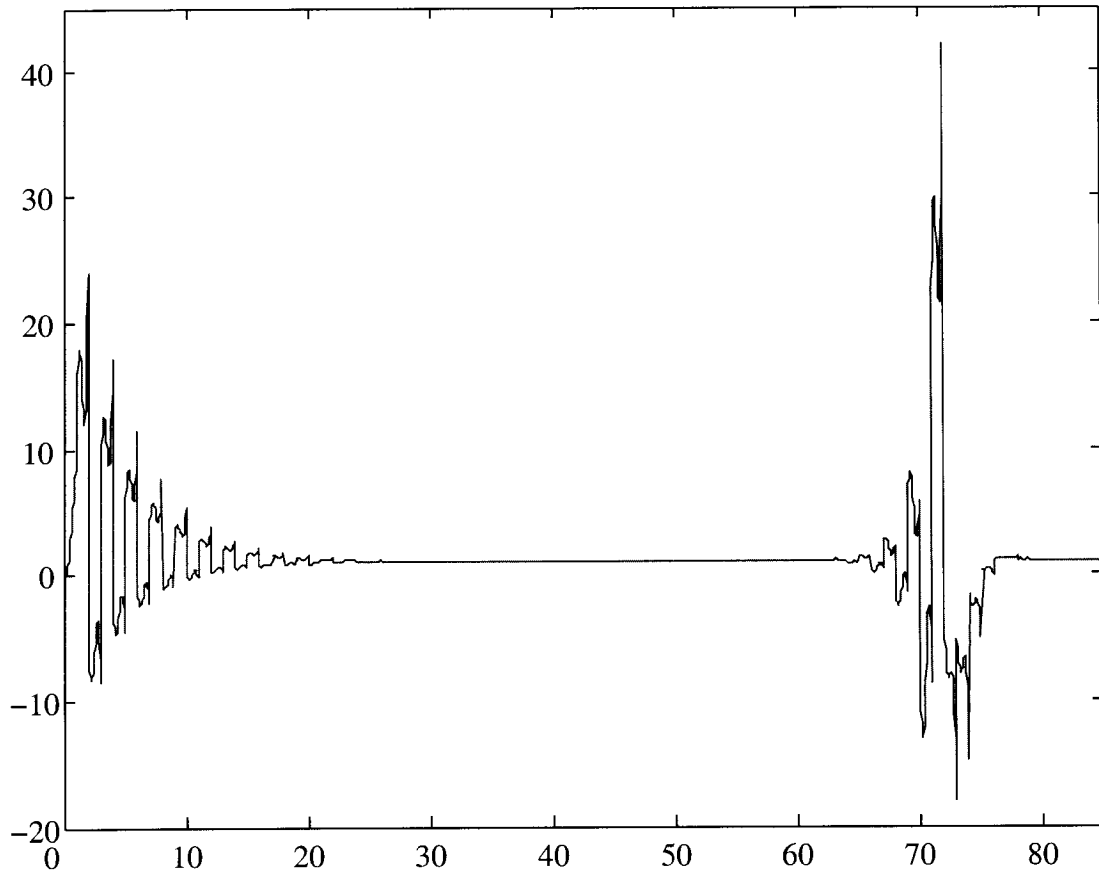


Figure 4.10: Continuous-time output of the closed-loop system in Example 1 with GSHFs using the proposed multi-layer scheme, when the plant model changes from \mathbf{P}_1 to \mathbf{P}_4 (Scenario one).

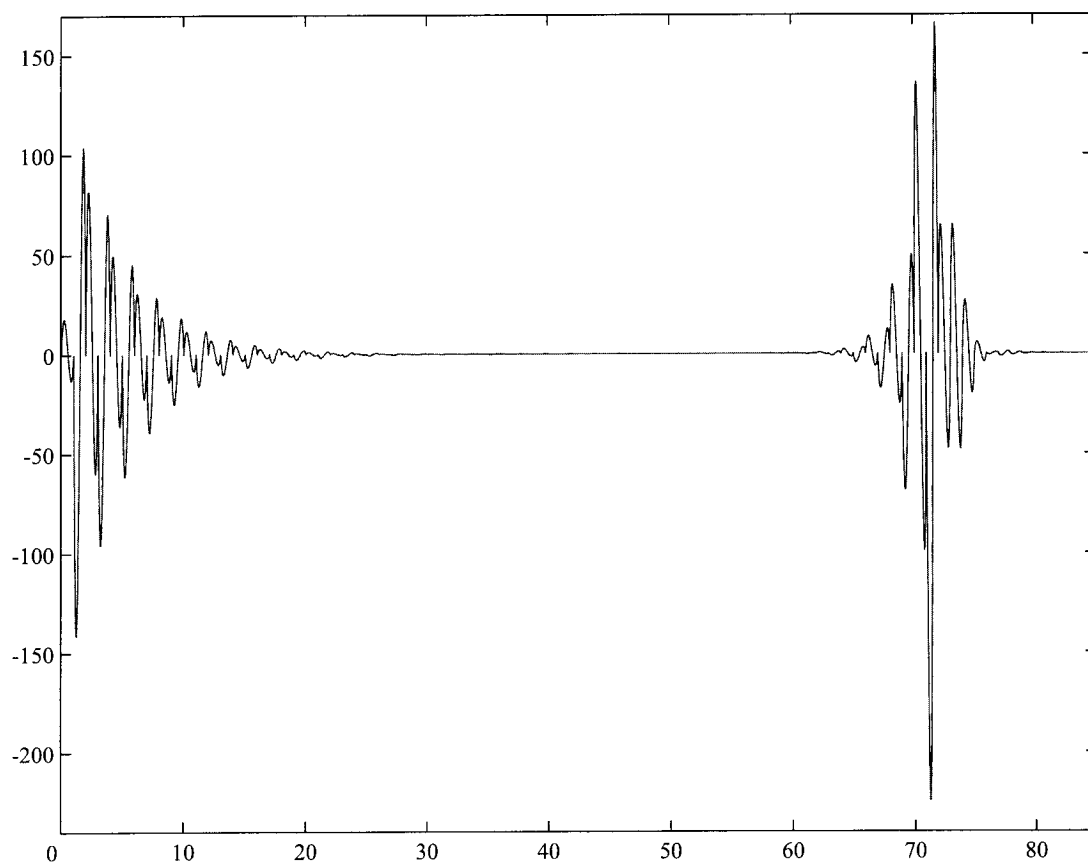


Figure 4.11: Continuous-time control signal of the closed-loop system in Example 1 with GSHFs using the proposed multi-layer scheme, when the plant model changes from \mathbf{P}_1 to \mathbf{P}_4 (Scenario one).

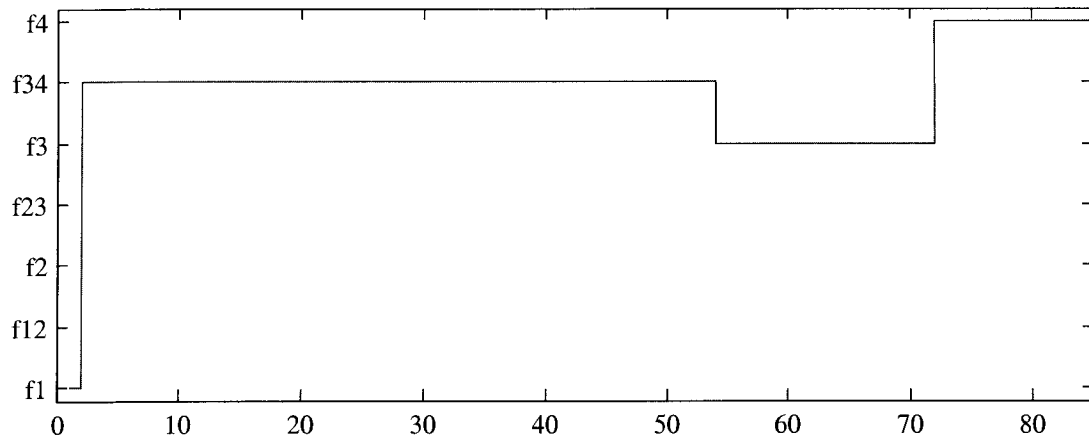


Figure 4.12: Switching instants of the multi-layer scheme in Example 1, when the plant model changes from \mathbf{P}_1 to \mathbf{P}_4 .

LQG optimal controller instead of GSHFs are presented in Figure 4.18, which shows a transient response by 5 orders of magnitude greater than the proposed multi-layer structure with GSHFs.

It is to be noted that choosing a less conservative safety time will result in finding the correct GSHF in shorter time.

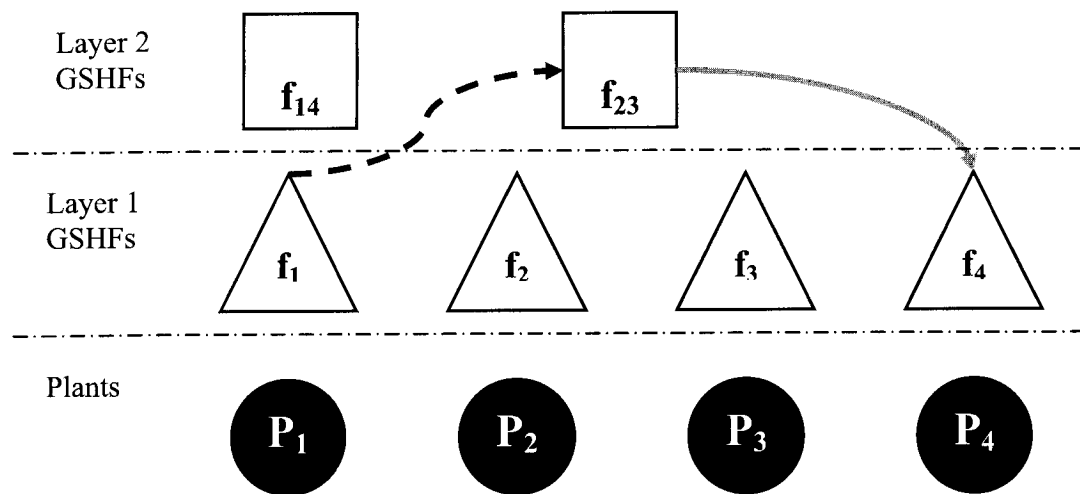


Figure 4.13: Scenario No. 2 for switching, when the plant model changes from P_1 to P_4 . The dashed arrow shows an unstable switching, while the solid arrow shows switching to a stabilizing GSHF.

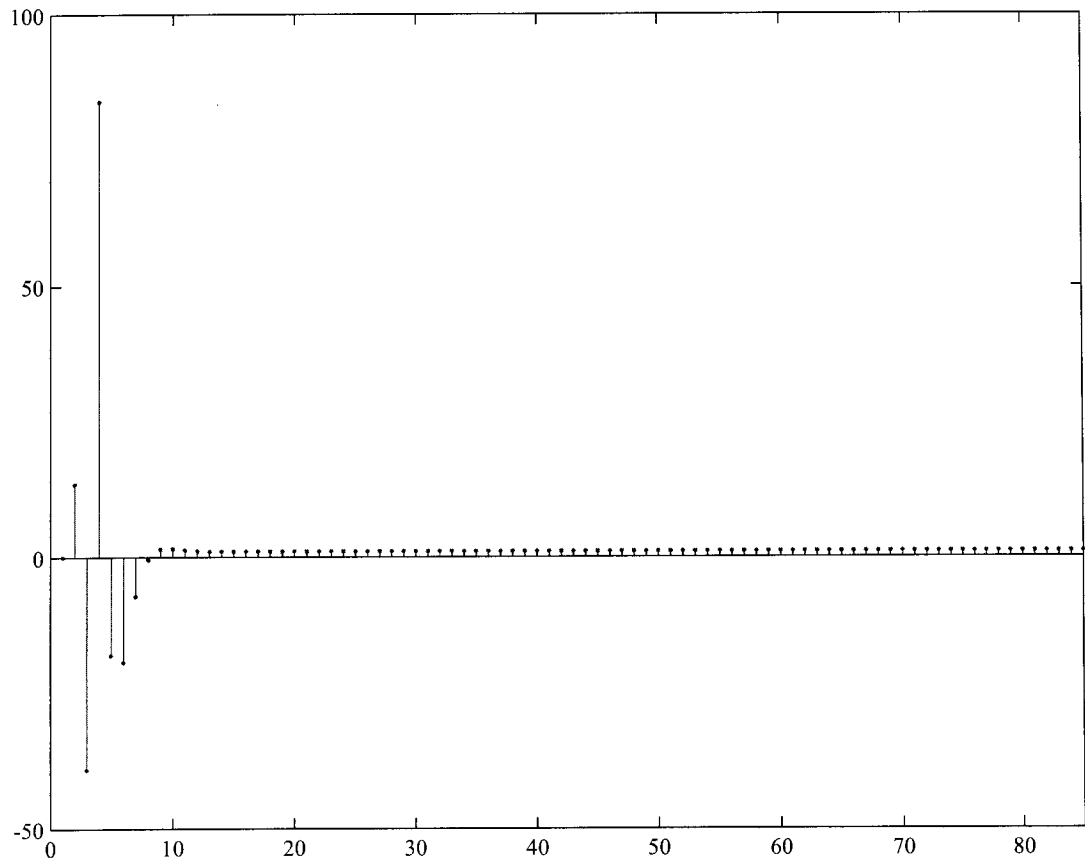


Figure 4.14: Discrete output of the closed-loop system with GSHFs at discrete points of time using the single-layer scheme, when the plant model changes from \mathbf{P}_1 to \mathbf{P}_4 .

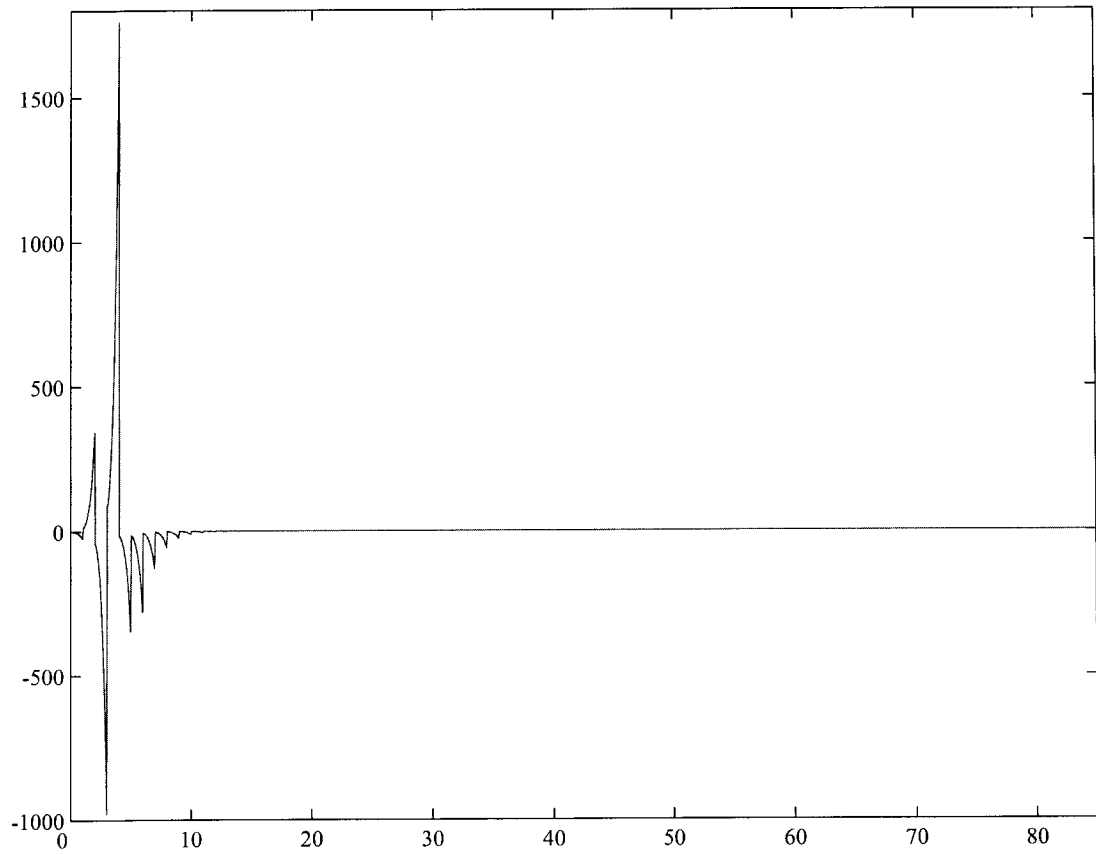


Figure 4.15: Continuous-time output of the closed-loop system for Example 1, using the single-layer scheme of [1], and first set of GSHFs when the plant model changes from \mathbf{P}_1 to \mathbf{P}_4 .

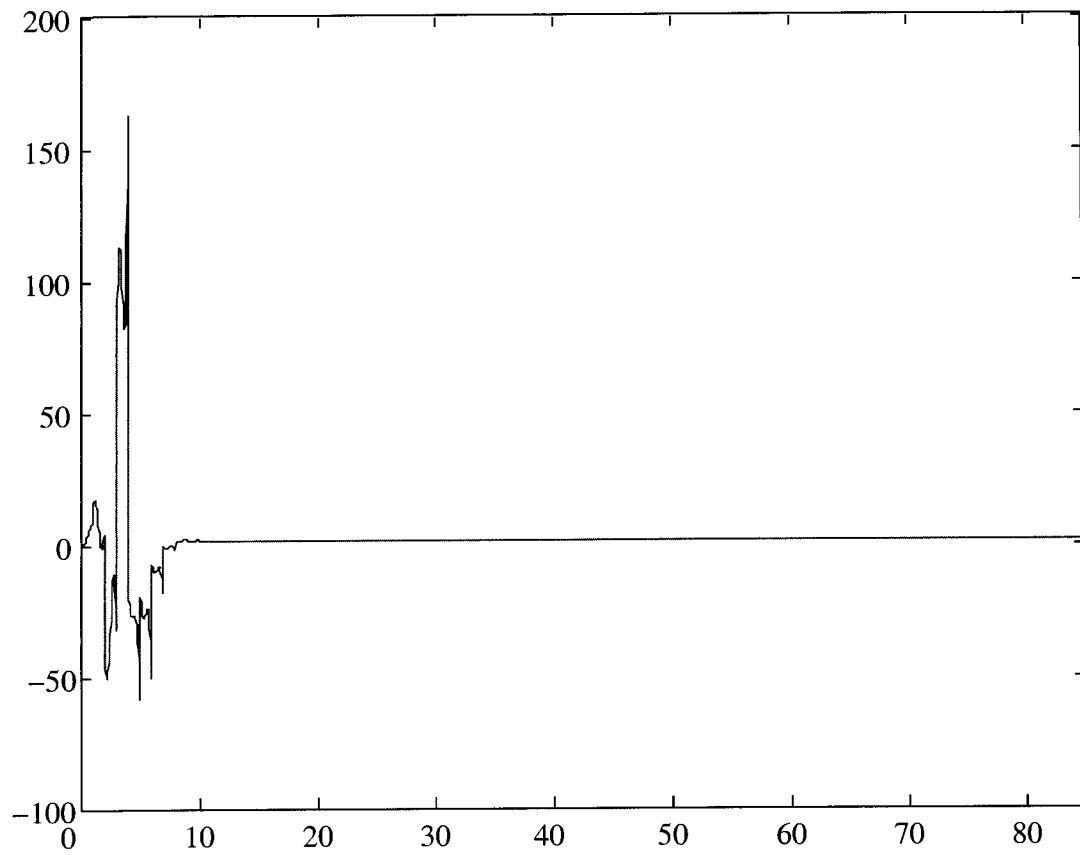


Figure 4.16: Continuous-time output of the closed-loop system for Example 1, using the single-layer scheme of [1], when the plant model changes from \mathbf{P}_1 to \mathbf{P}_4 .

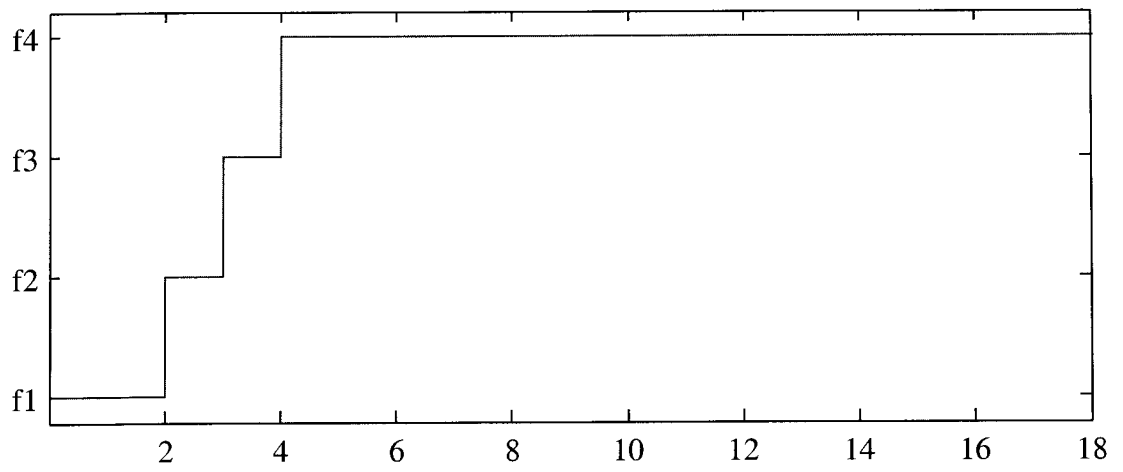


Figure 4.17: Switching instants of the single-layer scheme for Example 1, when the plant model changes from \mathbf{P}_1 to \mathbf{P}_4 .

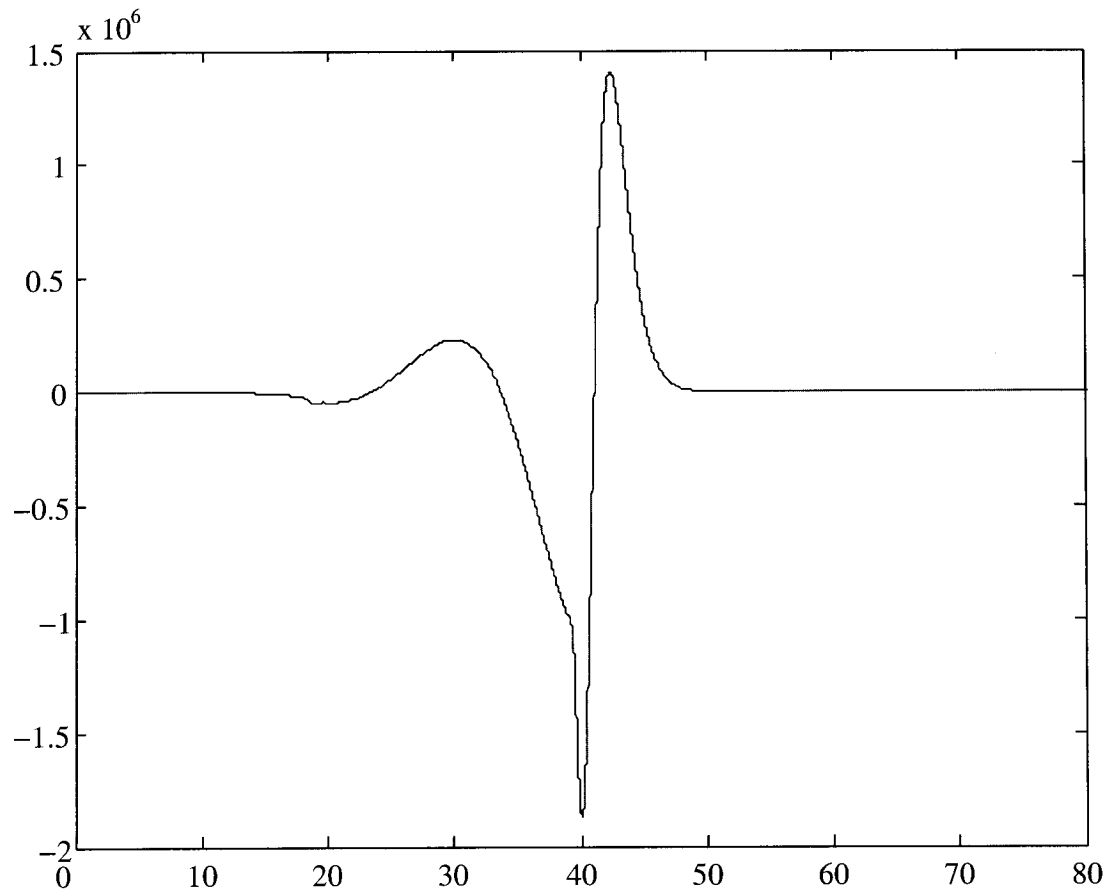


Figure 4.18: Output of the closed-loop system for Example 1 with optimal continuous-time LTI controllers using the single-layer scheme of [2], when the plant model changes from \mathbf{P}_1 to \mathbf{P}_4 .

Chapter 5

Conclusions and Future work

5.1 Conclusions

In this thesis, a new switching control mechanism using generalized sampled-data hold functions (GSHF) is proposed to regulate an uncertain plant whose model belongs to a finite set of known plants. Switching control methods can outperform traditional adaptive control techniques when the plant is highly uncertain and/or the *a priori* information required in conventional adaptive control methods is not available. A brief history of switching control is given in Chapter 1, and digital control of continuous-time using generalized sampled-data hold functions (GSHF) and its advantages were reviewed in Chapter 2.

The existing switching control methods often consider a family of plants in which controllers are structured as a “single-layer”. In this type of structure usually a one to one relationship exists between plant models and controllers. Furthermore it is often assumed that each controller stabilizes only one member of the family of plant models

and destabilizes all other ones.

The algorithm proposed in this work uses different layers of GSHFs that are designed off-line, where layer #1 consists of one high-performance GSHF for each plant model and other layers consist of simultaneous stabilizing GSHFs for certain subsets of the family of plant models. The switching mechanism is based on the discrete-time equivalent model and a discrete-time upper bound signal which is generated and compared to the samples of the norm of the output error at each sampling instant. Assuming that bounds on the norm of the reference signal and the unmeasurable disturbance are given, it is guaranteed that while the system searches for the correct GSHF in the first layer, it switches to at most one destabilizing GSHF and finally locks onto the correct one. The system switches to the next controller if the current controller destabilizes the system, or the current controller stabilizes the system but does not belong to layer #1.

In Chapter 3 a switching control scheme is proposed, which is computationally efficient in obtaining bounding functions or auxiliary signals compared to the existing methods [50], [2]. The required control computations are also much less than continuous-time switching control techniques. Moreover, the proposed switching control method utilizes the benefits of output control using GSHFs which can, in general, outperform traditional LTI controllers. Simulation results show effectiveness of the method compared to the traditional single-layer methods.

One of the shortcomings of switching control methods is the bad transient response which is mainly contributed by switching to many destabilizing GSHFs before the system locks onto the correct GSHF. Each switching to a destabilizing GSHF will usually cause a big overshoot, which will be accumulated before the correct GSHF is found. Addition of new layers of GSHFs can potentially reduce the number of *unstable switchings* as shown

in the algorithm proposed in Chapter 4.

One of the main concerns in multi-layer switching architecture is designing the higher layer controllers, i.e. the controllers that must stabilize more than one plant model. As discussed in chapter 4, it is not required for the algorithm to have all controllers in the higher layers. Only a certain subset of simultaneous stabilizers are sufficient in order to guarantee that with at most one unstable switching, the objective is achieved.

As a result it is suggested that using generalized sampled data hold functions which can be easily implemented using computer systems, choosing a proper decision making strategy, one can achieve overall system stability when the plant is highly uncertain, e.g. when some plant parameters change suddenly. It is to be noted that for the multi-layer switching control, it is required to choose a switching strategy which does not switch to the correct controller more than once. In other words, if one uses a switching scheme such as the one presented in [66], which does not lock onto the correct GSHF first time it switches to it, then it is not guaranteed that there will be no more than one unstable switching while the system searches for the correct controller.

5.2 Future Work

The problem considered in this work addresses a very diverse and general group of applications. With the new advancements in computer technology and recent developments in systems control theory, one can find a more computationally efficient switching strategies for multi-variable systems. The field of digital switching control seems to be very fertile, and numerous exciting ideas might be considered as possible direction of future work. some of which are as follows in the rest of this section.

As noted in chapter 4, after switching to different higher layer GSHFs (which is, in fact, simultaneous stabilizers), the system must switch to the highest layer, and then immediately move on a switching path towards the lower layers, and should eventually switch to a controller in the first layer. Therefore, one may want to find the minimum time required to stay on a GSHF before it can be concluded that it stabilizes the system. Note that the existing switching mechanisms usually use a bounding function to determine instability and there is no method to verify stability by examining the output signal in general. Note also that the system must switch from a higher layer GSHF to a lower layer one, even if it is stable; i.e. it should wait for a sufficiently long time (which is referred to as the *safety time* throughout this work) so that if the norm of the output error does not hit the corresponding upper bound signal, it can be concluded that the system is stable, although it should continue searching for the correct controller. One can assume that this “so called” *safety time* is obtained through experiments. However it would be very useful to find the safety time analytically, using the worst-case scenario in terms of initial state and disturbance signal. The results obtained may be very conservative though.

Moreover, in this thesis it has been implicitly assumed that the probability of each model in the set of candidate models to be the correct one at any time is equivalent. In other words, it is assumed that the probability distribution function (PDF) for the real plant over the candidate model is uniform. However for a more effective switching strategy, one can use an online supervisor to collect some statistical data, or use a given PDF for the models and the corresponding conditional probabilities. As a result each time the system is ready to switch (due to instability or stability in a layer other than #1), it should switch to the highly probable models first. This can be used in the switching logic in order to set privilege of different paths of traversing the graph constructed by GSHFs in different

layers. In other words, in the multi-layer switching structure the decision making unit may sometimes issue a command from a set of possible commands, among which some may have bigger weights based on the probabilities assigned to them. This has been discussed in Chapter 4 very briefly, but can be investigated in more details in the future.

The proposed switching method can also be very effective in decentralized control of highly uncertain large scale systems. The uncertainty can be in the subsystem level, or in interconnection level. One can use classical decentralized adaptive control methods to control such systems. In the decentralized adaptive control literature, some assumptions are usually made on the interacting subsystems. The main assumption which is often made in this case is on imposing a bound on the magnitude of the subsystems' interconnections [67], [68]. There have been some attempts to relax some of these assumptions. For example, a decentralized adaptive scheme is proposed in [69] which does not require any *a priori* information on the subsystems' high-frequency-gain signs.

Furthermore, in [70] and [71] it is shown that under certain conditions, the interconnection gain assumptions can be relaxed, by estimating the interconnection outputs acting on each subsystem; however, all of the assumptions normally made for the centralized adaptive control case must hold for each subsystem in the decentralized adaptive control problem. If the subsystem or the corresponding interconnections are highly uncertain, one can use a proper decentralized switching strategy [69]. One can use a multi-layer decentralized switching control architecture to improve the transient performance of the system. On the other hand, it is known that discrete-time controllers are very effective in decentralized systems. It was also shown in [55] that discrete-time LTI controllers can potentially stabilize certain class of decentralized systems that cannot be stabilized by any continuous-time LTI controllers. The equivalent discrete-time model of the system is

first obtained, and an appropriate technique is then used to design a digital controller to stabilize the system.

Also the idea of using a combination of adaptive controllers and switching GSHFs can be investigated in order to provide solutions for the applications in which the nature of the problem includes both slow and sudden changes in the dynamics of the plant.

In logic-based switching control, the controllers include not only familiar dynamic components but logic driven elements as well. In other words the decision making unit as referred to in this thesis, can be regarded as a discrete event system (DES) supervisor, which is responsible for controlling the state machine consisting of different states in which the switching mechanism might get into, along with the switching and/or stabilizing events. The automaton that can be defined in this way is a means to use DES techniques in multi-layer switching control.

Modelling the system using a DES has several advantages. By using well developed tools and techniques in DES literature not only one can achieve an online supervisor that operates in the decision making unit, but it would also be possible to use the model in order to design a proper multi-layer structure according to the problem specifications. In many real world applications of switching control, one may face a specification which permits more than one destabilizing switching, e.g. two or three destabilizing switching may be permitted. This translates to fewer simultaneous stabilizers required in the multi-layer structure. Also some switching paths may be more critical than the others, and the specification may require that while searching for the correct controller the switching mechanism avoid too many unstable switchings. In some other cases the cost of having one or two destabilizing switchings would not be very different. Determining which simultaneous stabilizer is required in the configuration and which one is not can be a

hard task in general. Hence, the DES model can also help construct a proper multi-layer structure off-line.

The basic switching mechanism for which a multi-layer digital version is proposed in this work is based on the works by Miller and Davison [2]. One can also consider other switching mechanisms which can be used in a multi-layer structure.

Bibliography

- [1] S. Zahirazami and A. G. Aghdam, “Switching control using generalized-sampled data hold functions,” *to appear in Proceedings of the Conference on Control Applications, 2005.*
- [2] D. E. Miller and E. J. Davison, “Adaptive control of a family of plants. In D. Hinrichsen and B. Mårtensson, editors, *Control of Uncertain Systems: Proceedings of an International workshop, Bremen, West Germany, June 1989*, volume 6 of *Progress in Systems and Control Theory*, pages 197-219, Boston, 1990. Birkhäuser Press,”
- [3] D. R. Mudgett and A. S. Morse, “Adaptive stabilization of linear systems with unknown high frequency gains,” *IEEE Transactions on Automatic Control*, vol. AC-30, no. 6, pp. 549–554, June 1985.
- [4] J. C. Willems and C. I. Byrnes, “Global adaptive stabilization in the absence of information on the sign of the high frequency gain. In A. Bensoussan and J. L. Lions, editors, *Analysis and Optimization of Systems: Proceedings of the Sixth International Conference on Analysis and Optimization of Systems*, volume 62 of *Lecture Notes in Control and Information Sciences*, pages 49-57, Berlin, 1984. Springer-Verlag,”

- [5] T. H. Lee and K. S. Narendra, "Removing the high-frequency gain assumption in discrete adaptive control," in *Proceedings of the 24'th IEEE Conference on Decision and Control*, pp. 1198–1202, IEEE, 1985.
- [6] R. D. Nussbaum, "Some remarks on a conjecture in parameter adaptive control," *Systems and Control Letters*, vol. 3, no. 5, pp. 243–246, November 1983.
- [7] A. S. Morse, "A three-dimensional universal controller for the adaptive stabilization of any strictly proper minimum-phase system with relative degree not exceeding two," *IEEE Transactions on Automatic Control*, vol. AC-30, no. 12, pp. 1188–1191, December 1985.
- [8] A. S. Morse, "A $4(n+1)$ -dimensional model reference adaptive stabilizer for any relative degree one or two, minimum phase system of dimension n or less," *Automatica*, vol. 23, no. 1, pp. 123–125, January 1987.
- [9] G. Tao and P. A. Ioannou, "Model reference adaptive control for plants with unknown relative degree," in *Proceedings of the 1989 American Control Conference*, pp. 2297–2302, IEEE, 1989.
- [10] B. Martensson, "The order of any stabilizing regulator is sufficient information for adaptive stabilization," *Systems and Control Letters*, vol. 6, no. 2, pp. 87–91, July 1985.
- [11] D. E. Miller and E. J. Davison, "On necessary assumption in continuous time model reference adaptive control," in *Proceedings of the 28'th IEEE Conference on Decision and Control*, pp. 1573–1578, IEEE, 1989.

- [12] Y. Zhang and P. A. Ioannou, "Robustness of nonlinear control systems with respect to unmodeled dynamics," *IEEE Transactions on Automatic Control*, vol. 44, no. 1, pp. 119–124, Jan 1999.
- [13] F. Ikhouane and M. Krstic, "Robustness of the tuning functions adaptive backstepping design for linear systems," *IEEE Transactions on Automatic Control*, vol. 43, no. 3, pp. 431–437, Mar 1998.
- [14] B. Fidan, Y. Zhang, and P. A. Ioannou, "Adaptive control of a class of slowly time varying systems with modeling uncertainties," *IEEE Transactions on Automatic Control*, vol. 50, no. 6, pp. 915–920, June 2005.
- [15] D. E. Miller and E. J. Davison, "A new self-tuning controller to solve the servomechanism problem," in *Proceedings of the 26'th IEEE Conference on Decision and Control*, pp. 843–849, IEEE, 1987.
- [16] D. E. Miller and E. J. Davison, "An adaptive controller which can stabilize any stabilizable and detectable LTI system. In C. I. Byrnes, C.F. Martin, and R. E. Saeks, editors, *Analysis and Control of Nonlinear Systems*, pages 51-58. Elsevier Science Publishers B. V., Amsterdam, 1988,"
- [17] D. E. Miller and E. J. Davison, "An adaptive controller which provides lyapunov stability," *IEEE Transactions on Automatic Control*, vol. AC-34, no. 6, pp. 599–609, June 1989.
- [18] D. E. Miller and E. J. Davison, "The self-tuning robust servomechanism problem," *IEEE Transactions on Automatic Control*, vol. 34, no. 5, pp. 511–523, May 1989.

- [19] D. E. Miller and E. J. Davison, "An adaptive tracking problem," *International Journal of Adaptive Control and Signal Processing*, vol. 6, no. 1, pp. 45–63, January 1992.
- [20] A. S. Morse, "Supervisory control of families of linear set-point controllers," in *Proceedings of the 32'nd IEEE Conference on Decision and Control*, pp. 1055–1060, IEEE, 1993.
- [21] K. S. Narendra and J. Balakrishnan, "Improving transient response of adaptive control systems using multiple models and switching," in *Proceedings of the 32'nd IEEE Conference on Decision and Control*, pp. 1067–1072, IEEE, 1993.
- [22] M. S. Branicky, "Analyzing continuous switching systems: Theory and examples," in *Proceedings of the 1994 American Control Conference*, pp. 3110–3114, IEEE, 1994.
- [23] M. Chang and E. J. Davison, "Control of unknown systems using switching controllers: an experimental study," in *Proceedings of the 1994 American Control Conference*, pp. 2984–2989, IEEE, 1994.
- [24] K. S. Narendra and J. Balakrishnan, "Improving transient response of adaptive control systems using multiple models and switching," *IEEE Transactions on Automatic Control*, vol. 39, no. 9, pp. 1861–1866, September 1994.
- [25] M. Chang and E. J. Davison, "Control of unknown systems using switching controllers: The self-tuning robust servomechanism problem," in *Proceedings of the 33'rd IEEE Conference on Decision and Control*, pp. 2833–2838, IEEE, 1994.

- [26] K. Ciliz and K. S. Narendra, "Multiple model based adaptive control of robotic manipulators," in *Proceedings of the 33'rd IEEE Conference on Decision and Control*, pp. 1305–1310, IEEE, 1994.
- [27] K. S. Narendra and J. Balakrishnan, "Intelligent control using fixed and adaptive models," in *Proceedings of the 33'rd IEEE Conference on Decision and Control*, pp. 1680–1685, IEEE, 1994.
- [28] M. Chang and E. J. Davison, "New directions in industrial control: Intelligent control - an experimental study applied to a multivariable hydraulic system. In I. Lasiecka and B. Morton, editors, *Control Problems in Industry: Proceedings from the SIAM Symposium on Control Problems*, San Diego, California, July 1994, volume 21 of *Progress in Systems and Control Theory*, pages 65-95. Birkhäuser Press, Boston, 1995,"
- [29] M. Chang and E. J. Davison, "Intelligent control: Some preliminary results. In B. A. Francis and A. R. Tannenbaum, editor, *Feedback Control, Nonlinear Systems, and Complexity*, volume 202 of *Lecture Notes in Control and Information Sciences*, pages 67-87. Springer-Verlag, London, 1995,"
- [30] A. S. Morse, "Supervisory control of families of linear set-point controllers - part 1: Exact matching," *IEEE Transactions on Automatic Control*, vol. AC-41, no. 10, pp. 1413–1431, October 1996.
- [31] M. W. Spong and L. Praly, "Energy based control of underactuated mechanical systems using switching and saturation. In A. S. Morse, editor, *Preprints of the Blick Island Workshop on Control using Logic-Based Switching*, pages 86-95, 1995,"

- [32] A. V. S. Efstratios Skafidas, Robin J. Evans and I. R. Petersen, "Stability results for switched controller systems," *Automatica*, vol. 35, no. 4, pp. 553–564, April 1999.
- [33] C. J. Bett and M. D. Lemmon, "Bounded amplitude performance of switched l_p systems with applications to hybrid systems," *Automatica*, vol. 35, no. 3, pp. 491–503, March 1999.
- [34] Y. Xudong, "Logic-based switching adaptive stabilization of feedforward nonlinear systems," *IEEE Transactions on Automatic Control*, vol. 44, no. 11, pp. 2174–2178, November 1999.
- [35] A. S. Morse, "Recent problems in parameter adaptive control," In *I. D. Landau, editor, CNRS Colloquium on Development and Utilization of Mathematical Models in Automatic Control*, pp. 733–740, 1983.
- [36] B. Martensson, "The order of any stabilizing regulator is sufficient a priori information for adaptive stabilization," *Syst. Contr. Lett.*, pp. 87–91, 1985.
- [37] M. Fu and B. R. Barmish, "Adaptive stabilization of linear systems via switching control," *IEEE Transactions on Automatic Control*, vol. AC-31, no. 12, pp. 1097–1103, December 1986.
- [38] M. Chang and E. J. Davison, "Switching control of a family of plants," in *Proceedings of the 1995 American Control Conference*, pp. 1015–1020, IEEE, 1995.
- [39] M. Chang and E. J. Davison, "Adaptive switching control of LTI MIMO systems using a family of controllers approach," *Automatica*, vol. 35, no. 3, pp. 453–465, March 1999.

- [40] M. S. Branicky, "Analyzing continuous switching systems: Theory and examples," *Proc. American Contr. Conf.*, pp. 3110–3114, 1994.
- [41] M. Chang and E. J. Davison, "Control of unknown systems using switching controllers: An experimental study," *Proc. American Contr. Conf.*, pp. 2984–2989, 1994.
- [42] M. Chang and E. J. Davison, "Control of unknown systems using switching controllers: the self-tuning robust servomechanism problem," *Proc. 33rd IEEE Conf. Decision Contr.*, pp. 2833–2838, 1994.
- [43] A. G. Aghdam and E. J. Davison, "Pseudo-decentralized switching control," *Automatica*, pp. 317–324, 2003.
- [44] A. G. Aghdam and E. J. Davison, "Application of generalized sampled-data hold functions in decentralized switching control," *Proceedings of the American Control Conference, 2003*, vol. 2, pp. 1152–1158, June 4-6 2003.
- [45] A. G. Aghdam and E. J. Davison, "An optimization algorithm for decentralized digital control of continuous time systems which accounts for inter-sample ripple," *Proceedings of the 2004 American Control Conference*, vol. 5, pp. 4273–4278, 30 June - 2 July 2004.
- [46] D. Liberzon, "Switching in systems and control," *Birkhäuser*, June 1, 2003.
- [47] D. E. Miller and E. J. Davison, "An adaptive tracking problem," *International Journal on Adaptive Control and signal Processing*, vol. 6, pp. 45–63, 1992.

- [48] K. S. Narendra and J. Balakrishnan, "Improving transient response of adaptive control systems using multiple models and switching," *IEEE Trans. Automat. Contr.*, vol. 39, no. 9, pp. 1861–1866, Sep. 1994.
- [49] D. E. Miller and E. J. Davison, "An adaptive controller which provides an arbitrarily good transient and steady-state response," *IEEE Trans. Automat. Contr.*, vol. 36, no. 1, pp. 68–81, 1991.
- [50] I. Karuei, N. Meskin, and A. G. Aghdam, "Multi-layer switching control," *to appear in Proceedings of the American Control Conference, 2005.*
- [51] A. B. Chamma and C. T. Leondes, "On the finite time control of linear systems by piecewise constant output feedback," *International Journal of Control*, vol. 30, no. 2, pp. 227–234, 1979.
- [52] P. T. Kabamba, "Control of linear systems using generalized sampled-data hold functions," *IEEE Transactions on Automatic Control*, vol. 32, pp. 772–783, Sep. 1987.
- [53] P. T. Kabamba and C. Yang, "Simultaneous controller design for linear time-invariant systems," *IEEE Transactions on Automatic Control*, vol. 36, pp. 106–111, Jan. 1991.
- [54] S. H. Wang and E. J. Davison, "On the stabilization of decentralized control systems," *IEEE Transactions on Automatic Control*, vol. AC-18, pp. 473–478, 1973.
- [55] Ü. Özgüner and E. J. Davison, "Sampling and decentralized fixed modes," in *Proceedings of the 1985 American Control Conference*, pp. 257–262, IEEE, 1985.

- [56] T. Chen and B. Francis, "Optimal sampled-data control systems,"
- [57] A. G. Aghdam and E. J. Davison, "Decentralized control of systems, using generalized sampled-data hold functions," *Proceedings of the 38th IEEE Conference on Decision and Control, 1999*, vol. 4, pp. 3912–3913, 7-10 Dec. 1999.
- [58] A. G. Aghdam and E. J. Davison, "Application of generalized sampled-data hold functions to decentralized control structure modification," *Proceedings of the IFAC 15'th World Congress, Barcelona, Spain, 2002*.
- [59] Q. Yu, M. Er, M. Ni, and L. Shen, "Generalized sampled and hold functions-based controllers design for uncertain systems," *Proceedings of the IEEE International Symposium on Computer Aided Control System Design*, pp. 346–350, 22 - 27 Aug. 1999.
- [60] J. Sklansky and J. R. Ragazzini, "Analysis of errors in sampled-data feedback systems - part ii," *AIEE Transactions*, vol. 74, pp. 65–71, 1955.
- [61] E. I. Jury and F. J. Mullin, "The analysis of sampled-data control systems with a periodically time-varying sample rate," *IRE Transactions on Automatic Control*, vol. AC-24, p. 1521, 1959.
- [62] C. F. VanLoan, "Computing integrals involving the matrix exponentials," *IEEE Transactions on Automatic Control*, vol. AC-23, no. 3, pp. 395–404, June 1978.
- [63] S. Fekri, M. Athans, and A. Pascoal, "Rmmac, a novel robust adaptive control scheme - part ii: Performance evaluation," *43rd IEEE Conference on Decision and Control*, pp. 1140–1148, Dec. 2004.

- [64] A. S. Morse, "Supervisory control of families of linear set-point controllers-part 1: Exact matching," *IEEE Trans. Automat. Contr.*, pp. 1413–1431, 1996.
- [65] J. Doyle, B. Francis, and A. Tannenbaum, "Feedback control theory," *Macmillan Publishing Company, New York*, 1992.
- [66] S. H. Wang, "Stabilization of decentralized control systems via time-varying controllers," *IEEE Transactions on Automatic Control*, vol. AC-27, no. 3, pp. 741–744, June 1982.
- [67] D. T. Gavel and D. D. Šiljak, "Decentralized adaptive control: Structural conditions for stability," *IEEE Transactions on Automatic Control*, vol. AC-34, no. 4, pp. 413–426, April 1989.
- [68] L. Shi and S. K. Singh, "Decentralized adaptive controller design for large-scale systems with higher order interconnections," *IEEE Transactions on Automatic Control*, vol. AC-37, no. 8, pp. 1106–1118, August 1992.
- [69] Y. Xudong, "Decentralized adaptive regulation with unknown high-frequency-gain signs," *IEEE Transactions on Automatic Control*, vol. 44, no. 11, pp. 2072–2076, November 1999.
- [70] M. Makoudi and L. Radouane, "A robust decentralized model reference adaptive control for non-minimum-phase interconnected systems," *Automatica*, vol. 35, no. 8, pp. 1499–1508, August 1999.

- [71] S. Mukhopadhyay and K. S. Narendra, "Decentralized adaptive control using partial information," in *Proceedings of the 1995 American Control Conference*, pp. 34–38, IEEE, 1999.

Appendix A

Computing Integrals Involving Matrix Exponentials

A.1 An Efficient Matrix Exponential Integration Method

In order to compute integrals involving matrix exponentials, one can use the method proposed by Charles Van Loan in [62]. It is desired to relate the following integrals:

$$\begin{aligned} H(\Delta) &= \int_0^\Delta e^{As} B ds \\ Q(\Delta) &= \int_0^\Delta e^{A^T s} Q_c e^{As} ds \\ M(\Delta) &= \int_0^\Delta e^{A^T s} Q_c H(s) ds \\ W(\Delta) &= \int_0^\Delta H(s)^T Q_c H(s) ds \end{aligned} \tag{A.1}$$

to the elements of the exponential of a certain block triangular matrix.

The following theorem gives a very general solution to the problem.

Theorem 4 [62] Let n_1, n_2, n_3 and n_4 be positive integers, and set m to be their sum. If the $m \times m$ block triangular matrix C is defined by,

$$C = \begin{bmatrix} A_1 & B_1 & C_1 & D_1 \\ 0 & A_2 & B_2 & C_2 \\ 0 & 0 & A_3 & B_3 \\ 0 & 0 & 0 & A_4 \end{bmatrix} \quad (\text{A.2})$$

then for $t \geq 0$

$$e^{Ct} = \begin{bmatrix} F_1(t) & G_1(t) & H_1(t) & K_1(t) \\ 0 & F_2(t) & G_2(t) & H_2(t) \\ 0 & 0 & F_3(t) & G_3(t) \\ 0 & 0 & 0 & F_4(t) \end{bmatrix} \quad (\text{A.3})$$

where

$$\begin{aligned} F_j(t) &= e^{A_j t}, \quad j = 1, 2, 3, 4 \\ G_j(t) &= \int_0^t e^{A_j(t-s)} B_j e^{A_{j+1}s} ds, \quad j = 1, 2, 3 \\ H_j(t) &= \int_0^t e^{A_j(t-s)} C_j e^{A_{j+2}s} ds \\ &\quad + \int_0^t \int_0^s e^{A_j(t-s)} B_j e^{A_{j+1}(s-r)} B_{j+1} e^{A_{j+2}r} dr ds, \quad j = 1, 2 \\ K_1(t) &= \int_0^t e^{A_1(t-s)} D_1 e^{A_4 s} ds \\ &\quad + \int_0^t \int_0^s e^{A_1(t-s)} [C_1 e^{A_3(s-r)} B_3 + B_1 e^{A_2(s-r)} C_2] e^{A_4 r} dr ds \\ &\quad + \int_0^t \int_0^s \int_0^r e^{A_1(t-s)} B_1 e^{A_2(s-r)} B_2 e^{A_3(r-w)} B_3 e^{A_4 w} dw dr ds \end{aligned} \quad (\text{A.4})$$

The proof of the above theorem requires solving four differential equations. If the theorem is applied to the following matrix

$$\hat{C} = \begin{bmatrix} -A^T & I & 0 & 0 \\ 0 & -A^T & 0 & 0 \\ 0 & 0 & A & B \\ 0 & 0 & 0 & 0 \end{bmatrix} \quad (\text{A.5})$$

one will need to find the following matrix:

$$e^{\hat{C}t} = \begin{bmatrix} \hat{F}_1(t) & \hat{G}_1(t) & \hat{H}_1(t) & \hat{K}_1(t) \\ 0 & \hat{F}_2(t) & \hat{G}_2(t) & \hat{H}_2(t) \\ 0 & 0 & \hat{F}_3(t) & \hat{G}_3(t) \\ 0 & 0 & 0 & \hat{F}_4(t) \end{bmatrix} \quad (\text{A.6})$$

where

$$\begin{aligned} \hat{F}_3(t) &= e^{At} \\ \hat{G}_2(t) &= e^{A^T t} \int_0^t e^{A^T s} Q_c e^{As} ds \\ \hat{G}_3(t) &= \int_0^t e^{A(t-s)} B ds \\ \hat{H}_2(t) &= e^{-A^T t} \int_0^t \int_0^s e^{A^T s} Q_c e^{Ar} B dr ds \\ \hat{K}_1(t) &= e^{A^T t} \int_0^t \int_0^s \int_0^r e^{A^T r} Q_c e^{Aw} B dw dr ds \end{aligned} \quad (\text{A.7})$$

and hence all the integrals in (A.8) can be expressed in terms of submatrices of $e^{\hat{C}t}$.

$$\begin{aligned}
H(\Delta) &= \hat{G}_3(\Delta) \\
Q(\Delta) &= \hat{F}_3(\Delta)^T \hat{G}_2(\Delta) \\
M(\Delta) &= \hat{F}_3(\Delta)^T \hat{H}_2(\Delta) \\
W(\Delta) &= [B^T \hat{F}_3(\Delta)^T \hat{K}_1(\Delta)] + [B^T \hat{F}_3(\Delta)^T \hat{K}_1(\Delta)]^T
\end{aligned}
\tag{A.8}$$

Appendix B

Simulation Codes

B.1 MATLAB Codes

B.1.1 Single-Layer

The simulations in this thesis have been prepared using MATLAB version 7.0.1.24704(R14) Service Pack 1 from Mathworks.

```
clc
```

```
clear all warning off;
```

```
% 'LOADING THE SYSTEM...'
```

```
load GSHFSYSTEM2.mat; number_of_plants=4;
```

```
GSHF_DATA=[1 1 01; 2 2 02; 3 3 03; 4 4 04;
```

```
12 1 2; 34 3 4];
```

```

number_of_GSHFs=size(GSHF_DATA,1);
number_of_layers=size(GSHF_DATA,2)-1; T=1;

condition=0;

% 'LOADING COMPLETED.'
% ' '

% simulation parameters:

safety_time=50; T=1; syms t record_state=[];

for k = 1 : number_of_GSHFs
    for k2=1:number_of_layers

        F_index=GSHF_DATA(k,1);
        P_index=GSHF_DATA(k,k2+1);
        r{F_index,k2} = [0];

        [A{P_index},B{P_index},C{P_index},D{P_index}]=ssdata(PLNT{P_index});

```



```

        Ad{P_index} = expm(A{P_index}*T);
        Cd{P_index} = C{P_index};
        Dd{P_index} = D{P_index};

    end

end for k=1 : number_of_GSHFs
    for k2=1:number_of_plants
        F_index=GSHF_DATA(k,1);
        P_index=k2;
        Bd{P_index,F_index} = eval(int(expm(A{P_index}*(T-t))
            *B{P_index}*GSHF{F_index},t,0,T));

    end

end

for P_index = 1 : number_of_plants
    for k2 = 1 : number_of_GSHFs
        F_index=GSHF_DATA(k2,1);
    end
    gamma1{P_index} = max(abs(eig(Ad{P_index}-
        (Bd{P_index,P_index}*Cd{P_index})))));
end

T2 = 20;

```

```

ref = 1; N = 100; out = [0]; last = 4; lost = 1; inp = [ref ref];
track = [lost]; [G H J K] =
ssdata(feedback(ss(Ad{last},Bd{last,lost},Cd{last},Dd{last},-1),1));
X = zeros(2,size(Ad{1},1)); XC = zeros(T2+1,size(Ad{1},1));
Y_rec=[];

settled=1; lost0=lost; counter=0; lost00=lost; for j = 1 : N

    if lost0~=lost
        settled=0; % we are in switching mode
        counter=0; % ready to count
    else
        counter=counter+1; % counting just started
    end

    if counter*T>(safety_time); %%%%%%%%%%% safty time
        settled=1;
    end

    inp2 = [];
    j2 = 1;
    TT = (j2-1):1/T2:j2-1/T2;
    for temp = (j2-1):1/T2:j2-1/T2

```

```

t = temp;
inp2 = [inp2,eval(int(GSHF{lost}))*(ref-out(j))];
end

[YC,XC] = lsim(A{last},B{last},C{last},D{last},inp2',TT,X(2,:));
Y_rec = [Y_rec, YC'];

[Y,X] = dlsim(G,H,J,K,inp,X(2,:));
out = [out, Y(2)];
for k = 1 : number_of_GSHFs
    for k2=1:number_of_layers
        F_index=GSHF_DATA(k,1);
        P_index=GSHF_DATA(k,k2+1);

        r{F_index,k2} = [r{F_index,k2}, gamma1{P_index}*r{F_index,k2}(j)
        + norm(Cd{P_index}*(Bd{P_index,F_index}*out(j)
        +Bd{P_index,lost}*(ref-out(j)))))];%
    end
end

condition=( r{lost,1}(j+1) < abs(out(j+1)))
& ( r{lost,2}(j+1) < abs(out(j+1)));
record_state=[record_state lost];

```

```

lost0=lost;
%states4x2;
if condition
    lost=lost+1;
    if lost>4
        lost=1;
    end
end

if lost0~=lost
    [G H J K] = ssdata(feedback(ss(Ad{last},Bd{last,lost}
    ,Cd{last},Dd{last},-1),1));
end

track = [track,lost];
end

```

B.1.2 Multi-Layer

The multi-layer setup simulations are done using the following MATLAB codes. Note that the code tries to switch from \mathbf{P}_1 to \mathbf{P}_4 .

```
%clc
```

```

clear all warning off;

% 'LOADING THE SYSTEM...'
load GSHFSYSTEM2.mat;

number_of_plants=4;
% GSHF NAME - P1 - P2 - ... PN
GSHF_DATA=[1 1 1;
           2 2 2;
           3 3 3;
           4 4 4;
           12 1 2;
           34 3 4];

number_of_GSHFs=size(GSHF_DATA,1);
number_of_layers=size(GSHF_DATA,2)-1;
% 'LOADING COMPLETED.'

for k = 1 : number_of_GSHFs
    for k2=1:number_of_layers
        F_index=GSHF_DATA(k,1);
        P_index=GSHF_DATA(k,k2+1);
        r{F_index,k2} = [0];
        [A{P_index},B{P_index},C{P_index},D{P_index}]=ssdata(PLNT{P_index});
        Ad{P_index} = expm(A{P_index}*T);
    end
end

```

```

        Cd{P_index} = C{P_index};
        Dd{P_index} = D{P_index};
    end
end for k=1 : number_of_GSHFs
    for k2=1:number_of_plants
        F_index=GSHF_DATA(k,1);
        P_index=k2;
        Bd{P_index,F_index} = eval(int(expm(A{P_index}*(T-t))
        *B{P_index}*GSHF{F_index},t,0,T));
    end
end

end

for P_index = 1 : number_of_plants
    gamma1{P_index} = max(abs(eig(Ad{P_index}
    -(Bd{P_index,P_index}*Cd{P_index})))));
end

ref = 1; N = 100; out = [0]; last = 4; lost = 1; inp = [ref ref];
track = [lost]; [G H J K] =
ssdata(feedback(ss(Ad{last},Bd{last,last},Cd{last},Dd{last},-1),1));
X = zeros(2,size(Ad{1},1)); XC = zeros(T2+1,size(Ad{1},1));
Y_rec=[];

settled=1; lost0=lost; counter=0; lost00=lost; for j = 1 : N

```

```

if lost0~=lost
    settled=0; % we are in switching mode
    counter=0; % ready to count
else
    counter=counter+1; % counting just started
end

if counter*T>(safety_time); %%%%%%%%%%% Safty time
    settled=1;
end

inp2 = [];
j2 = 1;
TT = (j2-1):1/T2:j2-1/T2;
for temp = (j2-1):1/T2:j2-1/T2
    t = temp;
    inp2 = [inp2,eval(int(GSHF{lost}))*(ref-out(j))];
end

[YC,XC] = lsim(A{last},B{last},C{last},D{last},inp2',TT,X(2,:));
Y_rec = [Y_rec, YC'];

```

```

[Y,X] = dlsim(G,H,J,K,inp,X(2,:));
out = [out, Y(2)];
for k = 1 : number_of_GSHFs
    for k2=1:number_of_layers
        F_index=GSHF_DATA(k,1);
        P_index=GSHF_DATA(k,k2+1);

        r{F_index,k2} = [r{F_index,k2}, gamma1{P_index}*r{F_index,k2}(j)
            + norm(Cd{P_index}*(Bd{P_index,F_index}*out(j)
            +Bd{P_index,lost}*(ref-out(j))))];%
    end
end
condition=( r{lost,1}(j+1) < abs(out(j+1)))
& ( r{lost,2}(j+1) < abs(out(j+1)));
record_state=[record_state lost];

lost0=lost;
states4x2;

if lost0~=lost
    [G H J K] = ssdata(feedback(ss(Ad{last},
        Bd{last,lost},Cd{last},Dd{last},-1),1));
end
end

```



```
    track = [track,lost];  
end
```

The output of the code can be found in the Simulations Results section of Chapter 4.